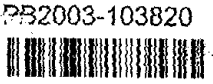

Final Report

on research carried out under

NIOSH-CDC Grant No. RO1-OH 03687-03

entitled

DEVELOPMENT OF NEW PERSONAL AEROSOL SAMPLERS

by

James H. Vincent, Ph.D., D.Sc. (Principal Investigator)

Samuel Y. Paik, Ph.D. (Research Assistant)

and

Douglas E. Evans, Ph.D. (Postdoctoral Fellow)

Submitted February 2003

TABLE OF CONTENTS

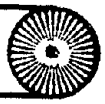

ABSTRACT

Aerosol samplers are important to industrial hygiene through their role in the measurement (and hence regulation) of workers' exposures to airborne particles. New health-related, particle size-selective aerosol standards require that such measurement should reflect the true physical nature of human exposure; that is, the manner in which they are inhaled and penetrate into the respiratory tract. This, in turn, has stimulated the search for new generations of practical sampling devices.

The inhalable fraction reflects what people actually inhale; that is, what passes through the nose and/or mouth during breathing. This is directly relevant to health effects in a wide range of working and other indoor environments. In turn, the thoracic subfraction is directly relevant to asthma and chronic pulmonary obstructive disease (COPD). These areas are components of the National Occupational Research Agenda (NORA). The primary broad objective of the proposed research was therefore to apply knowledge gained in previous research to the development of new small-scale, user-friendly personal aerosol sampling systems. More specifically we set out to (1) develop and use new knowledge of the theory of aerosol sampling to design new personal samplers for the inhalable aerosol fraction that are small, lightweight, convenient to use; (2) build a prototype inhalable aerosol sampler and test it for relevant conditions in the wind tunnel; and (3) test new samplers in actual workplaces.

After the research began, interest became more sharply focused on sampling for the inhalable aerosol fraction. This is where the greatest technical challenges lie since it involves the interface between the sampler and the uncontrollable (at least in practice) external wind environment. So it was decided that the final aims of the research should focus almost entirely on sampling at low flowrate for the inhalable fraction. This report mainly reflects that emphasis. However, a design study was carried out to realize a new prototype low-flowrate sampler for the thoracic fraction. But this was not tested in the laboratory or in the field.

Overall, this research proved the hypothesis that it is indeed possible to develop sampling instruments with desired performance characteristics based on an improved knowledge of the physics of aerosol sampling. The initial parts of the research comprised a set of laboratory investigations leading to the development of a prototype low-flowrate sampler for the inhalable aerosol fraction. During this work, we achieved a number of important new advances in aerosol sampling science, including identification of the limits of detection quantitation for the gravimetric assessment of small masses in sampler collection cassettes and substrates, and a better understanding of the aspiration efficiencies of sampling devices when sampling at low flowrates. These were important contributions towards the desired endpoint of a new low-flowrate sampler for the inhalable fraction.

SIGNIFICANT FINDINGS

Importantly, the research has demonstrated that, by due reference to appropriate physic scaling principles, it is possible to accurately characterize the performances of personal aerosol samplers using a small-scale sampler testing system. The sampler testing system and methods developed for this research enabled the testing and validation of the performances of aerosol samplers with

a high degree of reproducibility, at relatively low cost, and in short periods of time. It is expected that the future development of aerosol samplers will increasingly utilize such simplified testing systems, including the use of direct-reading instrumentation that would significantly reduce the costs, labor, and time requirements even further.

USEFULNESS OF THE FINDINGS

The progress that has been achieved in this project will greatly facilitate the future development of new sampling devices. This in turn will aid industrial hygienists in their ability to characterize workers' aerosol exposures and ultimately preserve the health of people in aerosol-laden workplace environments.

PUBLICATIONS ARISING OUT OF THE RESEARCH

A number of publications have already appeared in the peer-reviewed scientific literature arising out of this work, including:-

Paik, S.Y. and Vincent, J.H. (2002), Filter and cassette mass instability in ascertaining the limit of detection of nhalable airborne particulate, *American Industrial Hygiene Association Journal*, 63, 698-702.

Paik, S.Y. and Vincent, J.H. (2002), Aspiration efficiency for thin-walled nozzles facing the wind and for very high velocity ratios, *Journal of Aerosol Science*, 33, 705-720.

Paik, S.Y. and Vincent, J.H. (2002), Aspiration efficiencies of disc-shaped blunt nozzles facing the wind, for coarse particles and high velocity ratios, *Journal of Aerosol Science*, 33, 1509-1523.

Brixey, L.A., Paik, S.Y., Evans, D.E. and Vincent, J.H. (2002), Experimental studies to develop new aerosol samplers and methods for their evaluation, *Journal of Environmental Monitoring*, 4, 633-641.

Several more are in preparation, and will appear in due course.

THE PROPOSED RESEARCH

Background

In relation to the latest particle size-selective sampling criteria, the physical problem central to the research involved the aspiration of the inhalable fraction through the entry, and – where appropriate – the aerodynamic pre-selection of the desired subfraction. In either case, the selected health-related fraction is collected on a filter which can be subsequently analyzed after sampling. Such analysis may take the form of gravimetric assessment (i.e., weighing) to determine the total mass of particulate material collected and/or chemical quantitation to determine the mass contained within specific chemical species considered most relevant.

In general, so-called "*area sampling*" is carried out using instruments which sample air from the general environment in the general vicinity of the exposed person. This was the approach most commonly adopted in the years before the 1970s – at least for time-weighted average (TWA) or full-shift sampling – when sampling required an attendant operator and the required equipment was inevitably rather massive and required an external power source (and so was far from portable). "*Personal sampling*" only emerged with the advent of samplers and (particularly) pumps that could be miniaturized to the point where they could conveniently be carried by, or worn on the person of, the worker. The first commercial personal sampling pumps subsequently appeared around 1962, and by the early 1970s were becoming routine occupational hygiene tools. Now, three decades further on, personal sampling is widely regarded as the most satisfactory way to assess the exposures of workers. Pumps that can deliver upwards of 2 L/min for up to 12 hours are now commonplace and widely used by occupational hygienists. Nonetheless, to this day, such pumps are cumbersome (e.g., typically weighing between 25 and 40 ounces) and bulky, dictated in large measured by the batteries. So, they are considered inconvenient by certain segments of the workforce, including older workers and women. Further, in the wider context, where there is concern about the exposures of people to aerosols in the general living environment, current personal sampling pumps are not suitable for many of the groups of interest, including (again) older people and children.

Personal sampling pumps are now available that provide flowrates down to 0.1 L/min. These are much smaller than the ones referred to above, weighing only a few ounces and small enough to fit in a breast pocket. Such pumps are widely used for gas and vapor sampling, where sampling itself is not influenced or biased by anything like the aerosol mechanical forces that dominate aerosol sampling, and analytical methods are readily available for the determination of small collected samples. New knowledge about the physical performance characteristics of aerosol sampling heads now make it possible to think about integrating – for the first time – such small pumps into sampling systems for the routine measurement of personal aerosol exposures.

During the last two decades there has been great progress towards the setting of scientifically-based criteria for aerosol measurement in the workplace and elsewhere, led by the International Standards Organisation (ISO), the American Conference of Governmental Industrial Hygienists (ACGIH) and the Comité Européen Normalisation (CEN). All three bodies have moved during recent years towards international harmonization of particle size-selective criteria for health-related aerosol sampling. These are summarized in the current ACGIH-TLV booklet (ACGIH,

2002), and a full review is given in the recent book from the ACGIH Air Sampling Procedures Committee (Vincent, 1999). Such criteria are intended specifically as 'yardsticks' for the design of new sampling instrumentation. They focus attention firmly on the need for sampling to directly reflect the true physical nature of the human exposure. They identify firstly the *inhalability* of the human head itself, representing the efficiency, as a function of particle size, with which particles enter through the nose and/or mouth during breathing. This defines the *inhalable* fraction. They then identify the *thoracic* and *respirable* fractions as subfractions of that inhalable fraction. Here, the thoracic fraction describes the probability that an inhaled particle may penetrate into the lung below the larynx, and the respirable fraction the probability of penetration down to the alveolar region. Each of the three conventions is represented by a single curve describing it as a function of particle aerodynamic diameter. These will form the basis of future occupational exposure limits (OELs) for aerosols.

The adoption of criteria like those described is stimulating the re-assessment of existing sampling instrumentation as well as the search for new aerosol sampling matching those criteria. So far, just a small number of sampling instruments have been designed to specifically match the inhalability curve, and are available to occupational hygienists. One is the so-called "*IOM sampler*" (from SKC, Eighty-Four, PA), based on research conducted at the Institute of Occupational Medicine (Edinburgh, U.K.) during the 1980s in a body of work funded by the European Community. But more recent European-funded work has identified a number of other samplers which also appear to provide an adequate match (Kenny *et al.*, 1997). This opens up the real possibility that a range of options is available to industrial hygienists for inhalable aerosol sampling.

Most previous and current OELs for substances occurring as aerosols have been expressed in terms of so-called 'total' aerosol (for the coarser fraction) and respirable aerosol (for the finer fraction). But in the future, OELs for the coarser fraction will be expressed more specifically in terms of the new inhalable fraction, and OELs for the finer fraction will be expressed in terms of one or other of the respirable fraction (finest) and the thoracic fraction (intermediate). The choice will depend on the health effect of interest. The inhalable fraction will be applied for substances which are carcinogenic or may present a risk to health following systemic uptake from anywhere in the whole respiratory tract. The latter two fractions will be applied when the health effect is restricted to the respiratory tract, including asthma, chronic bronchitis and CPOD. With the introduction of these new criteria for aerosol sampling and exposure assessment comes the need to re-visit existing OELs and, where appropriate to conduct new exposure assessments for the purpose of new epidemiologic investigations. As will be seen from this report, the present research has provided the scientific basis for improved technical means to conduct such studies for working groups (e.g., some female and older workers) and – in the wider context – other populations (e.g., children) where it has not be possible to make adequate personal exposure assessments in the past.

The research described in this report was conducted under the direction of Professor James H. Vincent (Principal Investigator). Much of it was executed by Samuel Y. Paik (Research Assistant), for whom much of the contents of this report appeared in the doctoral dissertation that he defended successfully in August 2002. In addition, although he was not supported by this grant, Douglas E. Evans (Postdoctoral Fellow) provided valuable assistance with some parts of

the research, in particular that which addressed the question of sampling for the thoracic fraction. All those associated with the research are grateful for the support that came in the form of this grant.

Aims

Aerosol samplers are important to industrial hygiene through their role in the measurement (and hence regulation) of workers' exposures to airborne particles. New health-related, particle size-selective aerosol standards require that such measurement should reflect the true physical nature of human exposure; that is, the manner in which they are inhaled and penetrate into the respiratory tract. This, in turn, has stimulated the search for new generations of practical sampling devices.

The inhalable fraction reflects what people actually inhale; that is, what passes through the nose and/or mouth during breathing. This is directly relevant to health effects in a wide range of working and other indoor environments. In turn, the thoracic subfraction is directly relevant to asthma and chronic pulmonary obstructive disease (COPD). These areas are components of the National Occupational Research Agenda (NORA). The primary broad objective of the proposed research was therefore:-

- To apply the knowledge gained in previous research to the development of new small-scale, user-friendly personal aerosol sampling systems. Such systems would be suitable for use by female and older workers, as well as – in the wider indoor-air context – children.

The original specific objectives were:-

- To use new knowledge of the theory of aerosol sampling to design new personal samplers for the inhalable and thoracic aerosol fractions that are small, lightweight, convenient to use, and – hence – more user-friendly than current systems.
- To build a prototype inhalable aerosol sampler and test it for relevant conditions in the wind tunnel: (a) directly against the inhalability particle size-selective criterion, and (b) by comparison with a reference sampler for the inhalable fraction.
- To build a prototype thoracic aerosol sampler, and test it similarly in the wind tunnel.
- To modify both prototype samplers as appropriate, and optimize their designs and performances, leading to prototype practical systems.
- To explore methods for quantitating the small amounts of aerosol that will be collected by the new sampling systems.
- To test the new inhalable and thoracic aerosol samplers in workplaces by comparing them with reference samplers for those fractions from the current generation of sampling instruments.

The project had two important components. The first involved the appropriate scaling of the actual sampling head itself so that it would select and collect the desired aerosol fractions at the new much lower flowrate. The second involved the investigation of methods for the quantitation of the much smaller amounts of collected particulate material.

TECHNICAL REPORT

1. Introduction

Particle size-selective aerosol sampling

The first reference to "particle size-selective sampling" appeared in 1913 when McCrae found that particles observed by microscopy in lungs of miners post mortem were restricted to the range of one to seven micrometers. He thus identified the need to selectively measure relatively fine particles as the appropriate index of exposure for certain types of dust-related lung diseases, specifically pneumoconioses. By the 1950s, it became possible to identify the range of sizes of inhaled particles penetrating to the alveolar region of the lung. The British Medical Research Council (BMRC, 1952) defined respirable aerosol as the probability, as a function of particle aerodynamic diameter (d_{ae}, the diameter of a sphere of unit density with the same falling speed as the particle in question), that an inhaled particle will penetrate to the alveolar region of the lung. The ACGIH proposed its own respirable dust convention in 1968. In the 1970s, the International Organization for Standardization (ISO) formed a working group which, after several meetings, concluded that the idea of particle size-selective sampling should be expanded to cover all inhaled particles which may be related to all aerosol-related health effects. The inhalable aerosol fraction, referring to those particles that could be inhaled through the mouth or nose while breathing, would be important for the measurement of particles that constitute a risk to health, regardless of where they are deposited in the respiratory tract. In this case, relevant exposure limits should be based on the potential of the particles to be inhaled.

The concept of inhalability is a primary focus of the work described in this report. It is based on the physical fact, known from many wind tunnel experiments with 'breathing' mannequins, that only a portion of total aerosol in the inhaled air can enter a person's respiratory tract during breathing. However, most of the aerosol exposure limits defined by ACGIH and by other bodies in most countries have until recently been expressed in terms of 'total' dust, which assumes that all airborne particles have the same probability of being inhaled. Unfortunately, most 'total' aerosol samplers were originally developed without particular regard to specific quantitative criteria, and it has now become apparent that their performance characteristics may vary greatly from one instrument to another, as seen from the results of both wind tunnel studies and field studies respectively. For example, a large body of field work has shown unequivocally that the closed-face 37mm cassette, widely used in the U.S. as a personal sampler for 'total' aerosol, provides consistently lower concentrations than the IOM personal inhalable aerosol sampler (e.g., Tsai *et al.*, 1995a, and1996a; Werner *et al.*, 1996 and 1999; Spear *et al.*, 1997; Wilsey *et al.*, 1996; Kerr *et al.*, 2001a; and others). In all these studies, the IOM sampler was an appropriate reference instrument for the inhalable fraction (Bartley, 1998).

The conventions for the three aerosol fractions identified in the latest particle size selective sampling criteria are described in detail in the ACGIH monograph (Vincent, 1999). In summary, the *inhalable particulate matter* (IPM) fraction is given by

$$\text{IPM}\ (d_{ae}) = 0.5\ [1 + \exp\ (-0.06\ d_{ae})] \qquad (1)$$

in which d_{ae} is expressed in μm for d_{ae} up to 100 μm. In turn, the *thoracic particulate matter* (TPM) fraction is given by

$$\text{TPM}\ (d_{ae}) = \text{IPM}\ (d_{ae})\ [1\text{-F}(x)] \qquad (2)$$

where F(x) is the cumulative lognormal function with its median at d_{ae} = 11.64 μm and having a geometric standard deviation (σ_g) of 1.5. Finally, the *respirable particulate matter* (RPM) fraction is given by

$$\text{RPM}\ (d_{ae}) = \text{IPM}\ (d_{ae})\ [1\text{-F}(x)] \qquad (3)$$

where F(x) is now the cumulative lognormal function with its median at d_{ae} = 4.25 μm and having a geometric standard deviation (σ_g) of 1.5. These equations are consistent with the physical argument that both the thoracic and respirable aerosol conventions should be expressed as a fraction of the inhalable aerosol fraction. All three fractions are shown in Figure 1.

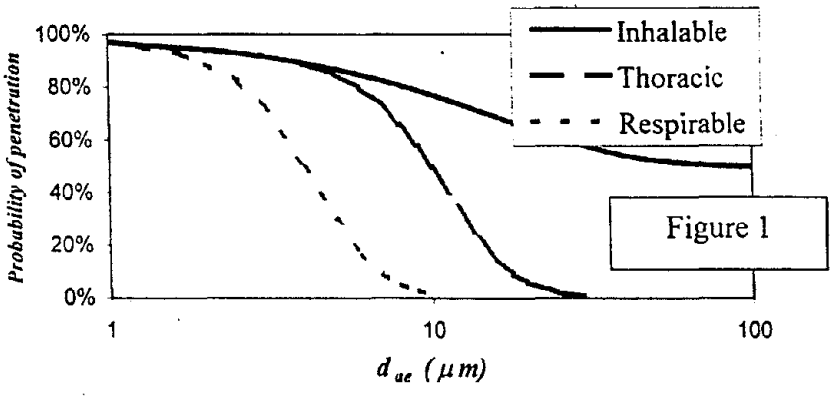

Figure 1

The concept of particle size-selective sampling is important not only because of its direct relevance to health effects but because it is defined as the primary basis of all future (and many current) occupational exposure limits relating to aerosol exposure (except for fibers). Therefore, the development of new sampling devices with performance characteristics conforming to particle size-selective criteria is a high research priority.

Aspiration efficiency

The investigation of sampler aspiration efficiency (A) was the goal of many of the experiments conducted in the research. It is the primary descriptor of aerosol sampler performance, defined as the efficiency with which particles are transferred from the atmosphere of interest into the body of an aspirating sampler. If A for an aerosol sampler, expressed as a function of d_{ae}, matches that of the nose and mouth during normal breathing (as defined by the IPM fraction), the sampler is considered to be an "inhalable aerosol" sampler. In turn, by reference to Equations (2) and (3), it seen to be the starting point for both thoracic aerosol and respirable aerosol samplers. Physically, there are a number of ways for formally defining aspiration efficiency. But for all the research

described in this report, where the distributions of air velocity and aerosol concentration could be assumed always to be uniform, it was appropriate that

$$A = c_s/c_o \tag{4}$$

for given particle size. The extent to which c_s differs from c_o depends on the ability of particles to follow the complex air motion in the vicinity of the sampler inlet.

Modeling aspiration efficiency

For the assessment of the performance of aerosol samplers, aerosol scientists have developed a number of research tools, mainly aimed at describing the nature of airflow near aerosol samplers and how particles are transported in these flows. One approach is to solve all the rigorous mathematical equations relevant to the system in question. This approach is based on a full description of flow fields and particle trajectories. However, all such approaches so far have been numerical simulations, and no deterministic models have yet been devised. The other approach is to describe the systems of interest using more intuitive physical models based on an understanding of the many features of air and particle transport. An example of the latter approach is what has become widely referred to as the "impaction" model. The impaction model describes the inertial forces that act on particles in the distorted airflow near a sampler entry, as a result of which the particles 'impact' into or out of regions of the flow field. Impaction models were first developed for thin-walled samplers facing the wind (Badzioch, 1959; Vitols, 1966; Davies, 1968; Voloschuck and Levin, 1968; Belyaev and Levin, 1974; Lipatov *et al.*, 1986; and others), where airflow into a thin-walled sampler was only minimally distorted by virtue of the very thin sampler wall. The general expression for aspiration efficiency for thin-walled samplers facing the wind is given by

$$A = 1 + \beta(R - 1) \tag{5}$$

which can easily be derived from physical arguments. Here β is the impaction efficiency and R is the ratio of freestream velocity (U) to sampling velocity (U_s), and the effect of gravity is neglected. It has been shown that β itself is a function of Stokes' number (St, embodying the effects of inertial forces) and R (Belyaev and Levin, 1974). This model was later developed to incorporate the effect of different sampler orientations relative to the wind (Durham and Lundgren, 1980; Tufto and Willeke, 1982; Vincent *et al.*, 1986; Hangal and Willeke, 1990).

Extensions of this approach were later developed to describe particle motion, and hence aspiration efficiency for the more complex flows associated with blunt samplers. Here the body of the sampler cannot be described as infinitesimally thin, so it plays a significant role over and above what is described by Equation (5). This new scenario has been described in a succession of modeling studies that set out to predict the ability of particles to follow the highly distorted streamlines, and in turn aspiration efficiency, for relatively simple blunt samplers (Vincent *et al.*, 1982; Vincent, 1987). Further extensions of this approach led to semi-empirical models that could be applied ultimately to personal samplers of the type used in practical occupational hygiene (Tsai and Vincent, 1993; Tsai *et al.*, 1995b; and Tsai *et al.*, 1996b). In all the empirical models described, from Belyaev and Levin onwards, the underlying rationale has been that,

while the general form of the equations contained in them are based on a sound understanding of the nature of the fluid and the particle dynamics, the equations themselves contained empirical coefficients that needed to be obtained by reference to experimental data. So, for example, whereas the 'classic' Belyaev and Levin model for thin-walled samplers contains just two empirical coefficients, by contrast the 1996 Tsai *et al.* model for personal samplers contains as many as 12 such coefficients. Such a large number of empirical coefficients suggests that the development of physical models for describing aerosol sampler performance, under for complex conditions like those pertaining to the real world, is still at a relatively early stage. It is therefore also clear that there is a continuing need to test samplers experimentally, to validate the samplers themselves and to improve the semi-empirical models. Much progress has been made toward these ends through the use of small wind tunnels and direct-reading instrumentation (Witschger *et al.*, 1998; Sreenath *et al.*, 1999; and Sreenath *et al.*, 2002), and the experience gained in these cited works has provided the starting point for much of what appears in this report.

Dimensionless parameters and scaling laws

It is a fundamental law of physics that any complete (dimensionally homogeneous) equation can be reduced to a functional relationship between a complete set of independent dimensionless products. Thus physical laws may be expressed in a form independent of the particular system of units employed in them (Pankhurst, 1964). Applying this principle to aerosol sampling, theoretical models that predict airflow into blunt aerosol samplers generally describe aspiration efficiency as a function of several dimensionless parameters that relate to both fluid and particle motion near the sampler (Vincent, 1989), thus

$$A = f(St, R, r, \alpha, B, \ldots\ldots) \qquad (6)$$

Here, St and R are as already defined, and r is the ratio of sampler orifice diameter to sampler or bluff body characteristic dimension, α is the orientation of the sampler with respect to the wind, and B is the sampler bluntness derived from the magnitude and shape of the aerodynamic blockage imposed by the sampler. In addition to these main factors, parameters such as the Reynolds number for the flow outside the sampler (Re_f) and the Reynolds number for the particle motion relative to the flow (Re_p) can be important under specific sets of conditions. And still others may include dimensionless groups to account for the effects of freestream turbulence, electrostatic forces and other relevant fluid mechanical effects. For Re_f and Re_p, in aerosol sampling research it has been customary to assume that changes in Re_f have little effect for the range of most conditions of practical aerosol sampling. Similarly, Re_p may be neglected over the range where particle motion relative to the air approximately follows Stokes' law. Regarding turbulence effects, the available evidence suggests that freestream turbulence has a weak effect over most of the ranges of conditions relevant to practical aerosol sampling (Vincent *et al.*, 1985).

The characterization of A in the manner indicated in Equation (6) provides an important starting point for the expression of scaling laws by which to relate the performances of sampling systems at full-scale and at small-scale respectively. Most studies in the past have utilized full-size mannequins and large wind tunnels to simulate workers' personal exposure to aerosols (e.g., Mark and Vincent, 1986; Vincent and Mark, 1990; Kenny *et al.*, 1997). These studies were

performed at great expense and effort, stemming largely from the difficulty in establishing uniform spatial and temporal aerosol concentration profiles inside the large wind tunnels. Many such problems may be resolved by using smaller wind tunnels provided that appropriate scaling between all the relevant variables can be carried out. For scaling, the ideal approach is to keep all the dimensionless variables – like those in Equation (6) – constant for the two systems in question. That is, assuming A is indeed solely a function of St, R, r, α and B, if these five dimensionless variables are kept constant for both small- and large-scale system, the resulting A of the samplers in each system should be the same.

Physical or dimensionless variable	***IOM sampler on life-size bluff body (full-scale)***	***Small-scale sampler on small bluff body (small-scale)***
Windspeed, U (m/s)	1	0.5
Sampling flowrate (L/min)	2	0.3
Orifice diameter, δ (mm)	15	8.2
Bluff body width, D (mm)	300	165
Sampling velocity, U_s (m/s) d_{ae} range (μm)	0.19 5 to 100	0.095 5.2 to 104.5
R	5.3	5.3
r	0.05	0.05
St range	0.005 to 2.02	0.005 to 2.02
α	averaged over 360°	averaged over 360°
B	equivalent for both systems	

Table 1

To illustrate the use of such scaling laws, Table 1 shows both the physical variables and dimensionless parameters for two physically-equivalent systems (as described in detail later). If R in the small-scale system were to be increased two-fold to close to 10, A would change by a certain value, as determined by experiment. Since the two-fold increase in R resulted in such a change in A in the small-scale system, a similar two-fold increase in R in the large-scale system should result in the same change in A as that in the small-scale system. Thus, experiments in the small-scale system would provide results applicable to the large-scale system, without requiring an actual experiment in the large-scale system.

Goals of the research

As stated earlier, the broad objective was to investigate the complex processes that determine the performance of aerosol samplers and apply what is learned to the design and validation of a prototype particle size-selective aerosol sampler. Toward these ends, semi-empirical models for predicting the aspiration efficiencies of aerosol samplers were developed or modified, first for the simple case of thin-walled samplers, then for blunt samplers and more complex personal samplers, gradually bridging the gap between idealized sampling systems and 'real-world' sampling systems. Based on the knowledge gained from these investigations, a practical goal of the research was to design a new, low-flowrate personal inhalable aerosol sampler to be used for industrial hygiene and environmental sampling applications.

The specific tasks of the research that were carried out in order to meet the objectives set at the beginning were as follows:-

- Determine the limit of detection (*LOD*) and limit of quantification (*LOQ*) of the gravimetric method for measuring the particulate material collected by aerosol samplers, for various IOM sampler cassettes and filters.

- Determine the effects of *St* and *R* on *A*, for sharp-edged, thin-walled samplers facing the wind, and improve an existing semi-empirical model that predicts their performances.

- Determine the effects of *St*, *R*, and *r* on *A*, for disc-shaped samplers facing the wind, and improve an existing semi-empirical model that predicts their performances.

- Determine the effects of *St*, *R*, and *r* on *A* for IOM samplers (original and modified) mounted on rotating bluff bodies.

- Determine the effects of *St* and *r* on *A* for blunt samplers mounted on rotating bluff bodies, for a wide range of *r*.

- Test a small-scale version of the IOM sampler in a small-scale sampler testing system and compare its aspiration efficiency with those obtained from full-scale sampler testing systems.

- Develop and validate a prototype low-flowrate personal inhalable aerosol sampler, both in the laboratory and in the field, by direct comparison with the IOM sampler.

This report describes how these tasks were executed and the results that were obtained.

2. Facilities and equipment

Small wind tunnel

Wind tunnels have been widely used in aerosol research. For general inhalation studies and for developing personal aerosol samplers, wind tunnels large enough to accommodate life-size mannequins have been typically used (e.g., Mark and Vincent, 1986; Hinds and Kuo, 1995; and Kenny *et al.*, 1997). By contrast, the wind tunnel used in the current research was much smaller, with a cross-sectional area of only 0.30 m × 0.30 m at the test section (see Figure 2). This had several advantages for the testing and development of aerosol samplers. Firstly, it was possible to achieve much better uniformity in spatial and temporal aerosol concentrations, which was necessary to obtain good reproducibility of aspiration efficiency data. Measurements of aerosol concentrations in our wind tunnel using a real-time dust monitor (Haz-dust II Real-time Personal Dust Monitor, SKC Inc., Eighty-four, PA) indicated mass concentration temporal and spatial variations of no greater than ±6%. A similar evaluation using isokinetic probes and gravimetry showed concentration variations less than ±5% along the central 0.15 m of the test section. By contrast, typical aerosol concentrations in the larger facilities referred to varied by as much as ±20% (Kenny *et al.*, 1997). Secondly, the small wind tunnel allowed tests to be conducted at

much lower cost, not only because small wind tunnels are generally less expensive, but also because much less aerosol needs to be generated. In addition, other associated costs (e.g., HEPA filters, air compressor, dust generator, etc.) are inevitably lower. Finally, the small wind tunnel is much more convenient in use, including its relatively easy cleaning, single (instead of multiple) aerosol injection points, etc. For these reasons,in recent years, many researchers have moved away from the need to use large wind tunnels (Witschger *et al.*, 1998; Sreenath *et al.*, 1999; Aizenberg *et al.*, 2000). Similar sentiments underlie similar work currently under way in Europe.

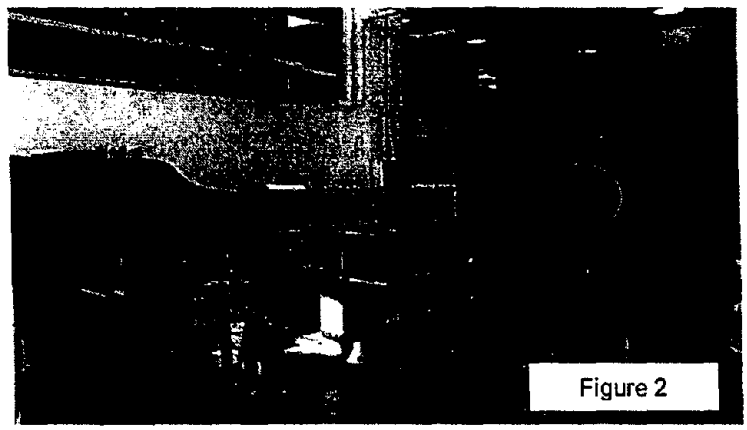

Figure 2

The small open-loop wind tunnel used in the current research was built by Engineering Laboratory Design (Lake City, MN), based on specifications required by this work and other related NIOSH-funded research. In this apparatus, air is drawn through an inlet plenum containing a HEPA (high efficiency particulate air) filter bank, passes through a honeycomb screen, and is accelerated through a 6.25:1 contraction before entering the test section. After passing through the test section, the air regains static pressure as it passes through a diffuser, and before discharge through another HEPA filter blank. Air motion is achieved by means of a tubular centrifugal fan located downwind of the test section. Aerosolized powders are introduced just upwind of the test section. A square-mesh grid is located just downstream of the aerosol injection point to faciliate the mixing of the injected aerosol and also to establish well-defined turbulence in the test section. Depending on the bar width, well-defined turbulence intensities and characteristic length scales are achieved at locations downwind of the grid (Baines and Peterson, 1951). In this work, a grid bar width of 0.84 cm and blockage of 31% produced turbulence intensity and length scale of about 5% and 2 cm, respectively, at a distance of 0.7 m downwind from the grid. The corresponding values 1.2 m from the grid were about 3.3% and 2.8 cm, respectively. A velocimeter (VelociCheck, Model 8330, TSI Inc., St. Paul, MN) was used to measure the velocity distribution across the width and height of the test section, with the turbulence grid in place. Velocity profiles were obtained 0.7 m and 1.2 m downstream of the grid (with thin-walled samplers in place), since these were the locations of the isokinetic and test samplers, respectively, in most of the experiments. For windspeeds up to 4 m/s (which covers the range of local windspeeds found in typical workplaces), the velocity across the height and width of the test section were found to vary by less than ±10%.

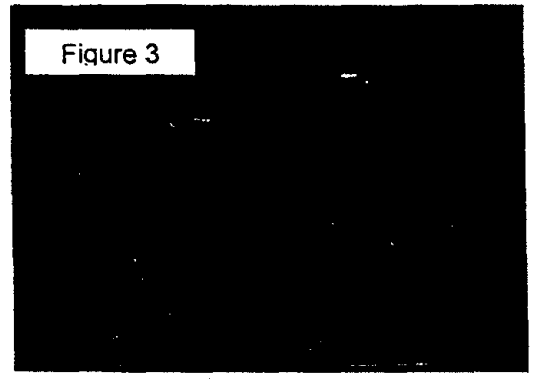

Aerosol generation

Aerosol generators: For the early pilot studies, a 'Reist' aerosol generator developed at the University of North Carolina (see Figure 3) was utilized. Its mechanism is similar to the turntable dust feeders used by others (e.g., see Vincent, 1989). This device consists of a vibrating, rotating dust cylinder that permits a reasonably steady delivery of dust to a turntable groove. An idler wheel keeps the dust cylinder in place while allowing it to rotate. The grooves are packed with dust and picked up by a manually height-adjustable aspirator connected to a supply of clean, dry compressed air. The air is passed through a venturi-type aspirator, and a wide range of dust pickup rates (on the order of several milligrams per second) is achieved by means of using different groove widths, groove locations, and turntable speeds. To determine the spatial and temporal uniformity of aerosol concentrations generated by this system, the Haz-Dust II Real-time Personal Dust Monitor was used (TSI Inc., St. Paul, MN). For the determination of spatial concentration variability, a thin-walled probe connected to the Haz-Dust II inlet was placed, in random order, at 8 evenly-spaced locations along the height and width of the wind tunnel. Spatial variability was calculated as the relative standard deviation (RSD) of the 8 probe measurements and it was determined to be about ±6%. Temporal variability in temporal concentration was calculated as the RSD of the real-time concentrations taken every second over a 4-minute duration, and was also determined to be about ±6%. Although this generator was able to produce a relatively constant output, there were some disadvantages to its use. It was bothersome to have to manually adjust the height of the aspirator before each experiment. Also, the vibration of the turntable caused large amounts of dust to escape the cylinder and never reach the grooves. For these reasons, an alternative aerosol generator was sought and found.

For the majority of the experiments, a Topas SAG (Solid Aerosol Generator) 410 (Topas GmbH, Dresden, Germany) was utilized (see Figure 4). This device consists of a powder reservoir and segmental feeding belt with defined constant small volumes. The feeding belt moves small proportions of the powder to an aspirating nozzle, similar to the one described for the Reist dust generator. A scraper is used to facilitate movement of the powder onto the feeding belt. The amount of aerosol being ejected is determined by adjustable knobs for both the speed of the belt and the speed of the scraper. We found that this aerosol generation system had improved stability over the Reist dust generator because the distance between the aspirator and feeding belt was kept constant by virtue of the aspirator design. In addition, the scraper allowed a steady movement of powder onto the belt, so vibration was not necessary. To evaluate the spatial uniformity of aerosol concentrations using this new generator, isokinetic probes were placed at two locations along the inner half of the wind tunnel test section (within which all the samplers

would be installed for all the experiments). The spatial difference in concentration for the two probes never differed by more than ±5% for the three particle sizes tested (d_{ae} = 13, 34 and 89.5 μm). Temporal stability was similarly good.

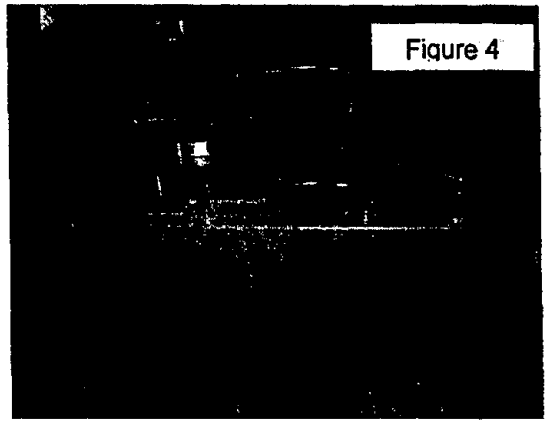

To reduce unwanted particle agglomeration, prior to each expeirment, the test powders were heated in an oven overnight at 80°C prior to aerosolization and a 300W infrared lamp kept the dust warm (to minimize moisture uptake) while the dust generator was operating. In the early experiments, a 2 mCi Kr^{85} neutralizer (TSI Inc., Model 3012, St. Paul, MN) was used in-line to neutralize the aerosol to Boltzmann equilibrium before injection into the dispersion chamber of the wind tunnel. However, its use was discontinued for the main body of the research. This was because the column of the neutralizer tended to collect significant amounts of particulate material, and so the material frequently – and inconveniently – needed to be removed and washed out. Nonetheless, to minimize any effects of particle charging, the dust generator, aerosol injection line and all sampling tubes were grounded.

The aerosol was introduced at the injection point in the direction opposite to the freestream flow, and a 0.15 m × 0.15 m mixing plate (as suggested by Stairmand, 1941) was placed just behind the injection nozzle to create enough turbulence to uniformly mix the dust.

Test powders

Two types of powders were used in the current research. Arizona road dusts (ARD) (Powder Technology, Burnsville, MN) were used to characterize sampler performance in the early experiments. Composed primarily of silicon dioxide, ARD was originally intended for use to test air filters to protect vehicle engines. Filter-testing has since been its most important application. The ARD used in the research was highly disperse and available in three grades – 'fine', 'medium' and 'coarse'. Based on Coulter-counter analysis (obtained from the supplier), the 'fine' grade had a geometric mean (GM) and geometric standard deviation (GSD) of 9 μm and 3.9, respectively. The 'medium' grade had a GM and GSD of 12.42 μm and 3.14, respectively, and the 'coarse' grade had a GM and GSD of 32 μm and 2.5, respectively.

For aspiration efficiency measurements as a function of particle size, narrowly-graded powders of fused alumina ('Duralum', Washington Mills Electrominerals, Manchester, England) were used. Such fused alumina powders have been widely used for aerosol studies since the 1980s

(Mark *et al.*, 1985). They are considered to be essentially 'monodisperse' (geometric standard deviation less than about 1.3) for the type of applications in the current research (Fuchs and Sutugin, 1966). The particular powder grades used throughout the research were the same as the ones originally used to produce aerosols calibrated by Mark *et al.* Other workers have used these same grades from the same supplier in their own research and confirmed that their more recent calibrations did not differ significantly from the original ones (e.g., L.C. Kenny, UK Health and Safety Laboratory, Sheffield, UK, personal communication). This was supported by information from the supplier that such 'optical grade' powders are manufactured to very high standards of quality assurance and consistency (see FEPA, 1993) by virtue of their primary industrial application as grinding powders. The data in Table 2 are based on photosedimentometer measurements from the manufacturer. The published specific gravity of Duralum (= 3.96), also obtained from the manufacturer, was used to calculate the particle aerodynamic diameters. Only the particle sizes used in the current research are presented. Comparison with the Mark *et al.* original calibrations (in parentheses) show that the powders were the same ones indeed. So, for the research described in this report, the Mark *et al.* original calibrations were used.

Grade designation	***Mass median sedimentation diameter (μm)***	***Mass median aerodynamic diameter (μm)***
F1200	3.0	6.0 (6.0)
F1000	4.5	9.0 (9.0)
F800	6.5	12.9 (13.0)
F600	9.3	18.5 (18.0)
F500	12.8	25.5 (26.0)
F400	17.3	34.4 (34.0)
F360	22.8	45.4 (46.0)
F320	29.2	58.1 (58.0)
F280	36.5	72.6 (74.0)
F240	44.5	88.6 (89.5)

Table 2

Bluff body apparatus

Many of the experiments required that the samplers be mounted on rotating bluff bodies to simulate how they would perform in actual workplaces. Because of the small cross-section of the wind tunnel, it was difficult to fit a turntable inside the test section, along with the bluff body and the sampling pumps that would need to rotate with the bluff body to prevent the tubes from tangling. Therefore, a method was devised to keep the pumps and turntable outside the test section, while allowing the bluff body and samplers to remain inside. A hole was drilled through the floor of the test section to accommodate a ¾-inch diameter wooden rod. Two ¼-inch stainless steel tubes were tapped into the sides of the rod and the ends of the tubes were bent at 45° angles away from the rod. Using elbows and screws, the bottom of the rod was attached to the center of the turntable and the top was attached to the bluff body. The bottom ends of the stainless steel tubes were connected to the sampling pumps with tygon tubing, and the sampling pumps were placed on top of the turntable. The top ends of the stainless steel tubes were connected to the test samplers with tygon tubing, and the samplers were attached to the bluff body using velcro. Thus, this apparatus was able to accommodate two samplers, one on each side of the bluff body, and each sampler was connected to its own pump through the stainless steel

tubes. In order to allow smooth rotation of the bluff body, teflon tape was tightly wound around the rod and PVC foam was wrapped around the tape to prevent dust from escaping the test section. The bluff body apparatus is shown in Figure 5.

Figure 5

Aerosol samplers and collection media

For the determination of total aerosol (reference) concentrations for most of the experiments, sharp-edged thin-walled probes (see Figure 6 below) were used under isokinetic conditions. For some of the experiments, where the performances of thin-walled probes were themselves the subject of investigation (see Section 5), the same probes were also used under anisokinetic conditions. Each such probe consisted of a cylindrical stainless steel tube, machined to have a sharp leading edge, and a 25-mm filter holder containing a glass fiber filter. A cone was placed around the filter holder to minimize aerodynamic blockage. Particulate material collected from the filter and inner tube wall were weighed separately using an electronic balance (Sartorius, Model MC201S, Sartorius Corporation, Edgewood, NY). In order to obtain the wall deposits, two 37-mm or 50-mm glass fiber filters (depending on the sampler orifice size) were pushed through the tube onto a third filter. The three filters were weighed together. By trial and error it was determined that this procedure provided consistently good recovery of the whole wall deposit. The sum of all the deposit obtained in this way and the mass collected on the primary 25-mm filter were used in the determination of aerosol concentration.

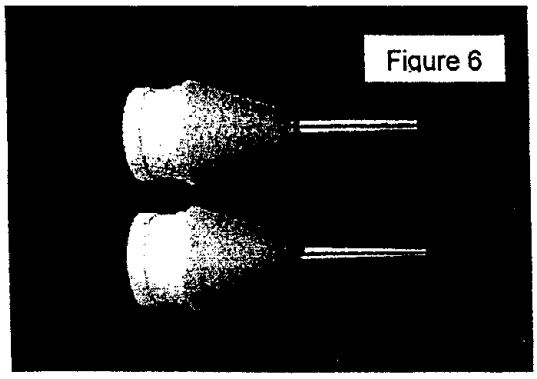

Figure 6

For the testing of blunt samplers, disc-shaped samplers and the personal samplers of interest were used. The disc-shaped samplers consisted of circular discs cut from cardboard that were placed around the tips of the thin-walled samplers (see Figure 7). The discs were located approximately 3 mm from the leading edge to minimize particle blow-off effects (as suggested by Mark and Vincent, 1986). The wall deposits were collected in the same manner as those used for the isokinetic and thin-walled samplers. IOM samplers were used for two primary purposes. First of all, they served as reference samplers for collecting the inhalable aerosol fraction. As mentioned earlier, the IOM sampler has received wide application in both research and industry, and has been shown in several studies to match the inhalable aerosol convention closely over a wide range of windspeeds relevant to workplaces. In the experiments, IOM samplers were usually mounted on bluff bodies (see above in Figure 5) to simulate their performances on actual workers in the field. In some cases, original versions of the IOM sampler also served as templates for the orifice adapters that were placed into their nozzles during the testing and design of new prototypes.

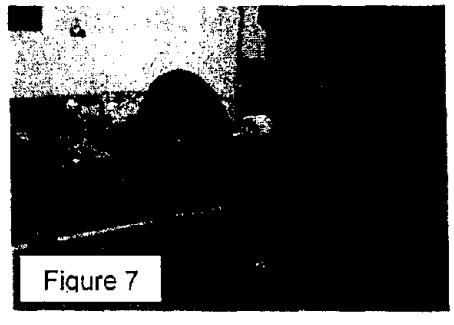

Figure 7

For the gravimetric analyses of samples, in the determination of aerosol concentrations glass fiber filters and stainless steel cassettes (where relevant) were chosen as representative sampling media for the majority of the research. Stainless steel cassettes are known to be much more stable, in terms of mass, than plastic cassettes (Smith *et al.*, 1998), and this was confirmed during the present research (see Section 3). Glass fiber filters were chosen because a comparison among various filters showed that glass fiber filters were optimal for sampling with 2 L/min (and lower-flowrate) sampling pumps due to their relatively low pressure drops. This combination produced very low mass variability and was therefore amenable to gravimetric analyses. For the field studies (see Section 9), however, both stainless steel and plastic IOM cassettes were used with MCE filters.

Analytical equipment

Gravimetric analysis (for the laboratory studies): The electronic analytical balance (Sartorius, NY, Model MC 210S) used for the gravimetric analyses in this research had a minimum readability of ±10 μg and a maximum tare weight of 210g. The high tare weight capacity of this balance enabled the filters and stainless steel cassettes to be weighed together on the balance, with sensitivity only weakly dependent on the tare weight (Mark, 1990). All the aerosol samples collected in the current laboratory-based research were in the milligram range or above. Thus the analytical balance was sufficient for the laboratory analyses. The balance was internally calibrated before every series of weighings and re-zeroed before each individual weighing. The

balance was also calibrated annually using the original equipment manufacturer's calibration procedures with weights traceable to the National Institute of Standards and Technology (NIST). In order to minimize the weighing imprecision of each measurement, all the samples were handled with teflon or metal forceps, and the samples were exposed to a Po-210 radioactive ion source to eliminate static electricity prior to weighing them. For the earliest experiments, the samples were initially desiccated and then conditioned overnight inside the balance room before each measurement. However, this was very time-consuming and labor-intensive. As described below in Section 3, it was found that the weighing imprecision of cassettes and filters was not significantly dependent on whether or not desiccation and conditioning had been carried out. This was because any changes in mass due to humidity could be corrected using blanks. Therefore, for the main bulk of the experiments, the samples were neither desiccated nor conditioned prior to weighing them.

Metal analysis (for the field studies, see Section 9): For the field studies, a lower *LOD* than what the balance could provide was required for sample analyses. This is because actual aerosol concentrations in the field would be much lower than that which was produced in the laboratory. Furthermore, the reduced flowrate of the prototype sampler would result in lower collected aerosol masses. In order to quantify these low mass concentrations accurately by a method other than gravimetric analysis, only the lead mass concentrations (and not the total aerosol masses) in the samples were quantified in the field studies. For the analysis of lead particulate, a Perkin-Elmer Model 3000DV (Perkin-Elmer Inc., Wellesley, MA) was used to quantify the samples, based on inductively-coupled argon plasma atomic emission spectroscopy (ICP-AES). The samples were analyzed for lead according to NIOSH Method 7300 (NIOSH, 1994), but where a microwave digestion procedure was used in lieu of the ashing technique. This enabled up to 24 samples to be prepared and analyzed on a given day. Lead masses could be quantified to the microgram level and this was therefore considered to be the most appropriate method for analyzing the field samples. All the metal analyses in this project were conducted in the Seoul National University (SNU) School of Public Health Industrial Hygiene Laboratory, with the participation of an experienced industrial hygiene technician. The Industrial Hygiene Laboratory at SNU participates in the inter-laboratory Proficiency Analytical Testing (PAT) program organized by the U.S. National Institute for Occupational Safety and Health (NIOSH) and the American Industrial Hygiene Association (AIHA).

In summary, the experimental procedures used throughout the whole course of the research were able to deliver highly reliable and consistent results.

3. Determination of the *LOD* and *LOQ* for gravimetric assessment of IOM samples

Background

In environmental air sampling, gravimetric analysis refers to a method by which the mass of an isolated sample of a substance is determined using an analytical balance. Typically, it involves weighing a sampling substrate before and after it is exposed to the environment in question, and calculating the difference that is associated with the collected material. For the assessment of airborne particulates in industrial settings, it is a common practice to aspirate air from a worker's breathing zone using a personal sampling pump and collect the aerosols onto a filter inside a

sampling head appropriate to the desired aerosol particle size fraction. This mass is then compared to the volume of air sampled to obtain an estimate of the aerosol mass concentration in the air for the fraction in question. In order to obtain an accurate measure of the collected mass, the mass must be significantly greater than the background variability of a blank sample that is analyzed according to the specific methodology employed.

In the gravimetric assessment of workplace aerosols, there is an increasing need to measure smaller and smaller collected masses. This is because lower concentrations of aerosol are now present in many workplaces, largely driven by the trend towards lower OELs. This trend is expected to continue as researchers gain more knowledge about the adverse health effects of various occupational aerosol exposures. Further, the desirability of using very light, low-flowrate sampling pumps for some aerosol sampling situations underlines the need to be able to accurately measure small collected particulate masses (Vincent *et al.*, 1999).

In order to accurately measure a small collected mass, it is important to know the *LOD* and *LOQ* of the measurement method used. These define the envelope for the practical implementation of gravimetric sample analysis. In most industrial hygiene situations, the *LOD* is defined as "*. . a stated limiting value designating the lowest concentration that can be detected and that is specific to the analytical procedure used . . .*" and the *LOQ* is "*. . a stated limiting value designating the lowest concentration that can be quantified with confidence and that is specific to the analytical procedure used. .*" (DiNardi, 1995). The *LOD* and *LOQ* can also be defined more simply in terms of collected particulate mass, instead of concentration. Assuming there is little variability in the mass of particulate once it has been collected, the *LOD* and *LOQ* are determined by the weighing imprecision of blank samples, determined through a series of weighings in a method evaluation (American Society of Testing and Materials, 2000). The instability of blank samples may be due to a number of factors, most notably moisture adsorption, but also electrostatic effects and handling damage. These need to be minimized or corrected in order to obtain low *LOD* and *LOQ*-values. The balance itself may also contribute to weighing imprecision, but its instability can be minimized by regular calibration to NIST (National Institute of Standards and Technology) standards.

Of particular interest in the current research and in industrial hygiene practice in general is the measurement of inhalable aerosols, as defined nowadays for many substances in the ACGIH list of TLVs, as well as in lists of OELs promulgated by a number of regulatory standards-setting bodies around the world. Here, as already mentioned, inhalable aerosol is defined as that fraction of airborne particles that may enter through the nose and/or mouth during breathing, for which one popular method is the use of a filter contained within a small cassette, as in the IOM sampler. As mentioned earlier, both the filter and the whole cassette assembly are weighed prior to and after sampling. While this method eliminates concerns about wall and inlet losses, since these are explicitly built into the measurement method, data assembled from field studies (NIOSH, 1996, cited by Smith *et al.*, 1998) have suggested that there is considerable mass variability in the cassettes themselves. The standard deviation of blank plastic cassette masses from the field studies was found to be an order of magnitude greater than that obtained for glass fiber filters in the Vaughan *et al.* (1989) study (0.19 mg versus 0.0167 mg, for measurements with an analytical balance of 10 μg readability). In response, Smith *et al.* set out to investigate the mass stability of plastic and stainless steel IOM cassettes containing glass fiber or PVC

filters. They found that when plastic cassettes were exposed to dry conditions inside a desiccator, their masses were reduced by as much as 1.5 mg in 4-5 days, and when they were subsequently left out in the weighing environment, their masses showed a similar rate of increase. Stainless steel cassettes, however, were mass-stable under conditions of both desiccation and room humidity. In later studies, Li and Lundgren (1999) and Lidén and Bergman (2001) reached similar conclusions about the amount of moisture lost or adsorbed by plastic IOM cassettes. To counteract the biases in plastic IOM cassettes, Smith *et al.* analyzed their data in fixed pairs of cassettes (with each cassette in a pair exposed to the same environmental conditions) to estimate sample accuracy when field blanks are used to correct samples. They calculated standard deviations in the weight differences for each pair, resulting in standard deviations of 0.013 mg and 0.009 mg for the plastic and stainless steel cassette assemblies, respectively.

While these standard deviations demonstrated the efficacy of correcting samples with field blanks, they were not determined from a method evaluation intended to represent standard deviations that would be obtained from actual field or laboratory blanks, as described in the new ASTM standard (ASTM, 2000). Therefore, it would be inappropriate to use these values as representative measures of weighing imprecision. The purpose of this part of our investigation, therefore, was to determine the magnitude of filter and cassette weighing imprecision, and hence *LOD* and *LOQ*, during instances when samples are collected and analyzed under typical laboratory conditions, using the ASTM method-evaluation guidelines. These values would be directly useful for most of the current research since all the laboratory samples collected from the wind tunnel studies were analyzed by the gravimetric method. In addition, the values would provide important information for the practicing industrial hygienist, since they should be close approximations of the *LOD* and *LOQ* that would be obtained from actual field studies, assuming that the samples are carefully transported to a laboratory for analysis.

The *LOD* and *LOQ* in this study were determined for an analytical procedure that involves weighing the sample masses within 1 to 2 days following exposure under relatively stable conditions (i.e., the samples were carefully transported to and from a wind tunnel laboratory and balance room and conditioned to the balance room environment before weighing). However, there may be instances in real-life occupational hygiene situations when a longer time between weighing samples before and after exposure is required or it is not possible to follow a strict analytical protocol. This may be applicable to situations when samples are collected in the field but analyzed days or weeks later in a laboratory. In these cases, it is less likely that a field blank correction, which is a required step in the analytical procedure, would be able to account for all the possible biases, since there is more opportunity for environmental changes. Probably the most important source of bias would be changes in humidity, or constant exposure to high or low humidity. Since desiccation is an easy means to expose sampling media to constant low humidity, a second experiment was conducted to determine the effect of desiccation on mass for various sampling media.

All these experiments complemented and extended the work reported earlier by Vaughan *et al.*, Smith *et al.* and Li and Lundgren. The results consolidated the body of useful information by which industrial hygienists may clearly identify the ranges of possibilities for the gravimetric assessment of collected inhalable particulate matter.

Theoretical framework

According to the ASTM standard for weighing collected aerosols (ASTM, 2000), weighing imprecision, s_w^2, is defined as

$$s_w^2 = s^2 \cdot (1 + 1/N_b), \tag{7}$$

such that s^2 is an estimate of the uncorrelated variance associated with each mass difference measurement (which requires two balance readings) and the term $1/N_b$ reflects the fact that sampled masses are more accurately determined by correcting them with the average of multiple blanks (N_b is the number of blanks). The variance of mass **difference** measurements is calculated because all gravimetric samples are determined as a difference between their masses before and after exposure. Equation (7) implies that at least one blank per batch is used for correction and that, when one blank is taken, $s_w^2 = 2s^2$.

If σ_w is the **actual** weighing imprecision (of which s_w is only an estimate), and it were known exactly, *LOD* would ideally be defined as (ASTM, 2000)

$$LOD \equiv \Phi^{-1}[1-\lambda] \cdot \sigma_w \tag{8}$$

where

$$\sigma_w^2 = \sigma^2 \cdot (1 + 1/N_b) \tag{9}$$

corresponding to Equation (7). Here Φ is the cumulative normal function, Φ^{-1} is the inverse function of Φ, and σ_w^2 is the actual variance of the sample. When a given measurement exceeds the *LOD*, this indicates the true presence of mass, with a false positive rate of λ (from 0 to 1). For example, if σ_w were known exactly to be 50 μg, only 5% of sample masses would exceed 82 μg if the true mass sampled were zero. This is known by referring to a table of standardized normal curve areas and finding the z-value corresponding to the area between 0 and z equal to 45% of the total area under the normal curve (Mendenhall and Beaver, 1994). The z-value ($= \Phi^{-1}[0.95]$) in this case is 1.645, so that 50 μg × 1.645 = 82 μg. However, since σ_w cannot be known exactly, it needs to be estimated. One way to do this is to use $\chi^2 = \nu \cdot s_w^2 / \sigma_w^2$, which follows a chi-square probability distribution. This type of probability distribution is appropriate here because variance estimates (s_w^2) are typically non-symmetric and dependent on sample size and actual variance (σ_w^2). The quantity ν designates the number of degrees of freedom determined from the sample size. In the present investigation, mass differences were obtained for six substrates in each batch and the variances from each batch (s_b^2) were averaged to give the value s^2 as a variance over all the batches. This results in $(n\text{-}1)\cdot B_n$ degrees of freedom, where n is the number of substrates per batch and B_n is the number of batches. The quantity s^2 was then plugged into Equation (7) to obtain s_w^2, and hence s_w. If we assume a chi-square probability distribution, where, at the 95% (i.e., 1-γ; γ=0.05) confidence level, the single-sided confidence limit on σ_w, based on $\nu = 25$ (e.g., 6 substrates and 5 batches) is $\sigma_{w1-\gamma}$ then

$$\chi_{1-\gamma,25}^2 = 25 \cdot s_w^2 / \sigma_{w1-\gamma}^2. \tag{10}$$

Referring back to Equation (8) we get

$$LOD_{1-\gamma} = \Phi^{-1}[1-\lambda] \cdot [25/(\chi_{1-\gamma,25}^2)]^{1/2} \cdot s_w. \quad (11)$$

In this, $\chi_{1-\gamma,25}^2$ is available from standard statistical tables and found to be 14.61. So

$$LOD_{1-\gamma} = \Phi^{-1}[1-\lambda] \cdot [25/(14.61)]^{1/2} \cdot s_w \rightarrow \Phi^{-1}[1-\lambda] \cdot 1.31 \cdot s_w.$$

If LOD is defined as $3s_w$, as it typically is, then

$$\Phi^{-1}[1-\lambda] \cdot 1.31 = 3$$

The z-value is 2.29, which corresponds to an area under the normal curve equivalent to 48.90% of the total area. This corresponds to a λ-value of 1.1%. Therefore, when a sample mass exceeds the LOD, we can state with 95% confidence that the mass is present, with a false positive rate of just 1.1%.

Again, if σ_w were known exactly, the LOQ would be defined as (ASTM, 2000)

$$LOQ \equiv \sigma_w / CV_{max} \quad (12)$$

where CV_{max} is the maximum relative error acceptable in a quantification. For example, if σ_w were exactly known to be 50 µg and CV_{max} was set at 10%, the LOQ would be 500 µg. Applying this to Equation (10), this gives

$$LOQ_{1-\gamma} = [\{25 / (\chi_{1-\gamma,25}^2)\}^{1/2} \cdot s_w] / CV_{max}. \quad (13)$$

When LOQ is defined as $10s_w$ where, as before, s_w is an estimate of σ_w, then we have

$$CV_{max} = [\{25 / (\chi_{1-\gamma,25}^2)\}^{1/2}] / 10 = 13\% \quad (14)$$

This means that, when a given measurement exceeds the LOQ (= $10s_w$), we may state with 95% confidence that the maximum relative error is ±13%. It is therefore important to note that, in order to quantify the amount of particulate in a sample with the precision specified above, the sample mass needs to exceed the LOQ, and not simply the LOD.

Assessment of LOD and LOQ for IOM sampler cassettes and filters

Plastic and stainless steel IOM sampler cassettes (see Tables 3 and 4 below) were analyzed by weighing them in combination with three different filter types. Nickel-plated plastic cassettes were analyzed in combination with glass fiber filters. The chosen filters are all commonly used for air sampling in occupational hygiene applications. All the weighings were carried out using the electronic balance already mentioned, with readability to ±10 µg. Prior to the weighings, the balance was calibrated using the original equipment manufacturer's calibration procedures with

weights traceable to the National Institute of Standards and Technology (NIST). In order to assess the *LOD* and *LOQ* for various cassette and filter combinations, the method evaluation suggested by the recent ASTM standard was adopted. In what follows, the combined filter/cassette assemblies will be referred to as "substrates".

Filters	***Cassettes***
25 mm GF/A filter from Whatman, Inc.	IOM sampler plastic cassette
25 mm silica-free PVC† filter from SKC Inc.	IOM sampler stainless steel cassette
25 mm teflon filter from SKC Inc.	IOM sampler nickel-plated plastic cassette

*Glass fiber A-type
†Polyvinyl chloride

Table 3

Abbreviation	***Cassette type***	***Filter type***
PG	Plastic	*GF/A*
NG	Nickel-plated plastic	*GF/A*
SG	Stainless steel	*GF/A*
PP	Plastic	*PVC*
NP	Nickel-plated plastic	*PVC*
SP	Stainless steel	*PVC*
PT	Plastic	*Teflon*
NT	Nickel-plated plastic	*Teflon*
ST	Stainless steel	*Teflon*

Table 4

The filters were initially exposed to a Po-210 source (to eliminate static electricity) before placing them into their respective cassettes. Then they were desiccated overnight in a chamber containing indicating silica gel at approximately 20% relative humidity. Apart from handling them during initial cassette assembly, the filters were never handled again directly. Each batch consisted of six substrates, and a total of five batches were weighed on separate days, or on separate times during the same day. After initial desiccation, individual batches were conditioned for 8 to 12 hours in the balance room environment, weighed, transported, and exposed for one hour (the duration of a typical sampling session in the laboratory) to the wind tunnel laboratory environment, reconditioned to the balance room environment, and then reweighed. Balance readings were taken after 30 seconds of stabilization and substrates were handled with metal forceps and latex gloves. In order to eliminate mass deviations arising from electrostatic effects, substrates were always exposed for a few seconds to the Po-210 source before weighing them. For the duration of this experiment, the temperature of the balance room was relatively constant at 21 to 22° C. The relative humidity (RH) of the balance room ranged from 16 to 22% (the measurements were taken during the winter when the relative humidity was low). The wind tunnel temperature and RH varied from 17 to 20° C and 24 to 27%, respectively.

The changes in mass were recorded for substrates in each batch, and intra-batch variances were calculated from these mass differences. To determine the overall standard deviation for each substrate type, the intra-batch variances pooled from the five batches were averaged. This

method of using pooled intra-batch variances as the basis for determining the standard deviation, and hence the *LOD* and *LOQ* of each substrate type, largely eliminates the biases (i.e., changes in mass) that may result from moisture adsorption, desiccation, or other ambient effects. This is because intra-batch variances do not reflect actual changes in mass, which are corrected for separately by using blanks (in an actual exposure assessment), but simply reflect the deviations in mass among substrates within each batch. As such, no consistent correlation was found between intra-batch variances and the wind tunnel temperature, the balance room temperature, the wind tunnel RH, or the balance room RH.

The standard deviation calculations for all substrate types were expressed using one more significant figure than the mass differences on which they were based, according to convention (Parratt, 1961). Based on these standard deviations, the *LOD* and *LOQ* were calculated and tabulated (see Table 5). The results show that the differences in mass stability among the various cassette and filter media tested are relatively small. However, a few observations can be made. For both plastic and stainless steel cassettes, Teflon filters used in combination with them yield the lowest *LOD* and *LOQ* compared to the other filters. On the other hand, glass fiber filters, used in combination with all three types of cassettes, generally yield a higher *LOD* and *LOQ*. Nickel-plated plastic cassettes do not seem to provide improved stability over the plain plastic cassettes, although only one comparison is available.

	NG	PG	PT	PP	SG	ST	SP
LOD (mg)	0.16	0.16	0.13	0.17	0.20	0.12	0.13
LOQ (mg)	0.54	0.55	0.44	0.58	0.67	0.40	0.42

See Table 4 for list of abbreviations.

Table 5

Effect of reduced humidity on substrate mass variability

For this experiment, three of each type of substrate were analyzed and labeled according to Table 3. The substrates were desiccated in a chamber maintaining a relative humidity of approximately 20%. The substrates were weighed every 8 to 12 hours and always replaced into the desiccator when they were not being weighed. The duration of desiccation was approximately one week. It is generally known that 8 to 12 hours of desiccation between weighings is sufficient for the filters in the current study to reach a stable "dry" mass. Therefore, any significant change in mass over time would be attributable to the cassettes themselves.

The temperatures of both the balance room and desiccator were relatively constant at 21 to 23° C throughout the experiment. However, the RH in the balance room varied from about 30 to 60% (these mass measurements were taken during the summer), compared to the initial RH readings inside the desiccator (recorded at the beginning of each weighing session), which ranged from 21% to 23%.

The substrates utilizing plastic cassettes and nickel-plated plastic cassettes show consistent steady decreases in mass for surprisingly long periods as they were desiccated (see Figures 8 and

9 below). While it appears that the plastic cassette substrates stabilized at day 3, their masses decreased again after day 4. Stability was not reached, even after six days. The apparent initial stabilization is probably due to the higher balance room RH recorded during days 3 to 5, which may have resulted in readings higher than those expected from the trend of the curve down to that point (substrates were taken out of the desiccator briefly for weighing, during which they were exposed to the balance room humidity). The masses of nickel-plated plastic cassettes do however seem to have stabilized after about three days, and through the sixth day. From these results, it is immediately clear that there is a real bias induced by the desiccation for both plastic and nickel-plated plastic cassette substrates.

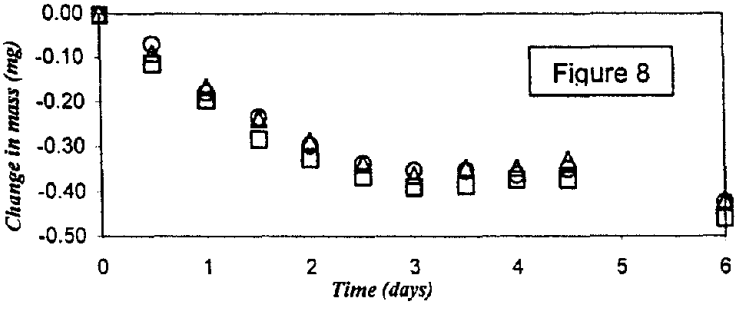

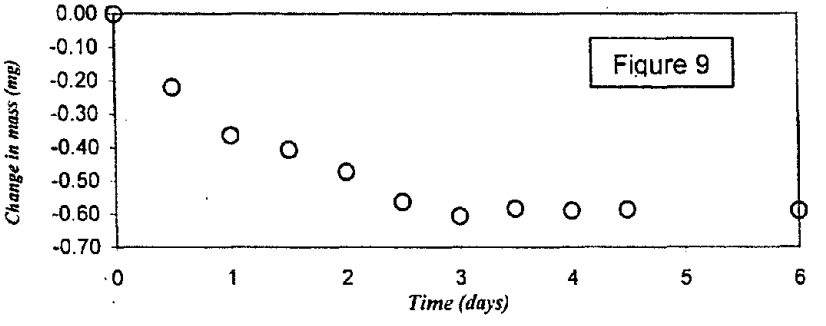

For the plastic substrates with PVC and glass fiber filters, the overall change in mass from day 0 to day 6 ranged from –0.38 to –0.49 mg (see Table 6).

Substrate type	*Total change in mass (mg)*
PP_1	-0.45
PP_2	-0.41
PP_3	-0.40
PG_1	-0.41
PG_2	-0.47
PG_3	-0.49
PT_1	-0.45
PT_2	-0.43
PT_3	-0.38

Table 6

For nickel-plated plastic cassettes with glass fiber filters, the situation is similar, with mass changes in the range from –0.54 to –0.64 (see Table 7)

Substrate type	*Total change in mass (mg)*
NG_1	-0.54
NG_2	-0.59
NG_3	-0.64

Table 7

By contrast, the situation is much better for stainless steel cassette substrates, as expected from the Smith *et al.* study. These substrates had relatively stable masses that varied in both positive and negative directions without obvious bias (see Figure 10). They did not show any systematic decrease or increase in mass. Their overall change in mass from day 0 to day 6 ranged from –0.04 to +0.05 mg (see Table 8), approximately ten times smaller in magnitude than that for plastic and nickel-plated plastic cassette substrates.

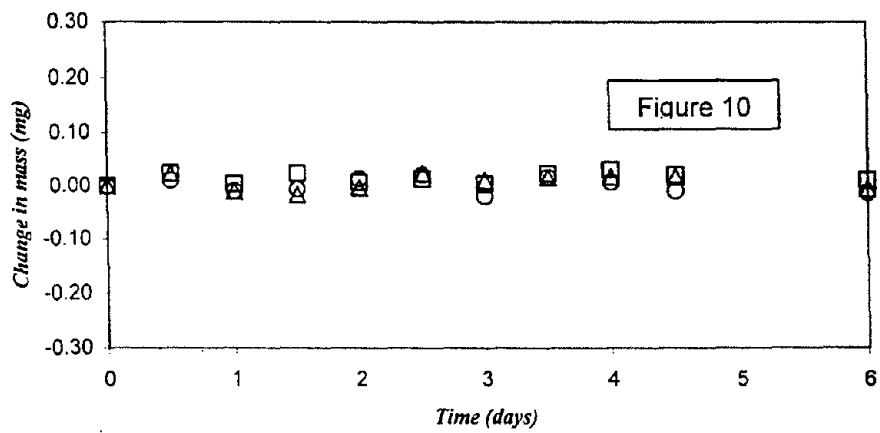

Substrate type	*Total change in mass (mg)*
SP_1	0.03
SP_2	-0.03
SP_3	-0.04
SG_1	0.05
SG_2	-0.02
SG_3	0.00
ST_1	0.00
ST_2	0.01
ST_3	-0.03

Table 8

Discussion and interpretation

In this part of the research, different combinations of widely-used inhalable aerosol sampling filters and cassettes were analyzed. The observed measures of weighing imprecision were used to

determine their respective *LOD* and *LOQ*-values, and these values provided a useful comparison of the limits of sampling performance across different sampling media. The *LOD* and *LOQ* determined for the various substrates suggested only small differences in weighing imprecision. While teflon filters seemed more stable than glass fiber filters, no cassette type had a clear advantage over the others. But regardless of the type of cassette or filter used, an *LOD* equal to or lower than 0.20 mg and an *LOQ* equal to or lower than 0.67 mg can be expected.

Probably more important than the type of cassette or filter used is the method employed in performing the analysis. The method described in this study assumed that samples would be analyzed within 1 to 2 days of exposure and that two blanks would be used to correct each sample, as recommended by NIOSH Method 0500 (NIOSH, 1994). By assuming that these blank corrections would largely eliminate the biases resulting from each substrate type's unique response to ambient conditions (most notably humidity), the *LOD* and *LOQ* were primarily based on the uncorrectable environmental instabilities associated with each substrate type. Therefore, it makes sense that the *LOD* and *LOQ* were comparable across the different substrate types, even if they were to differ significantly in their response to ambient conditions, this being largely accounted for by correcting with blanks.

One way to lower the *LOD* and *LOQ* would be to use several blanks. For example, if three blanks were used for each batch instead of two, the *LOD* and *LOQ* for nickel-plated plastic substrates would fall to 0.15 and 0.51 mg, respectively, instead of 0.16 and 0.54 mg. If ten blanks were used per batch, the *LOD* and *LOQ* would be further reduced to 0.14 and 0.46 mg, respectively. The *LOD* and *LOQ*-values that would result from using three and ten blanks per batch are shown in Table 9. However, using multiple blanks can only lower the *LOD* and *LOQ* to a certain extent, since they simply improve how accurately the blanks account for the variability that is correlated among all the substrates of a specific type.

No. of blanks		*NG*	*PG*	*PT*	*PP*	*SG*	*ST*	*SP*
3	LOD (mg)	0.15	0.16	0.12	0.16	0.19	0.11	0.12
3	LOQ (mg)	0.51	0.52	0.41	0.55	0.63	0.38	0.40
10	LOD (mg)	0.14	0.14	0.11	0.15	0.17	0.10	0.11
10	LOQ (mg)	0.46	0.47	0.37	0.50	0.57	0.35	0.36

Table 9

In the second experiment, the actual loss in mass for plastic cassettes was seen to be smaller in magnitude than reported by Smith *et al.* (1998). However, these two sets of results do not contradict one another since Smith *et al.* recorded cassette masses over a longer period of time (53 days) and the plastic cassette substrates in the current study did not reach a stable mass. For plastic and nickel-plated plastic cassettes, a blank correction would be much more important than for stainless steel cassettes under these circumstances. Plastic and nickel-plated plastic cassettes would be subject to greater potential error, proportional to the magnitude of the blank correction. Therefore, in situations where a longer time (i.e., more than 1 to 2 days) is required between collecting samples and analyzing them, or a less strict analytical protocol is followed, only stainless steel cassettes would be expected to yield accurate measurements of sample mass.

Conclusions from this part of the research

This study took a close look at the gravimetric method for aerosol sample analysis and provided estimates of the *LOD* and *LOQ* for several sampling substrates of the type widely used for collecting inhalable aerosols. Additional studies on the effect of particulate masses on sample variability would further elucidate these lower limits.

The comparison of the *LOD* and *LOQ* for various substrates showed that only minor differences existed between them. In each case, sample masses equal to or higher than 0.20 mg could be confidently detected and sample masses equal to or higher than 0.67 mg could be confidently quantified. These values were similar to those determined by Lidén and Bergman (2001) (they calculated an *LOQ* of 0.50 mg). The new values showed that, by correcting samples with field or laboratory blanks (depending on the application), it is not necessary to store samples for a one-week duration in a temperature and humidity-controlled weighing room before and after weighing, as recommended by Lidén and Bergman, in order to obtain good weighing precision. In practical terms, if a sample were taken over an 8-hour working shift at the flowrate of 2 L/min required in the use of the IOM sampler, the confidence in exposure concentration measurements would decrease steadily in the range from about 0.7 mg/m^3 down to about 0.2 mg/m^3. At this lower point, the collected mass would barely be detected let alone accurately quantified. This has several implications about the utility of the gravimetric method. Many TLVs established by the ACGIH have inhalable particulate values less than 1 mg/m^3 (e.g., insoluble and soluble nickel compounds, cadmium compounds, etc.). If an industrial hygienist were to use gravimetric analyses to assess worker exposures to aerosols that are of the order of 1 mg/m^3 or less, these estimates would fall somewhere near or between their *LOD* and *LOQ*. In other words, a majority of the samples would not be accurately quantified (the relative error may be greater than the maximum allowable, defined during the calculation of the *LOQ*). In addition, as TLVs (and OELs generally) are increasingly lowered, as they inevitably will be, the ability to gravimetrically quantify worker exposures will be even further diminished. Moreover, any reduction in sampling flowrate, as proposed in the present research, would result in the collection of even lower sample masses. It is therefore imperative that analytical methods with much greater sensitivity than the gravimetric method be developed and used. Two such methods are inductively-coupled plasma mass spectrometry (ICP-MS) and ICP-AES, which can analyze metals at nanogram and microgram levels, respectively. These should be the preferred methods in the future, at least for the measurement of inhalable metal aerosols (Vincent *et al.*, 1999). The ability to quantify small particulate concentrations will continue to be a significant challenge for occupational hygiene science and the practicing industrial hygienist.

Finally, in summary, this part of the research has established a firm foundation for the analysis of samples that would be collected throughout the present research wherever the gravimetric analytical method is used. It provides the necessary guidance in determining the appropriate amount of aerosol that needed to be generated in future experiments and for what duration.

4. A preliminary investigation of the effect of sampling flowrate

Background

The Tsai *et al.* (1996b) semi-empirical model for the aspiration efficiencies of personal aerosol samplers predicts that a 20-fold reduction in flowrate for an IOM sampler does not change its A significantly when mounted on a full-size mannequin. This is a somewhat surprising prediction. But if it were true the IOM sampler itself, without any modifications, would be sufficient as part of a lightweight sampling system, since it would be able to collect the inhalable aerosol fraction using a much smaller sampling pump. However, because the model contains several empirical coefficients fit to a limited set of experimental data, it is questionable whether the model would hold for the large values of R corresponding to a low-flowrate version of the IOM sampler. Nonetheless, the purpose of this preliminary experiment was to determine whether or not an IOM sampler operating at a very low flowrate of 0.1 L/min would indeed collect the same aerosol mass concentration as another IOM sampler running at the recommended flowrate of 2 L/min.

Experimental methods

Mass concentrations of aerosolized Arizona road dust (ARD) powders were measured using two IOM samplers, with pumps sampling air at 2 L/min and 0.1 L/min, respectively. Mass concentrations were measured for different aerosol coarseness levels and windspeeds. There were a total of 9 sets of conditions, executed randomly, with three repeats of each condition. The different sampling conditions are shown in Table 10.

1. $U = 0.5$ m/s Dust grade: coarse	2. $U = 0.5$ m/s Dust grade: medium	3. $U = 0.5$ m/s Dust grade: fine
4. $U = 1.0$ m/s Dust grade: coarse	5. $U = 1.0$ m/s Dust grade: medium	6. $U = 1.0$ m/s Dust grade: fine
7. $U = 2.0$ m/s Dust grade: coarse	8. $U = 2.0$ m/s Dust grade: medium	9. $U = 2.0$ m/s Dust grade: fine

Table 10

The duration of each sampling trial was approximately 30 minutes, and a total of 27 trials were conducted. In order to compare the performances of the two samplers, the ratios of their mass concentrations were calculated. The IOM samplers were mounted on each side of a miniature bluff body (see earlier Figure 5), since it was not possible to fit a life-size mannequin inside our small wind tunnel. This approach was taken in consideration of studies carried out by Witschger *et al.* (1998) and Aizenberg *et al.* (2000) suggesting that using a smaller-than-full-size bluff body did not change sampler performance significantly. The bluff body was rotated at a constant slow rate of 2 revolutions per minute (rpm). The ARD powders were aerosolized using the Reist dust generator described earlier.

Results

Results from the experiment indicate that the IOM sampler, running at 0.1 L/min, collected very different mass concentrations than the IOM sampler running at 2 L/min (see Table 11 for the

ratios expressed as $cIOM_2/cIOM_{0.1}$). In general, the two samplers are closer to unity for finer particles and lower windspeeds. The *LOD* and *LOQ* were determined from the method described in the previous section, except that the paired mass differences were based on actual dust samples, rather than blanks. The resulting *LOD* and *LOQ* were found to be 0.16 and 0.53 mg, respectively. The range of masses collected was 0.43 to 43 mg, and only one mass measurement was below the *LOQ*.

	U = 0.5 m/s	U = 1.0 m/s	U = 2 m/s
Coarse	0.585	0.374	0.238
	0.625	0.403	0.097
	0.630	0.318	0.139
Medium	0.843	0.403	0.223
	0.738	0.374	0.189
	1.010	0.480	0.247
Fine	0.797	0.652	0.202
	0.782	0.700	0.178
	0.900	0.375	0.164

Table 11

Discussion and interpretation

A least-squares multiple linear regression analysis, using SAS (Statistical Analysis System, Cary, NC), was conducted to see how dust grade and windspeed affected the concentration ratio of the 2 L/min IOM sampler and 0.1 L/min IOM sampler. Both dust grade and windspeed had a significant effect ($p < 0.05$) on concentration ratio, with a combined adjusted R^2-value of 0.82. Windspeed, however, had a much greater effect, as evidenced by its larger (in terms of magnitude) regression coefficient (-0.370). The regression coefficient for dust grade was –0.075. The negative sign on the regression coefficients for both dust grade and windspeed indicated that the concentration ratio was inversely proportional to both dust grade and windspeed. The *LOD* and *LOQ* calculated for dust loadings up to 43 mg were only slightly higher than those calculated for blank glass fiber filters. This indicated that the dust loadings did not contribute much to overall filter and cassette mass instability.

The most likely reason for the departure from unity when comparing the two samplers was the difference in velocity ratio, *R*, for the two samplers. For an IOM sampler operating at 2 L/min, the *R*-value is 5.3 when $U = 1$ m/s. However, for an IOM sampler operating at 0.1 L/min, the *R*-value is 106, again assuming that $U = 1$ m/s. For higher windspeeds, the difference in *R* would be even greater. As mentioned earlier in this report, it is well known that the aspiration efficiencies of samplers are largely dependent on *R* . Thus, it is not surprising that such a large difference in *R* would significantly affect *A* for the two samplers.

What was immediately clear from the results was that the Tsai *et al.* model predictions were not accurate for the large range of *R* tested in these experiments. In fact, upon closer examination of the basis of the model, the range of *R* tested in the experimental data set upon which the model was based was found to be in the range only from 0.2 to 14. By contrast, in the current experiments, the range of *R* was from 2.7 to 212. Clearly, the model was not designed to accommodate such large values of *R*.

Conclusions from this part of the research

This study represented the first of a series of wind tunnel studies in this body of work aimed at investigating the sampling characteristics of aerosol samplers. It demonstrated the importance of backing up theoretical sampler predictions with carefully executed experiments. The study addressed the basic question of whether the flowrate of a sampler plays a large role in determining its performance. It was found that the sampling flowrate and windspeed, both embodied in the dimensionless variable R, play a vital role, as does the size of the particles being sampled. Above all, the study pointed to the need to better characterize the performance of samplers at large values of R, especially since – as it has become clear – existing models are not able to accurately predict the effects of R at these large values.

In summary, this part of the research showed that it was possible to obtain meaningful results in the new experimental system, and it pointed to the important role of R in determining aspiration efficiency. This characterization would be an important theme throughout the research (see below), leading to development of a practical sampler with desired performance characteristics.

5. Aspiration efficiency for thin-walled nozzles facing the wind at high velocity ratios

Introduction

In this part of the research we investigated the aspiration efficiencies of sharp-edged, thin-walled probes facing the wind, for an especially wide range of R. This type of sampler represents the most idealized form of aerosol sampler and, by virtue of its simplicity, it is one of the most extensively studied of all aerosol samplers (as summarized by Vincent, 1989). The investigation of thin-walled probes represents the first step toward understanding the more complex flows pertaining to blunt samplers. In the context of the current research, this study served two major goals. First of all, it served as a validation of the experimental methods described earlier in this report in that it produced data that were directly comparable to the large body of experimental data and theoretical knowledge obtained over the past 40 years by many researchers. Secondly, the study investigated sampling conditions outside the range of those studied previously and provided important insights into the effect of R on sampler A, especially for large R where, as described in Section 4, current knowledge of A is particularly weak.

Background

Interest in thin-walled probes first came from the need to collect 'representative' samples of aerosols in ventilation ducts and exhaust stacks, which could be obtained under isokinetic conditions. Common applications of thin-walled, isokinetic probes were the determination of particulate emissions from the stacks of industrial plants. More recently, isokinetic probes have been useful in laboratory testing of the performances of practical air samplers, of the type used in environmental and occupational hygiene, by providing reference concentrations from which test samplers' aspiration efficiencies can be determined.

The study of thin-walled probes has also been driven by the need to understand more complex airflow scenarios pertaining to the wider family of 'blunt' aerosol samplers, of which thin-walled

probes are simply a limiting case. Such studies have provided important insights not only into the nature of human inhalation of aerosols but also the performances of aerosol samplers aimed at collecting particle size-selected fractions (Vincent, 1995).

Most of the published experimental data and theory on the performance of thin-walled, cylindrical probes have been limited to relatively narrow ranges of R. The upper end of the range of R studied in most previous research has not exceeded about 5 (Badzioch, 1959; Vitols, 1966; Davies, 1968; Zenker, 1971, Belyaev and Levin, 1974; Jayasekera and Davies, 1980; Davies and Subari, 1982; Lipatov *et al.*, 1986; and others). However, interest has been stirred in studying aerosol aspiration for a much wider range of R. This is largely driven by the desire for new blunt samplers to accurately sample according to specific particle size-selective criteria at lower flowrates (which results in higher R-values) in order to use lighter sampling pumps for industrial and environmental hygiene applications (Vincent *et al.*, 1999). The study of aspiration into thin-walled samplers at high R-values would provide fresh insights into the physics of aerosol sampling under such conditions that may then be generalizeable to blunt samplers. In addition, however, for aerosol scientists, there is scholarly interest in identifying how far the classic model of Belyaev and Levin (1974) for thin-walled probes facing the wind can be extended for wider ranges of R and St than previously studied.

With all the preceding in mind, the aim of the present study was to revisit existing thin-walled probe theory and to examine the extent to which it predicts A for high levels of R, especially in the range above 5. New wind tunnel experiments were conducted for thin-walled probes with R-values up to as great as 50. This far exceeds the range of any previous such experiments.

Theoretical framework

Badzioch (1958) was among the first to study A for thin-walled probes as a function of R and St. From physical reasoning, based on considerations of the ability of particles to 'follow' an air flow that is changing direction in the vicinity of the sampler entry, he argued that

$$A = 1 + \beta(R - 1). \tag{15}$$

In this expression, the term β is an efficiency by which particles 'impact' onto the plane of the sampling orifice, governed entirely by inertial considerations. In this way, it may be expressed as a function of St, tending towards zero for $St \to 0$ and tending towards unity for $St \to \infty$. Equation (15) was later confirmed by Voloshchuck and Levin (1968), Davies (1968), and Zenker (1971), all of whom concurred that β is a function of St but not of R. However, in 1974, Belyaev and Levin noted the suggestion of Rüping (1968) that β should be a function of R as well as St, leading them to propose that β should take the form

$$\beta = 1 - 1/\{1+G(St)\}, \tag{16}$$

in which G may depend on R. It was acknowledged that this expression was purely empirical, but that it satisfied the boundary conditions at very high and very low St-values for the expected physical behavior of the system in question. Belyaev and Levin carried out experiments in which they visually tracked the trajectories of monodisperse *Lycopodium* spores in the vicinities of

thin-walled tubes and so determined aspiration efficiency from the positions of the limiting trajectories. This is the so-called "direct method" (Vincent, 1989). Their experiments were performed for R-values from 0.2 to 5 and St-values from 0.18 to 2.03, and they used the results to find an empirical form for the function G as a function of R, thus

$$G = 2 + (0.62/R) \tag{17}$$

Belyaev and Levin noted that this equation held with "sufficient accuracy for practical purposes." Equations (15) to (17) then became the most widely-accepted form of what has come to be known as the "impaction model for a thin-walled sampler facing the wind" (Vincent, 1989). Many researchers have tested this model, and found that it agrees well with experimental data for St ranging from about 0.04 to 2 and R ranging from about 0.03 to 11 (Davies and Subari, 1982; Jayasekera and Davies, 1980; Belyaev and Levin, 1974; Lipatov *et al.*, 1986; Gibson and Ogden 1977; and Zenker, 1971). Although there have been some discrepancies between predicted and measured A at $R < 0.2$, these have been attributed to particle bounce/splash effects which tend to increase measured A-values when using the indirect method (Lipatov *et al.*, 1988). Therefore the Belyaev and Levin model has become widely regarded as 'universal'.

It is important to note, however, that the Belyaev and Levin model contains two empirical coefficients (in G), and that these were fitted to a limited set of experimental data, with relatively narrow ranges of R and St. It remains to be seen whether this model can accurately predict A for more extreme conditions of R and/or St.

Experimental methods

The experiments were carried out in the small wind tunnel. Fused alumina powders (nominal Grades F800, F400 and F240) corresponding to mass median d_{ae} of 13, 34, and 89.5 μm, respectively, were aerosolized using the Topas SAG 410. The aerosols were injected into the airflow inside the wind tunnel just upwind of the mixing plate. The compressed air supply to the aerosol generator was maintained at 2 bar, sufficient to provide an agglomerate-free aerosol. To test for the presence of unwanted particle agglomerates in the dispersed aerosol, particle samples impacted onto glass slides placed briefly inside the wind tunnel were viewed under the microscope. There was no visible evidence of agglomeration for any of the particle sizes for the operating conditions specified. The particles were not neutralized prior to injection into the wind tunnel. This follows the practice in most of the earlier studies using such powders, guided by the evidence that electrostatic effects on A while particles are moving outside the sampler are not significant (as reviewed by Vincent, 1989). While the Kr^{85} neutralizer (TSI Inc., St. Paul, MN) was used in the preliminary tunnel study described earlier, its use was discontinued for the main body of the research. Nonetheless, as a precautionary measure, the dust generator, aerosol injection line, and all sampling tubes were grounded. For the experiments, three sharp-edged, thin-walled probes were used. The first of the three tubes was placed on the axis of the wind tunnel working section at a distance 0.7 m downstream from the turbulence-generating grid. This was far enough away (a) not to be influenced by the recirculating flows immediately behind the grid structures and for the freestream turbulence characteristics to have become reasonably isotropic (Baines and Peterson, 1951), yet (b) not so far for there to have been significant particle loss from the freestream due to gravitational settling. Overall, the role of such grid-generated

turbulence was to facilitate the mixing of aerosol and provide well-defined turbulence intensity and length scale in the test region of the wind tunnel. The first tube was operated isokinetically (R = 1). The other two tubes were placed symmetrically, but offset from the wind tunnel axis and separated by 0.10 m, at a distance 1.2 m downstream from the turbulence-generating grid. These latter two samplers were operated anisokinetically to provide the desired range of values of R. Usually, in a given experimental run, two different R-values were thus represented. For each experimental sampling session, this system yielded three test samples, the single upstream one to provide the reference concentration (c_0) and the other to provide two separate values of the aspirated concentration (c). For R-values greater than unity, particle bounce and blowoff were expected to be negligible, since air diverges into the tube under these conditions (Lipatov *et al.*, 1988). This was confirmed when it was found that greasing the outside surfaces of the tubes did not affect the measured concentrations. To check for particle bounce or blowoff from the inner tube walls (which is a more likely scenario for R > 1), the deposits on the inner walls were visually inspected. Here, too, there was no visible evidence in the depositional patterns suggestive of particle bounce or blowoff from the inner walls. The aspiration efficiencies of the test probes were determined using the so-called "indirect method" (Vincent, 1989), utilizing the earlier Equation (1).

It was expected that, due to a combination of particle settling and re-mixing along the length of the wind tunnel test section, the average aerosol concentration would change as a function of position along the axis of the wind tunnel, to an extent dependent on the size of the particle and windspeed. Corrections were therefore applied to the upstream isokinetic probe concentrations to account for particle size-dependent decreases in aerosol concentration between the upstream reference and downstream test probe positions. That is, in order to obtain c_0 for the calculation of A, the upstream concentration measured by the isokinetic probe was divided by the appropriate correction factor ($C_{upstream}/C_{downstream}$) in order to obtain the true reference concentration at the downstream position. The correction factors were based on a large set of experimental data. The experiments were conducted by means of isokinetic sampling (i.e., R = 1) at both the upstream and downstream positions, for a single windspeed (U = 1 m/s), held constant for all the experiments reported in this study, and for four particle sizes. The samplers were positioned in the exact same manner as that described in the previous section. Four repeats for each particle size were performed and the calculated upstream to downstream ratios are shown in Figure 11.

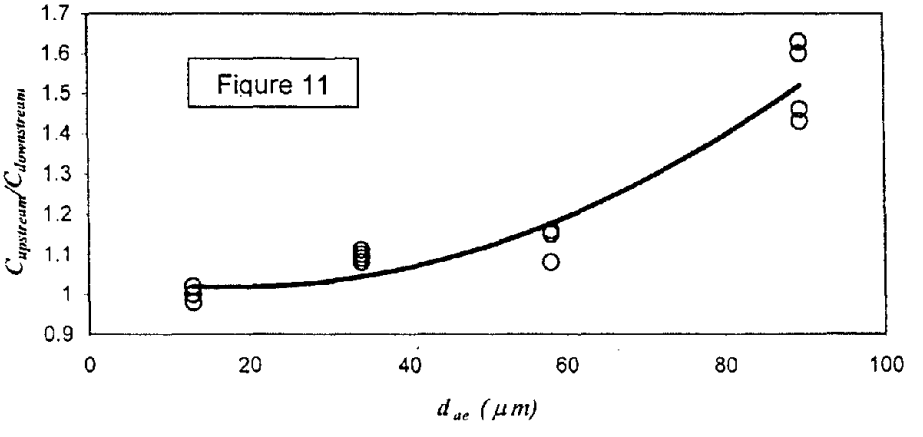

The results indicate that the aerosol concentrations do indeed change as they move along the test section. As expected, the greatest changes occurred for the largest particles. The results also confirm that the aerosol concentration, for all particle sizes and to within experimental error, was consistently the same at each of the two downstream locations. Therefore, an empirical correction factor was determined from the ratios of upstream to downstream concentrations for each particle size and windspeed, where the downstream concentrations were averaged concentrations from the two downstream positions. A second order polynomial regression curve was fit to all the data using the spreadsheet program Microsoft Excel (Microsoft Corporation, Redmond, WA). The resultant fitted equation is

$$C_{upstream} / C_{downstream} = 1.05 - 0.0034 \cdot d_{ae} + 0.0001 \cdot d_{ae}^2 \qquad (18)$$

where d_{ae} is expressed in [μm]. This empirical expression provides a good fit to the data, with an R^2-value of 0.92.

Experimental results for thin-walled probes

As already mentioned, the freestream air velocity in the wind tunnel was maintained at 1 m/s for all the experiments reported in this part of the research. So R was varied by changing the sampling flowrate and the tube diameter. Three particle sizes (characterized by d_{ae} = 13 μm, 34 μm and 89.5 μm) and two tube diameters (δ = 6.6 mm and 10 mm) were employed, so that St ranged from 0.051 to 3.68 and R from 0.5 to 50. Aspiration efficiency (A) was measured for this wide range of R and St, and two or three repeats were done for each combination of R and St. The full experimental results for A are shown below in Table 12. All sampled particulate masses exceeded the LOQ of 0.40 mg as determined for the current experimental system (filters and balance) using the method described earlier. A is plotted as a function of R for various values of St in Figures 12 to 14 (see below), where for conciseness, only the data pertaining to the 10-mm orifice are shown. Also shown in each of these figures is the dashed line representing the linear behavior predicted using the model of Belyaev and Levin. In the figures, the error bars represent 95% confidence intervals, derived from the standard deviations calculated from the repeat experimental measurements. The plots in Figures 12 to 14 indicate that, as R increases upwards beyond about 6, the theoretical model predictions from Belyaev and Levin ($A_{B\text{-}L}$) increasingly overestimate A compared to the measured values (A_m). A similar trend can be seen when all the results are plotted in the form of A_m versus $A_{B\text{-}L}$ (see Figure 15 below).

To show the practical significance of these results, Figure 16 (see below) is a bias map constructed to show more clearly the bias contained in the Belyaev and Levin model for the wide ranges of R and St pertaining to the experiments. The approach taken is similar to that adopted by a number of workers in studies of sampler bias (e.g., Lidén, 1994). In the present case, bias was defined as

$$\text{Bias (\%)} = \{(A_{B\text{-}L} - A_m) / A_m\} \times 100. \qquad (19)$$

d_{ae} (μm)	δ (mm)	R	St	A
13	6.6	0.5	0.078	0.96, 0.95
13	6.6	2	0.078	1.29, 1.25
13	6.6	6	0.078	1.37, 1.40
13	6.6	10	0.078	1.52, 1.72
13	6.6	25	0.078	2.09, 2.20
13	6.6	50	0.078	2.48, 3.60
89.5	6.6	0.5	3.68	0.61, 0.66
89.5	6.6	2	3.68	1.83, 1.90
89.5	6.6	6	3.68	4.85, 5.42
89.5	6.6	10	3.68	8.15, 8.41
89.5	6.6	25	3.68	16.80, 19.28
89.5	6.6	50	3.68	36.34, 33.67
13	10	0.5	0.051	0.99, 0.90, 0.89
13	10	2	0.051	1.19, 1.28, 1.29
13	10	4	0.051	1.30, 1.31, 1.34
13	10	6	0.051	1.35, 1.32, 1.29
13	10	8	0.051	1.46, 1.42, 1.49
13	10	10	0.051	1.36, 1.47, 1.50
13	10	16	0.051	1.56, 1.49, 1.51
13	10	25	0.051	1.61, 1.66, 1.60
13	10	50	0.051	2.45, 2.29, 2.01
34	10	0.5	0.351	0.73, 0.74, 0.71
34	10	2	0.351	1.48, 1.44, 1.57
34	10	4	0.351	2.24, 2.23, 2.16
34	10	6	0.351	2.40, 2.75, 2.61
34	10	8	0.351	3.35, 2.99, 3.09
34	10	10	0.351	3.27, 3.75, 3.76
34	10	16	0.351	5.26, 4.49, 4.73
34	10	25	0.351	6.61, 6.87, 7.39
34	10	50	0.351	14.85, 12.91, 11.54
89.5	10	0.5	2.43	0.67, 0.65, 0.63
89.5	10	2	2.43	1.81, 1.51, 1.73
89.5	10	4	2.43	2.99, 2.86, 3.17
89.5	10	6	2.43	4.33, 4.36, 4.89
89.5	10	8	2.43	5.90, 5.05, 6.51
89.5	10	10	2.43	5.77, 7.25, 6.60
89.5	10	16	2.43	9.88, 8.96, 10.09
89.5	10	25	2.43	14.92, 17.18, 16.79
89.5	10	50	2.43	27.10, 30.87, 30.87

Table 12

The bias in Equation (19) was calculated for each individual set of experimental conditions studied, and the results represented in the *R-St* plane were smoothed to generate lines of constant bias. This plot shows that the bias was always small when R was less than about 6, entirely consistent with the conclusions of earlier research. But it shows that there was an increasingly large positive bias in $A_{B\text{-}L}$ compared to A_m as R rose above 6. This trend can have considerable practical significance if it is desired to sample at large R-values, for whatever reason.

Discussion

Numerous studies by other workers have shown that, when R is relatively small ($R < 6$), the Belyaev and Levin model predicts A-values that agree very well with experimental data. It was therefore reassuring that the new experimental data presented here were also in such good agreement with the Belyaev and Levin model in the same range of R, thus validating the new experiments. It follows that the noted overestimate of the Belyaev and Levin empirical model for larger values of R, as shown in Figures 12 to 14, was a real effect. In turn, this suggests that the Belyaev and Levin model should no longer be regarded as universal.

Referring back to Equation (13), as already mentioned, the functional form for the 'impaction efficiency' in the context of aerosol sampling is plausible. But it is entirely empirical. Inside that empirical form, the parameter G contains two coefficients, as shown in Equation (17), which were originally obtained by fitting the model to the (then) available data. It is therefore quite appropriate to modify Equation (17) by a yet further empirical extension of the existing form. To achieve this, an additional term is needed that reverts back to the original form shown in Equation (17) when R is small. With this in mind, we considered

$$G = 2 + (0.62/R) + k_1 R^{k_2} \qquad (20)$$

where the last term on the right hand side provides the desired modification. The coefficients k_1 and k_2 were determined by non-linear least squares regression using the statistical package SYSTAT 10 (SPSS Science, Chicago, IL). A total of 105 data records from the experiments were used to determine the best-fit values for the unknown coefficients, yielding

$$k_1 = -0.910$$
$$k_2 = 0.103$$

with $R^2 = 0.99$, which indicates that the fitted relationship accounts for 99% of the variation in the overall data set of experimentally-measured A. For practical purposes, the modified model may therefore be expressed in terms of Equations (15) and (16) together with

$$G = 2 + (0.62/R) - 0.9R^{0.1} \qquad (21)$$

where rounding of the new coefficients in the manner shown does not significantly change the R^2-value. As shown by the solid lines on Figures 12 to 14, the revised empirical model provides an excellent fit with all the experimental data. The new model is satisfactory for predicting A (A_P, say) for the full range of R and St studied (see Figures 12 to 14).

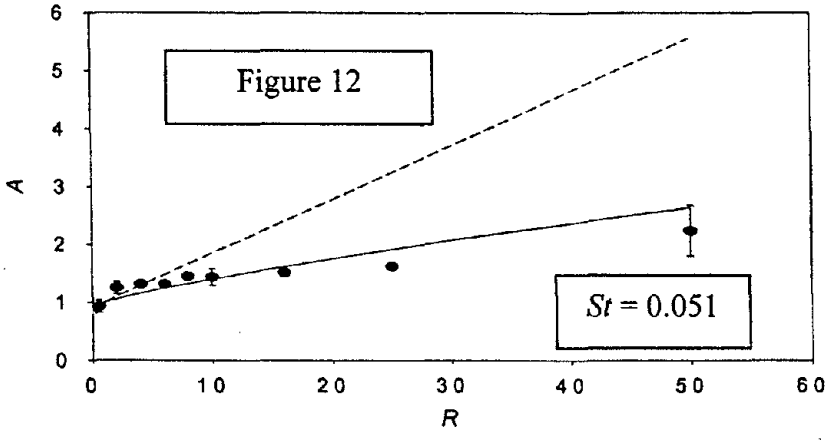
Figure 12
St = 0.051
A
R
0
1
2
3
4
5
6
0
10
20
30
40
50
60

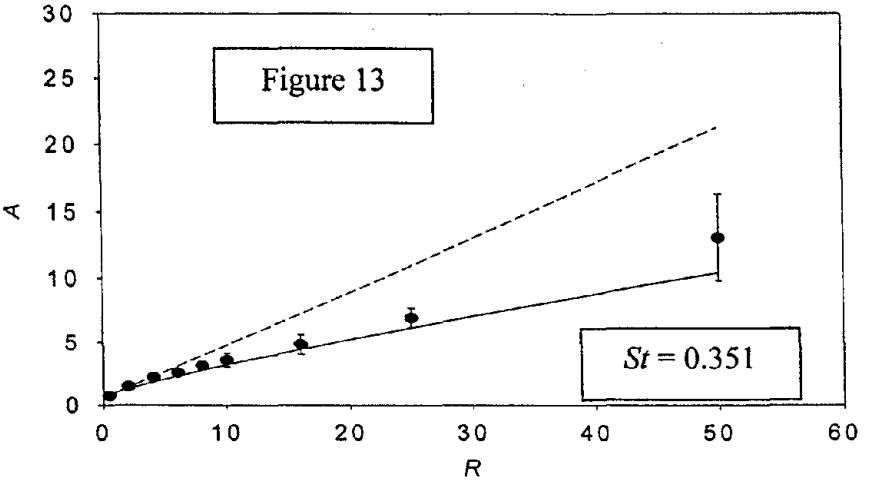
Figure 13
St = 0.351
A
R
0
5
10
15
20
25
30
0
10
20
30
40
50
60

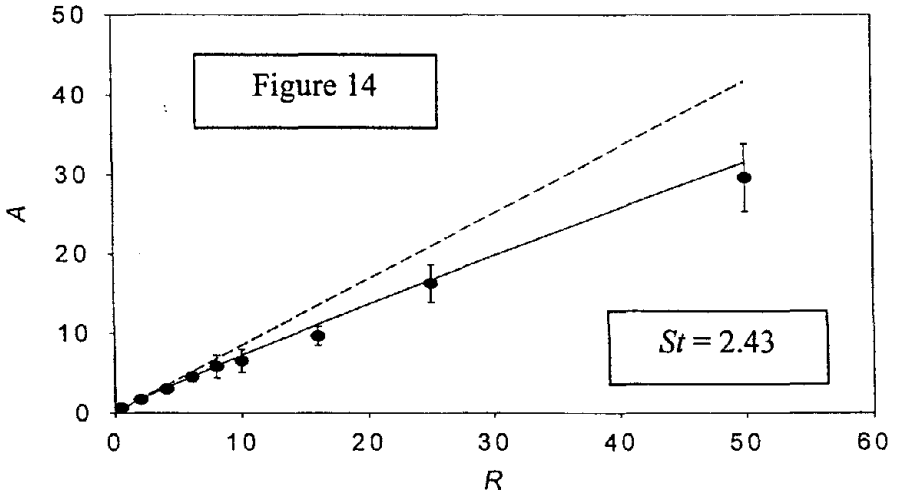
Figure 14
St = 2.43
A
R
0
10
20
30
40
50
0
10
20
30
40
50
60

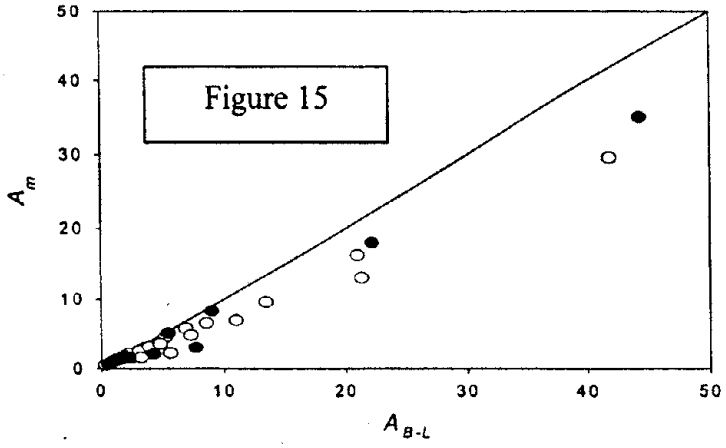

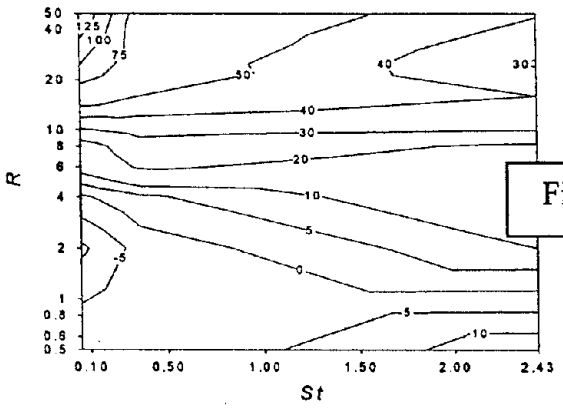

Figure 17 shows the same results in the form of a plot of A_P versus A_m. Also shown in Figure 17 are experimental data from a number of previous important studies. Agreement is seen to be consistently good, except for results corresponding to low R from studies involving the "indirect method," where particle blow-off from external surfaces of the sampling tubes would have caused over-sampling (according to Lipatov *et al.*, 1988). In general, therefore, the new semi-empirical model predicts A well for the full range of $0.03 \leq R \leq 50$ and $0.04 \leq St \leq 3.68$, a large portion of which was investigated in the present study. Additionally, since the data obtained for the smaller tube are not significantly different from those obtained from the larger one, there is no indication that the tube size has any independent influence on A. This supports the majority of researchers (as summarized in Vincent, 1989) who have contended that the size of the sampling tube, by itself, does not have a significant effect on A.

Figure 18 is another bias map, similar to the one in Figure 16, but now showing bias contours in the R-St plane of the modified aspiration efficiency model's predictions against the new experimental data. Now it is seen that bias of the model predictions is less than 10% for almost all the R and St combinations studied experimentally.

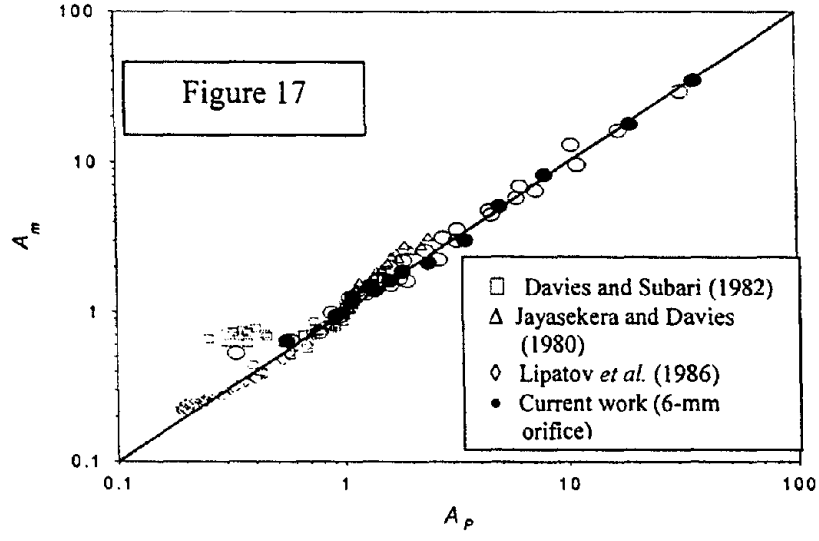

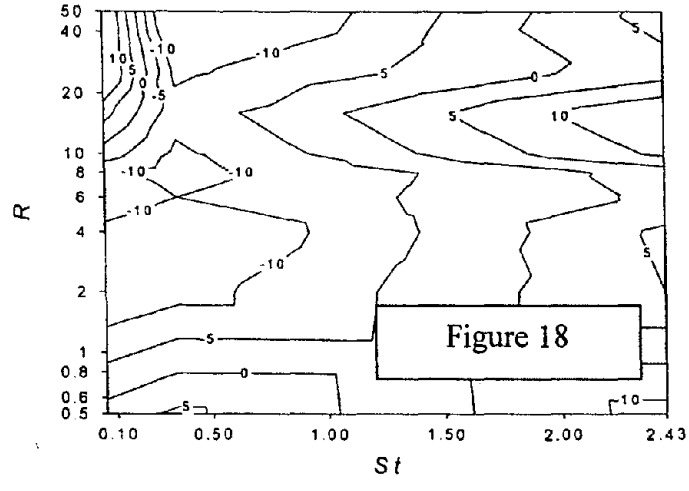

As already mentioned, Equation (15) is a basic expression for the A of a thin-walled sampling probe facing the wind that is fully justifiable on physical grounds provided that the main mechanism influencing A is particle inertia (as embodied by St). The central ingredient that defines the role of St in the aspiration process is β (within which St is contained), and this has so far been described only by empirical expressions, guided by physical considerations of expected behavior in the limits of high and low St. Rüping (1968) was the first to suggest any dependence of β on R. But it was Belyaev and Levin (1974) who were the first to demonstrate this dependence experimentally, and they arrived at the form shown in Equations (15) and (16) by reference to the unambiguous results of their own experiments performed using the "direct method." Even so, they were not able to articulate a physical rationale to explain what they had observed.

In the current study, a much wider range of R was studied experimentally. The experiments showed that, while $A_{B\text{-}L}$ agreed well with A_m for $R < 6$, encompassing the range of conditions studied by Belyaev and Levin, it progressively overestimated A_m for increasingly higher values of R (see Figures 12 to 14). Within the framework initiated by Belyaev and Levin, the search for a

physical explanation for this change in behavior at higher R is not really justified because the original model for G did not itself contain any physical arguments. However, it is of interest to consider the validity of the underlying physical assumption that the whole aspiration process is principally controlled by inertia, as embodied in the basic working expression for aspiration efficiency given by Equation (15). Since, as argued earlier, it was possible to discount significant electrostatic effects, only gravity and turbulence remained as potential influential factors in the aspiration process. As noted earlier, freestream turbulence was consciously introduced into the airflow in the wind tunnel working section. The presence of such turbulence has been considered by some in relation to its possible effects on aspiration efficiency (Vincent *et al.*, 1985). But the limited evidence given in that paper suggested that aspiration is governed mainly by the time-averaged mean flow (similar to that observed in smooth, laminar air flow) and not significantly influenced by the superimposed random motions of the airflow and the particles associated with the turbulence. With regards to gravity, the correction factors accounted for the gravity-associated change in aerosol concentration from the upstream to downstream sampler positions, where the aerosol concentrations were measured by isokinetic samplers. However, there may have been a gravity effect that depended on the flowrate of the samplers. For the range of R-values in the experiments, the corresponding range of mean air velocity across the plane of the sampling orifice was 0.02 m/s $\leq U_s \leq$ 2 m/s. For the largest value of R and the largest particles used in the experiments, the settling speed of the particles falling under the influence of gravity would therefore have been of the same order of magnitude as the horizontal translation velocity of the particles passing through the sampler entry plane. So it would not indeed have been surprising if there were to be an effect associated with gravity in this case. The new data reported in this paper were inspected in the light of this possibility. The Froude number ($Fr = U_s^2/g\delta$, where g is the acceleration due to gravity) represents the ratio between inertial and gravitational forces. So an empirical expression involving Fr in the modified equation for G was sought. However, no form could be found that provided agreement with the experimental data even nearly as good as that exhibited by the new equations proposed here. It was therefore concluded that, irrespective of possible underlying physical explanations not yet accessible, these new equations provide a good working empirical model for describing the aspiration efficiency of thin-walled probes for R-values up to at least 50.

The results from this study have implications for the more general case of blunt sampling. Most notably, empirical or semi-empirical models that have been proposed for idealized or actual practical blunt samplers, based on experimental data for limited ranges of R (e.g., Tsai *et al.*, 1993, 1995b and 1996b), may need to be re-evaluated if they are to be applied to conditions where R is larger.

Conclusions from this part of the research

In this section we have described a study aimed at investigating the aspiration efficiencies of idealized thin-walled probes at large values of R. The large experimental data set was also used to determine the applicability of the Belyaev and Levin thin-walled sampler model to wider ranges of R and St beyond those tested in earlier studies. A limitation was found in the Belyaev and Levin model for R-values greater than about 6, most notably in the empirical form of the parameter G that Belyaev and Levin introduced to account for the R-dependency observed in their own experiments. When a correction was applied to G (in the form of a simple additional

empirical parameter, again involving R), it was found to provide a very good fit ($R^2 = 0.99$) to all the experimental data, including the new ones generated during the present experimental study, for the widest ranges of R and St examined thus far.

While more study would be required to determine the exact physical nature of aspiration into thin-walled samplers, especially at large R where, it is expected, the effects of gravity should become apparent, the modified model greatly extends the range for which it would be possible to predict the aspiration efficiency of particles into thin-walled samplers. In order to gain similar confidence in the impaction models for blunt samplers, the next section proceeds to describe a study conducted to investigate A for blunt samplers at similarly large R-values so that such models may, in their turn, also be modified.

6. Aspiration efficiency of disc-shaped blunt nozzles facing the wind

Introduction

This section of the report describes an investigation of disc-shaped blunt nozzles facing the wind, for a wide range of particle aerodynamic diameter d_{ae}, and again for a very wide range of velocity ratio R. By virtue of its simple shape and axisymmetry, the disc-shaped sampler represents the next level of complexity from sharp-edged, thin-walled samplers. A thorough investigation of its sampling characteristics was aimed at narrowing the gap between the current knowledge of thin-walled samplers and that for more complex blunt samplers, eventually to the extent of the type commonly used for practical industrial hygiene applications (as described later in this report).

Background

As described in the previous section, the simplest scenario for investigating aerosol sampler performance involves the aspiration of particles into a sharp-edged, thin-walled probe facing the wind, where the wall of the nozzle is sufficiently thin as to have very little effect on aspiration efficiency. A more practical scenario of equivalent simplicity is the one involving a nozzle with finite wall thickness facing the wind. This is what is referred to as a "blunt sampler." Here, the effect of the sampler wall thickness is embodied in r, the ratio of the sampler orifice diameter and the outer diameter of the sampler body.

Some of the earlier blunt sampler basic experimental research focused on the aspiration of aerosols into disc-shaped samplers facing the wind (Vincent *et al.*, 1985; Chung and Ogden, 1986). Vincent (1987) developed a semi-empirical model to predict the aspiration of aerosols into blunt samplers facing the wind, for which Chung and Ogden estimated the empirical coefficients by reference to the available experimental data. This model, however, has not yet been tested for experimental conditions beyond the limited ranges examined in those earlier experimental studies.

The study described in the previous section showed that the classic model of Belyaev and Levin (1974), derived on the basis of experimental data for A at quite small R-values, progressively overestimated A for R greater than about 6. The original Belyaev and Levin model for thin-walled sampler A was therefore modified to accommodate these larger R-values. As an extension

of that simplest case, this study revisited the existing model for the equivalent simple blunt sampler scenario, and examined how it too applies for *R*-values outside the range previously studied experimentally. New experiments were conducted to investigate blunt sampler *A* under such conditions. Specifically, *A* was studied for an axisymmetric disc-shaped sampler facing the wind, with *R* from 0.5 to 25 and for d_{ae} ranging from 13 to 89.5 μm. The particle size range was chosen to encompass the coarse inhalable fraction that is of considerable current interest to occupational hygienists and occupational exposure standards-setting bodies.

Theoretical framework

The general nature of streamlines near a blunt sampler is highly distorted, resulting from the competing effects of the divergence of the air to pass around the bluff body of the sampler and of the convergence of a portion as it enters the sampling orifice. Based on this description, particles may 'impact' into the sampled air in the diverging portion of the flow or 'impact' out of the sampled air in the converging portion. For the case of a disc-shaped blunt sampler facing the wind, the blunt sampler model can be summarized in terms of the following set of working equations (Vincent, 1989):

$$
\begin{aligned}
St &= (d_{ae}^2 \rho^* U) / (18 \eta \delta) \\
\phi &= (r^2 / R) \\
St_1 &= St\, r\, \phi^{-1/3} \\
\beta_1 &= 1 - 1 / \{1 + G_1(St_1)\} \\
A_1 &= 1 + \beta_1 (\phi^{-1/3} - 1) \\
St_2 &= St \phi^{1/3} \\
\beta_2 &= 1 - 1 / \{1 + G_2(St_2)\} \\
A_2 &= 1 + \beta_2 [(r / \phi^{1/3})^2 - 1] \\
A &= A_1 A_2
\end{aligned}
\qquad (22)
$$

In this system of equations, the final outcome is the result of the combination of two transmission efficiencies for particles crossing the divergent and convergent portions of the flow, respectively, immediately in front of the sampling orifice. In this set of equations, $r = \delta/D$, where δ is the diameter of the sampling inlet and D is the diameter of the sampler body. The derived secondary dimensional quantity, ϕ, has useful physical meaning in that it represents the ratio of the sampling flowrate to the flowrate of air geometrically incident onto the sampler body. The terms β_1, β_2 and St_1, St_2 are the impaction efficiencies and Stokes' numbers respectively for particle transport in the two flow regions mentioned, and G_1 and G_2 are empirical coefficients. Chung and Ogden determined the latter by fitting the model to their own limited experimental data for d_{ae} up to only about 12 μm, and obtained $G_1 = 0.25$ and $G_2 = 6.0$.

Experimental methods

The experimental facilities and methods used in the present work were essentially the same as those in the earlier study for thin-walled sampling probes. The experimental set-up for the blunt sampler studies is shown in Figure 19. Here, as in our study of thin-walled samplers described in Section 4, a sharp-edged, thin-walled probe, operated isokinetically, was used to measure the reference total concentration of aerosols in the wind tunnel test section. Again, the sum of the

wall deposit and the mass collected on the primary 25-mm filter was used to determine the reference freestream aerosol concentration, c_0.

Disc-shaped bluff body samplers, with a range of body and orifice diameters, were used as the test samplers. The samplers consisted of circular discs cut from cardboard, which were placed over sharp-edged, thin-walled tubes and located approximately 3 mm from the leading edge to minimize particle blow-off effects (as described by Mark and Vincent, 1986). One such sampler consisted of a 6.6-mm diameter tube and 130-mm diameter disc, and the other sampler consisted of a 10 mm-diameter tube and 100 mm-diameter disc. In this way, r-values of 0.05 and 0.10, respectively, were achieved.

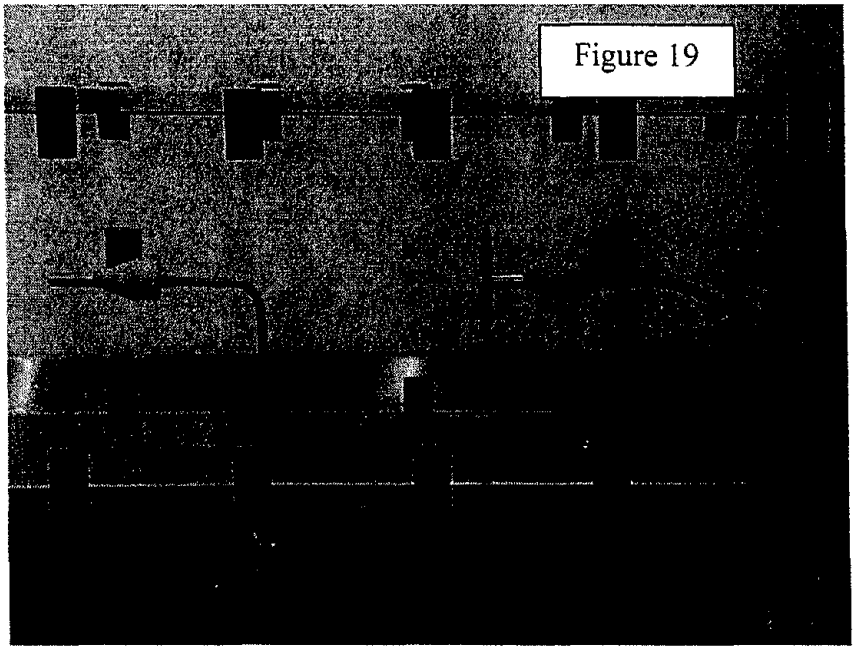

Figure 19

The isokinetic thin-walled reference probe (R = 1) was placed on the center axis of the wind tunnel working section at a distance 0.7 m downstream from the turbulence-generating grid at the working section. The disc-shaped sampler to be tested was also placed on the center axis of the wind tunnel, approximately 0.5 m downstream of the thin-walled probe. The disc-shaped samplers were operated at a range of flowrates to provide the desired range of R-values. For each experimental sampling session, this system yielded two test samples, the upstream one to provide the reference concentration (c_0) and the downstream one to provide the aspirated concentration (c_s). Once again, aspiration efficiency in each experiment was determined from $A = c_s/c_0$, again after adjusting for the particle size-dependent differences in the undisturbed upstream and downstream aerosol concentrations.

The windspeed in the wind tunnel was again maintained at 1 m/s for all the experiments reported here. So R was varied by changing the sampling volumetric flowrate and tube diameter. Three nominal particle sizes (d_{ae} = 13 μm, 34 μm and 89.5 μm), two tube diameters (δ = 6.6 mm and 10 mm), and two disc diameters (D = 100 mm and 130 mm) were employed, such that St ranged from 0.051 to 3.68, R from 0.5 to 25, and r from 0.05 to 0.10. Based on assessment of the

variability of data from such experiments, as ascertained from the thin-walled probe study, it was considered sufficient to perform just two repeats for each combination of R, St and r.

Results

The full experimental results for A are shown in Table 13. It is seen that, from the two repeat runs for each specific set of conditions, together with the wide range of conditions studied, the experiments are highly reproducible. The repeat measurements of A for any given set of experimental conditions never differ by more than 10%, and most of the data pairs differ by less than 5%. This is far better than the precision obtained in the earlier disc-shaped sampler studies cited above, and in wind tunnel aerosol studies in general.

d_{ae} (μm)	δ (mm)	D (mm)	r	R	St	A
13	6.6	130	0.05	0.5	0.078	0.94, 0.95
13				2	0.078	0.92, 0.94
13				6	0.078	0.97, 1.07
13				10	0.078	0.87, 0.83
13				16	0.078	0.94, 0.89
13				25	0.078	0.98, 0.94
34				0.5	0.531	0.79, 0.81
34				2	0.531	0.88, 0.84
34				6	0.531	0.93, 0.93
34				10	0.531	1.12, 1.05
34				16	0.531	1.14, 1.15
34				25	0.531	1.36, 1.26
89.5				0.5	3.68	0.62, 0.63
89.5				2	3.68	0.94, 1.00
89.5				6	3.68	1.45, 1.37
13	10	100	0.10	0.5	0.051	0.94, 0.94
13				2	0.051	0.94, 0.95
13				6	0.051	1.00, 0.99
13				10	0.051	1.09, 1.09
13				16	0.051	1.04, 1.06
13				25	0.051	1.12, 1.01
34				0.5	0.351	0.89, 0.87
34				2	0.351	0.97, 0.99
34				6	0.351	1.23, 1.23
34				10	0.351	1.27, 1.25
34				16	0.351	1.41, 1.30
34				25	0.351	1.69, 1.54
89.5				0.5	2.43	0.83, 0.86
89.5				2	2.43	1.09, 1.11
89.5				6	2.43	1.69, 1.64
89.5				10	2.43	1.89, 1.96
89.5				16	2.43	2.51, 2.69
89.5				25	2.43	3.28, 3.49

Table 13

In Figure 20 (see below), the new experimental results (open circles) are compared with predicted values calculated from the earlier model with the coefficients as determined by Chung and Ogden. They are plotted in the form of measured aspiration efficiency (A_m) versus predicted aspiration efficiency (A_V). Also shown are the A_m-data (open triangles and squares) from the two earlier studies that exceeded the LOQ of 0.40 mg.

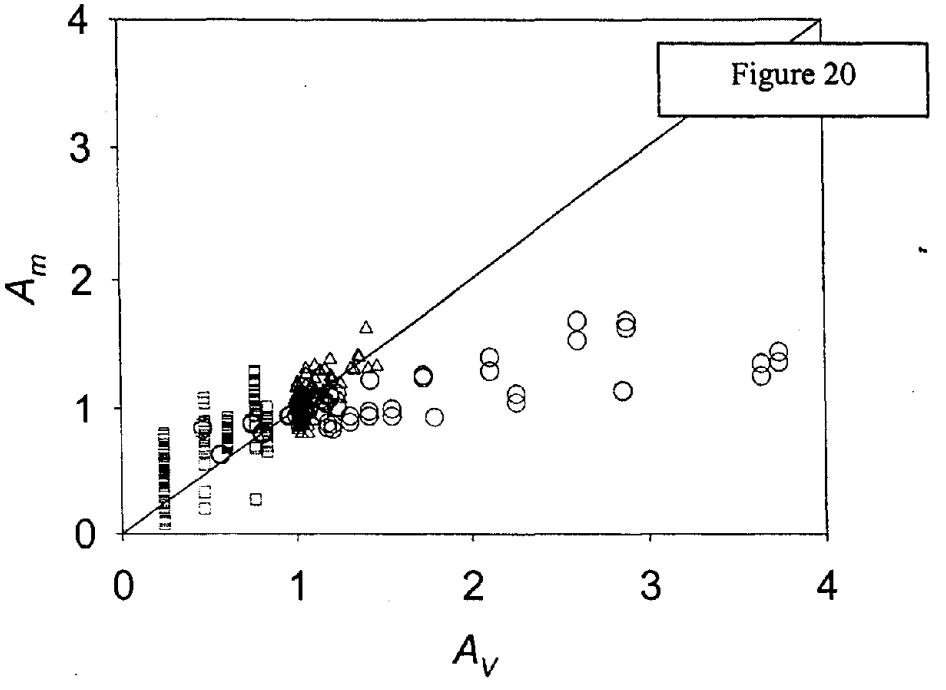

Figure 20 shows that the model greatly overestimates A when A is greater than about 1. The model, however, somewhat underestimates A when compared to the earlier data of Vincent *et al.* (1985). Figure 21 maps the bias between the model and the new measurements from the present study, as a function of both St and R, using

$$\text{Bias (\%)} = \{(A_V - A_m) / A_m\} \times 100 \qquad (23)$$

In Figure 21 it can be seen that when R is greater than about 2, the model increasingly overestimates A compared to the new data. However, the magnitude of the bias is generally uniform across the range of St. Overall, it now becomes clear that this model, with its current empirical coefficients, is not satisfactory in predicting A accurately for the wider range of R and St, even for this simple sampler configuration.

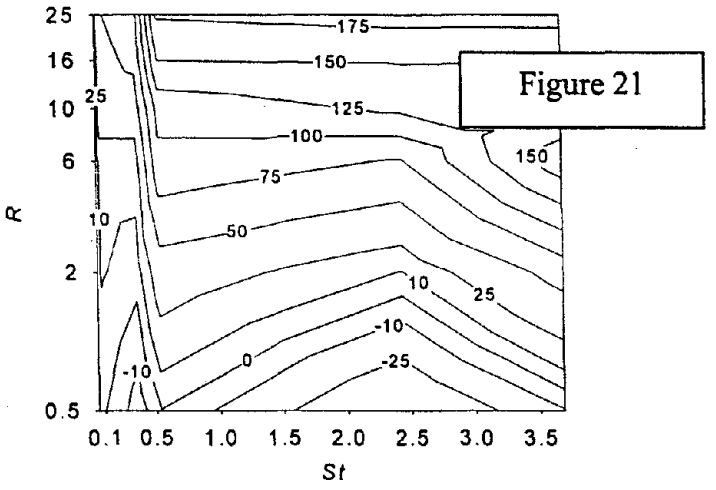

Figure 21

To investigate the effects of r, experimental data for $r = 0.05$ are compared with those for $r = 0.10$. The results are shown below in Figure 22, and it is seen that A is generally larger for $r = 0.10$ across the whole range of A. A simple linear regression of these data shows that $A_{r=0.10} = 1.15 \cdot A_{r=0.05}$ with $R^2 = 0.82$. Here, therefore, the dependence of A on r is relatively weak.

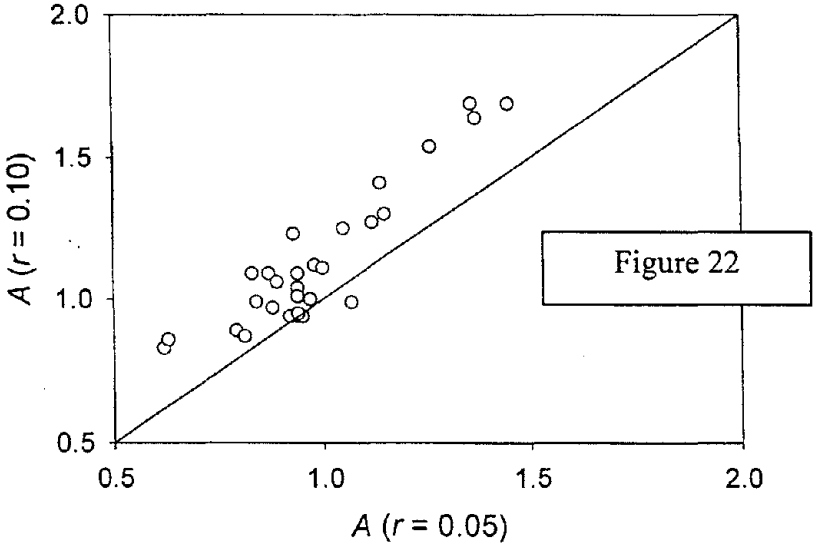

Figure 22

Discussion

Experimental data for A for disc-shaped samplers facing the wind are scarce. Only two earlier studies have been reported for this simple, axisymmetric blunt sampling scheme, and the results from one of them may have been confounded somewhat by turbulence effects (Vincent *et al.*, 1985). Yet such studies provide important insights into the nature of the performances of aerosols of much more complicated geometries, like those used in practical occupational and environmental hygiene situations. Since the empirical coefficients in the original model described in the set of Equations (22) were determined from such scant data, it was not

surprising to find that the original model did not predict A well for the new data, which were obtained for a much wider range of conditions. Nonetheless, within the range of R, St and r investigated in the earlier studies, inspection of these new data showed that they did agree quite well with those data (see Figure 20). Where the departure from the model becomes apparent is for conditions where R-values extend out beyond the range studied earlier. This pattern is similar to that observed in the earlier work for thin-walled sampling probes (see above). So, again, the research points to the need for a modified aspiration efficiency model.

In the original model, the coefficients G_1 and G_2 were presented as simple empirical constants, and these were estimated by Chung and Ogden by fitting the model to their own data. Following what was learned from the thin-walled probe study, forms for these two coefficients were sought that depended on other parameters, most notably R and r. Several empirical forms were considered, but the simplest and most satisfying was the one that replaced the impaction expressions in Equations (22) by

$$\beta_1 = 1 - 1 / \{1 + k_1(R/r)^{k_2}(St_1)\}$$
and
$$\beta_2 = 1 - 1 / \{1 + k_3(R/r)^{k_4}(St_2)\} \qquad (24)$$

Whereas in the thin-walled probe study it was sufficient to include R in the modifying term, r is now also introduced in order to represent the effect of the sampler wall thickness. The new coefficients k_1, k_2, k_3 and k_4 were determined by a non-linear least squares regression, again using the statistical package SPSS 11.0 (SPSS Science, Chicago, IL). A total of 66 data records from the new experiments were used to determine the best-fit values for the unknown coefficients, yielding

$k_1 = 1.26$
$k_2 = -0.68$
$k_3 = 1.59$
$k_4 = 0.40$

with $R^2 = 0.97$, indicating that the fitted relationship accounted for 97% of the variation in the overall data set of experimentally measured A. Figure 23 (see below) shows the comparison between predicted A ($A_{P\text{-}V}$, say, using the revised model) versus measured A (A_m), and it is seen that the new model is satisfactory in predicting A for the full range of R, St, and r examined in the current investigation. It also predicts A well for data from the earlier studies ($R^2 = 0.80$ for all the data). In particular, the new model predicts A much better than the previous one when compared against the Vincent *et al.* data from 1985 (see Figures 20 and 23). It is also encouraging that the R^2-value obtained from the new model is indicative of a much better fit than that obtained in the Chung and Ogden study (where the R^2-value was only 0.49). This is probably due to the more improved experimental method utilized in the current study, which largely stems from the use of a more stable, miniature wind tunnel and all its experimental advantages. A bias map is shown in Figure 24, where it is seen that the bias is now less than 10% for all R and St combinations studied experimentally. This further reinforces the accuracy of the new model. The comparison with Figure 21 is striking. Now, it can be said that the new model predicts A well for the full range of experimental conditions reported here and previously.

The effect of R on A: Figure 25 shows that, as in the case of the thin-walled sampler facing the wind, the A for axisymmetric, disc-shaped blunt samplers facing the wind increases with increasing R. The rate of this increase is largest for high St-values. Closer inspection of the new semi-empirical model for the blunt sampler reveals the important finding that the effect of R on A is much weaker than for thin-walled samplers facing the wind. Furthermore, not only is the rate of increase in A with R greatest for large St-values, but the magnitude of the reduction in A for the disc-shaped sampler compared to the thin-walled sampler is greatest for large values of R and St.

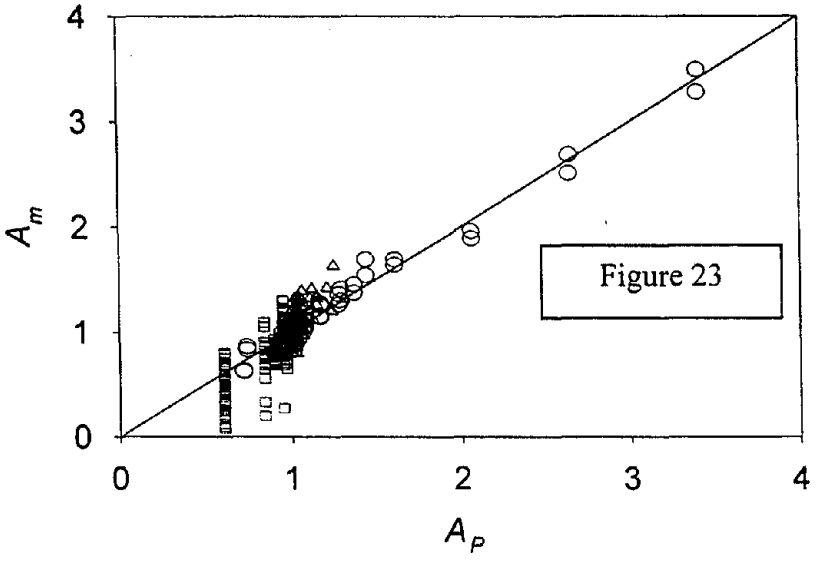

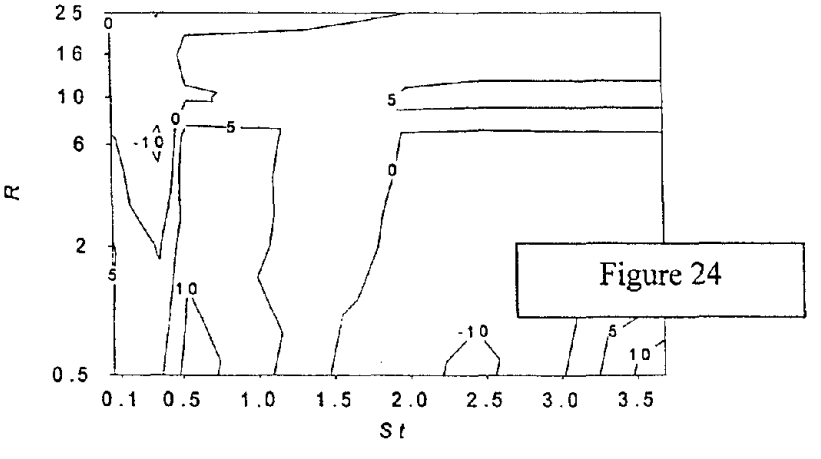

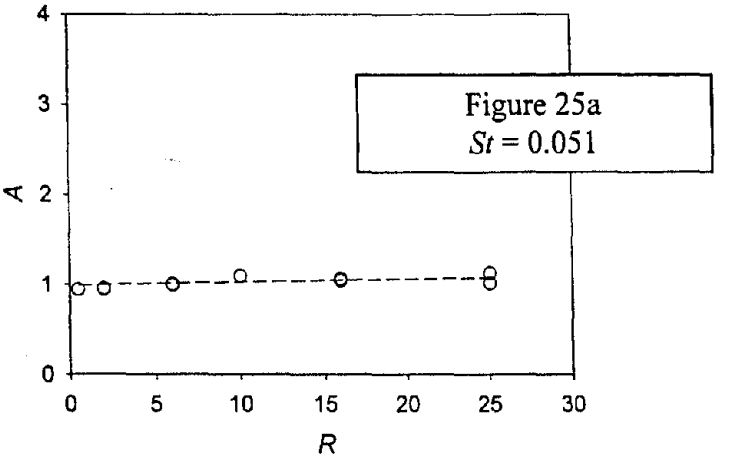
Figure 25a
St = 0.051
A
R
0
1
2
3
4
0
5
10
15
20
25
30

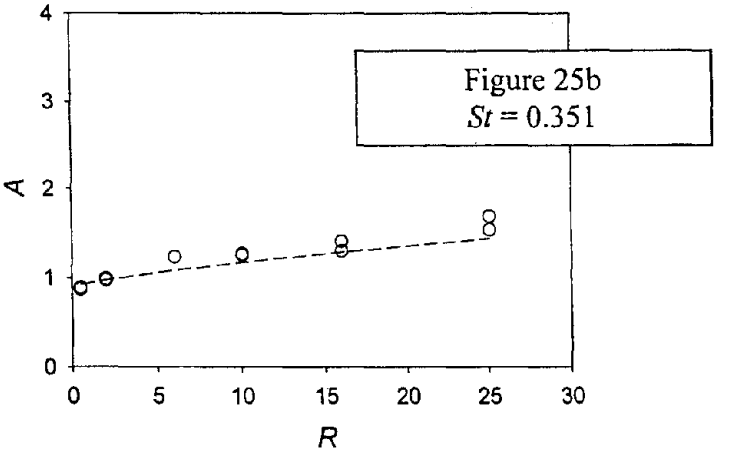
Figure 25b
St = 0.351
A
R
0
1
2
3
4
0
5
10
15
20
25
30

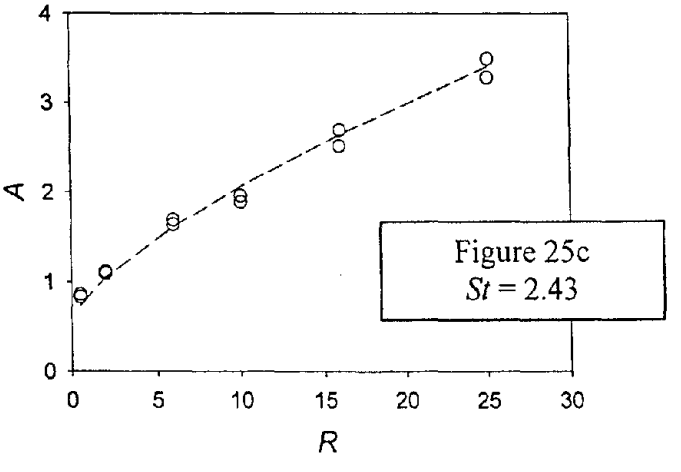
Figure 25c
St = 2.43
A
R
0
1
2
3
4
0
5
10
15
20
25
30

The effect of *St* on *A*: The effect of *St* on *A* is of the greatest general interest because it embodies the important role of particle size, which is the basis of particle size-selective criteria used to set aerosol standards and, in turn, guides the design of aerosol samplers. For a blunt sampler facing the wind under subisokinetic (i.e., $R > 1$) conditions, we now know from the new semi-empirical model for the blunt sampler that *A* increases with increasing *St*, and the rate of this increase is greatest when *R* is high. However, the effect of *St* on *A* is much weaker than for thin-walled samplers facing the wind. Thus, the sampler wall has a similar dampening effect on the influence of *St* on *A* as it does on the influence of *R* on *A*. Since, as described earlier, the general nature of streamlines near a blunt sampler is a 'divergent-convergent' pattern, one would have to attribute the presence of the converging portion as largely responsible for this dampening effect. This is the region where particles may 'impact' out of the sampled air flow and thus not be included in the collected sample. Of course, the relative sizes of the diverging and converging flow regions would be highly dependent on the degree of super or subisokinetic sampling. Another notable difference between the thin-walled and blunt sampling scenarios is the shape of their *A* curves. For thin-walled samplers, *A* begins to level off at large *St*-values, whereas for blunt samplers, *A* seems to increase steadily throughout the full range of *St*. For thin-walled samplers, given their simple airflow geometry, it seems intuitive that when *St* reaches a certain magnitude, any further increase in *St* would not increase *A* significantly because there is only a finite number of particles available to 'impact' into the flow. For blunt samplers, perhaps a higher *St*-value would be necessary to reach a ceiling limit of *A*, since the particles must travel through more complex flows involving both diverging and converging portions.

The effect of *r* on *A*: From the above, it has become apparent that sampler 'bluntness', represented here by *r*, reduces the influence of *R* and *St* on *A*. While it is clear that the mere presence of the disc largely reduces *A*, less is known about the effects of reducing or increasing the size of the disc. In the current experiment, two *r*-values are examined, 0.05 and 0.10. A comparison of measured *A* for these two samplers (see Figure 22) indicates that a larger *r*-value generally results in a larger measured *A*, irrespective of the values of *R* and *St*. This is to be expected since the sampler becomes physically closer to a thin-walled sampler as *r* approaches unity. However, as shown in Figure 22, it is very interesting to see that a two-fold increase in *r* produces approximately only a 15% increase in *A* (and perhaps even less when measuring orientation-averaged *A* under more 'realistic' conditions). This has important implications to real-world personal aerosol samplers, for which a reasonable practical assumption is that orientation is uniformly averaged from 0° to 360°. In the real-world scenario, relatively small samplers are placed on the body of the person whose aerosol exposure is to be assessed, in which case, the body of the wearer becomes, in the fluid mechanical sense, part of the overall blunt sampler system. For example, assuming a torso width of 300 mm and a sampling orifice diameter of 15 mm, as for the IOM sampler increasingly used by occupational hygienists, the resulting *r*-value is 0.05. If the torso width were reduced to 150 mm, for the same 15 mm orifice sampler, the resulting *r*-value would be 0.10. If the effect on *A* of doubling the *r*-value from 0.05 to 0.10 is small, then we would be able to say with confidence that the sampler mounted on the smaller torso would have a similar performance to that mounted on the larger torso. In relation to the testing of practical personal aerosol samplers (e.g., as described by Mark and Vincent, 1986; Kenny *et al.*, 1997; and others), this would in turn enable personal samplers to be tested in smaller, more practical, wind tunnels because such testing would no longer be constrained by the need to accommodate full-size mannequins. It would be interesting to more precisely define the

range of r within which the r-value has a minimal impact on A. This would provide more flexibility in choosing the size of the mannequins and sampler orifices, in accordance with scaling laws (Ramachandran *et al.*, 1998), when developing and testing particle size-selective samplers.

Conclusions from this part of the research

The study described in this chapter followed up the work described in the previous section for the aspiration efficiencies of idealized thin-walled nozzles facing the wind, extending the work to simple axisymmetric disc-shaped blunt samplers, also facing the wind. Such studies, while highly idealized, provide important insights into the aerosol sampling process that can be carried over to the interpretation of the performances of practical sampling devices like those used in the real world of occupational and environmental hygiene. In this way, these studies provide an important link with what follows in the rest of this report.

A large set of new experiments was conducted to determine A, as a function of St and r, and over an especially wide range of R. A comparison with the earlier model, with coefficients estimated by Chung and Ogden, indicated that the model overestimated A for R-values greater than about 2. As was the case for the classic Belyaev and Levin model for thin-walled samplers facing the wind, the original model was limited by the oversimplification of its empirical coefficients. When these were modified to take account of the effects of both R and r, the resulting new model was found to provide a very good fit with both the new experimental data and with the ones published earlier. Thus, the range of applicability of the new, modified model was greatly improved.

A particularly interesting and useful result was found in the effect of r on A. A two-fold increase in r produced only a 15% increase in A. This suggests that for many practical purposes, it may be assumed that changes in r may have a small effect on A. In relation to the testing of personal aerosol samplers in wind tunnels, this opens up the possibility of using smaller-than-life-size mannequins (or representative bluff bodies), and yet obtain results that remain meaningful in relation to full-scale. This work therefore lies firmly in the growing overall body of work aimed at identifying simpler and more manageable protocols for the testing of aerosol samplers, including the important related studies in the laboratory of Willeke and his colleagues (e.g., Witschger *et al.*, 1998; Aizenberg *et al.*, 2000).

7. Orientation-averaged aspiration efficiency of original and modified IOM samplers mounted on slowly-rotating bluff bodies

Introduction

We now move on to describe two sets of experiments intended to characterize the orientation-averaged aspiration efficiencies of IOM samplers mounted on rotating bluff bodies. The first set of experiments represented a logical next step from the investigation of disc-shaped samplers described in the previous chapter. IOM samplers were mounted on simplified, three-dimensional rectangular bluff bodies that were rotated horizontally at a slow constant rate. The orientation-averaged A-values were measured as functions of St, R and r. The samplers were mounted on bluff bodies to best simulate the performances of such samplers in the field, where they would be

mounted on actual workers. The second set of experiments focused on the effect of r on orientation-averaged A, for a much wider range of r than examined previously. These experiments were performed in response to the results obtained for the disc-shaped sampler study, which seemed to suggest that within a certain range, r would not have a large effect on A. The experiments were intended to satisfy our curiosity regarding the potential use of simplified, miniature bluff bodies to test and develop personal inhalable aerosol samplers.

Investigation of orientation-averaged aspiration efficiency A for a broad range of velocity ratio R and Stokes' number St

In the work described in earlier sections of this report, we looked closely at the effects of St, R and r on sampler aspiration efficiency. These investigations were important in determining the performances of thin-walled and blunt samplers under relatively simple sampling conditions. As useful as these studies were in increasing our collective knowledge in aerosol sampling, especially for wide ranges of R, aerosol sampling in the real world rarely occurs under such ideal conditions.

In order to address the reality that people do not usually face directly into the wind while they are working, a number of studies have investigated the A of the human head at various orientations with respect to the wind. Ogden and Birkett (1977) were the first to investigate this scenario. They measured A for a life-sized model human head and shoulders at 0°, 45°, 90°, 135° and 180° to the wind, for windspeeds ranging from 0.75 to 2.75 m/s, at breathing flowrates of 84 to 1340 ml/s, and for monodisperse particles with d_{ae} up to 30 μm. They concluded that, when the nose and mouth aspirated air at a constant rate, the human head behaved like a blunt sampler, with only small differences between nose- and mouth- breathing. The trends they observed when the nose and mouth were facing directly into the wind were broadly consistent with those predicted from the modified disc-shaped sampler model described in the previous chapter. For both the head and disc-shaped sampler, A-values were greatest for high R-values and lowest for small R-values, and the magnitude of these changes were greatest for large particles. When the model head was not facing into the wind, however, the A-values decreased as a function of d_{ae} (and hence, St) for all the conditions that were examined, with the exception of nose-breathing at a 45° orientation at $R = 8.4$. There was an approximately ten-fold variation in A (A ranged from 0.25 to 2.5) for all the different R-values and wind orientations that were examined. When the A-measurements of the model head were averaged across all orientations, the orientation-averaged A-values were found to lie within a much narrower range (from 0.3 to 1.2). Orientation-averaged A generally decreased as a function of d_{ae} and seemed to level off at around $d_{ae} = 30$ μm. This was true for the full range of R examined, which was determined to be 0.05 to 8.4. The decrease in orientation-averaged A was less marked, however, at relatively high R.

Ogden and Birkett's experimental data were limited to particles smaller than about 30 μm in d_{ae}. In order to examine the A of the human nose and mouth for particles up to 60 μm in d_{ae} and windspeeds up to 8 m/s, Armbruster and Breuer (1982) conducted a similar study using a model human head (without shoulders). Based on their published aspiration velocities for the nose and mouth, their R-values ranged from 0.13 to 5. Armbruster and Breuer observed very similar trends to those found in the Ogden and Birkett study. However, at increasingly large R-values and particle sizes, their calculated orientation-averaged A-values began to depart from those general

trends, increasing as a function of particle size. For both the nose and mouth, orientation-averaged A began to increase at around d_{ae} = 30 μm and it was greatest for d_{ae} = 60 μm. Since Ogden and Birkett only investigated particles up to 30 μm in d_{ae}, the two studies were complementary. The Armbruster and Breuer study, however, showed that even when the A of the nose and mouth were orientation-averaged with respect to the wind, R had a significant influence on A, especially for large particles. Vincent and Mark (1982) further expanded these investigations for particles up to d_{ae} = 100 μm. They observed similar trends for orientation-averaged A as those observed in the earlier studies and found that orientation-averaged A did in fact level off around d_{ae} = 30 μm and remained at around 0.5 for particles with d_{ae} all the way up to about 100 μm.

These studies became the basis of the inhalability curve, which has since been adopted as an international consensus standard for inhalable aerosol sampling. This convention assumed that, in general, a person has no preferred orientation with respect to the wind when he or she is working. Therefore, any sampler aimed to collect inhalable aerosol exposures to such individuals would have to conform to the inhalability curve. Ever since the standard was established, the development and testing of relevant sampling instruments has also usually involved the determination of A-values that were averaged across all orientations. This has been achieved either by rotating the mannequins at a constant rate (Kenny *et al.*, 1997), rotating them incrementally during sampling (Mark and Vincent, 1986), or measuring A at several orientations at once and averaging them in some appropriate way (Witschger *et al.*, 1998). Since the goal of the current experiments was to first determine how blunt samplers would perform in realistic field situations and then to use that knowledge as a basis for developing new samplers, the orientation-averaged A of IOM samplers, under various conditions, was examined. IOM samplers were chosen because of their simple geometries and because they incorporated cassettes that were capable of collecting all the particles that entered into their orifices. Thus, their performances reflected true aspiration efficiency. In order to achieve orientation-averaging, the bluff bodies were rotated slowly at a constant rate.

While attempts have been made to use mathematical models to predict A for samplers under orientation-averaged conditions (Tsai *et al.*, 1995b; Tsai *et al.*, 1996b), such models are largely semi-empirical by nature, containing up to 12 empirical coefficients. Earlier examination of the most recent model for such purposes suggested that it was not accurate for the wide ranges of conditions of interest in the current work (see Section 4). Therefore, no attempt was made to either improve the earlier models or develop new ones based on the newly obtained experimental data. However, such an exercise may be useful at some point in the future after more knowledge is gained about aerosol sampling under these relatively complex conditions.

To investigate orientation-averaged A, IOM samplers were mounted on both sides of a three-dimensional, rectangular bluff body, as shown in Figure 26. One of the IOM samplers contained a modified orifice adaptor, which effectively reduced the size of the orifice to 7.9 mm. This allowed both samplers to be mounted on the same bluff body, while allowing them to have different r-values. For the sake of simplicity and axial symmetry, the samplers were mounted centrally on the bluff body. While it was recognized that samplers are often asymmetrically located on the bodies of workers in practical sampling situations, a recent study had shown only small positional effects associated with the placement of samplers on mannequins (Kenny *et al.*,

1997). Other studies made similar simplifying assumptions about the position of test samplers on the body (Witschger *et al.*, 1998; Aizenberg *et al.*, 2000).

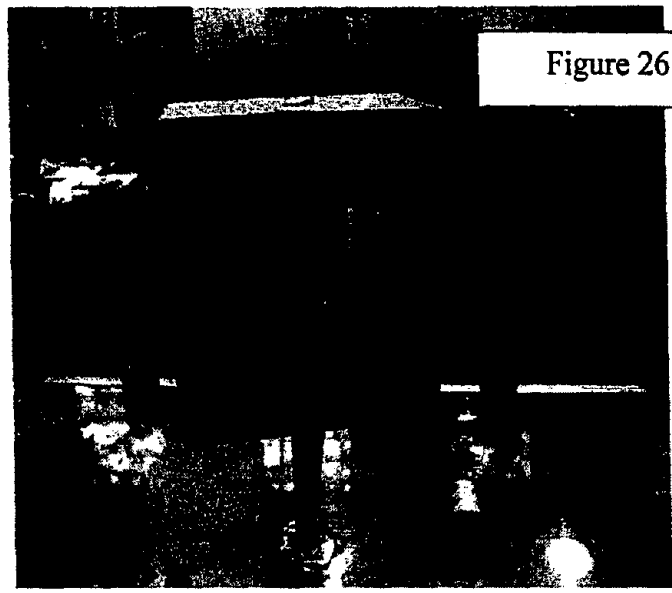

The dimensions of the bluff body were intended to reflect a simplified human torso. Its width-to-depth ratio was set at 2, which was intentionally slightly higher than the chest width-to-depth ratio determined from anthropomorphic data in order to account for the arms. Its width and depth were 120 mm and 60 mm, respectively, and its height was arbitrarily set equal to its width. The bluff body was rotated horizontally at a constant rate of 2 revolutions per minute (rpm) for orientation-averaging. The test sampler concentrations were measured using the gravimetric method, and reference concentrations were obtained from sharp-edged, isokinetic probes, after correcting them with the appropriate correction factors (as described in Section 4). As in the earlier experiments with thin-walled probes and disc-shaped samplers, fused-alumina powders of nominal grades F800, F400 and F240 were mechanically generated to produce aerosols of mass median d_{ae} 13, 34 and 89.5 μm, respectively.

Orientation-averaged A was determined for wide ranges of R and St, and for two values of r. Since U was kept constant at 1 m/s, R was varied by changing the sampling flowrate, providing an R-range from 2 to 15. Based on the different particle sizes that were investigated, St ranged from 0.03 to 3.08, and the two orifice diameters provided r-values of 0.125 (open circles) and 0.066 (open triangles), respectively. Three repeats were obtained for each combination of St, R, and r. The full experimental results for orientation-averaged A are shown below in Table 14 and they are displayed in graphical form in Figure 27. The dotted lines in the graphs represent model predictions from the disc-shaped sampler study described in the previous section.

d_{ae} (μm)	δ (mm)	D (mm)	r	Q (L/min)	R	St	*Orientation-averaged A*
13	7.9	120	0.066	1.47	2.0	0.06	0.98. 0.92, 1.07
13				0.50	5.9	0.06	1.29, 1.07, 1.08
13				0.20	15	0.06	1.76, 1.73, 1.49
34				1.47	2.0	0.44	0.64, 0.59, 0.74
34				0.50	5.9	0.44	0.43, 0.65, 0.59
34				0.20	15	0.44	1.67, 1.84, 1.50
89.5				1.47	2.0	3.08	0.52, 0.45, 0.50
89.5				0.50	5.9	3.08	0.86, 0.88, 0.68
89.5				0.20	15	3.08	3.15, 2.39, 2.20
13	15	120	0.125	5.3	2.0	0.03	0.98, 0.95, 1.05
13				2.0	5.3	0.23	1.13, 1.11, 1.06
13				0.71	15	1.62	1.49, 1.41, 1.31
34				5.3	2.0	0.03	0.77, 0.68, 0.73
34				2.0	5.3	0.23	0.58, 0.72, 0.61
34				0.71	15	1.62	1.45, 1.43, 1.44
89.5				5.3	2.0	0.03	0.68, 0.54, 0.60
89.5				2.0	5.3	0.23	0.82, 0.69, 0.75
89.5				0.71	15	1.62	2.38, 2.09, 2.10

Table 14

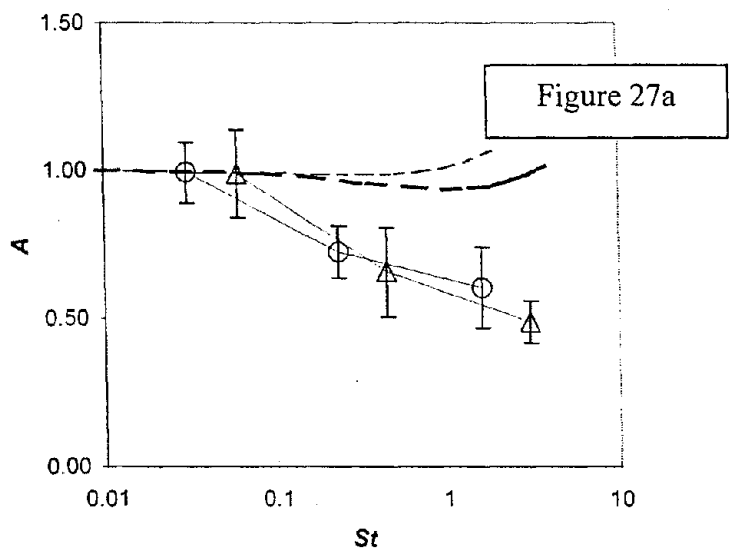

Figure 27a

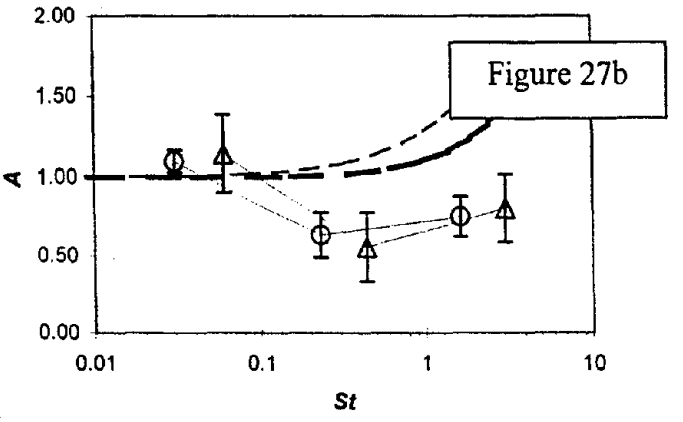

Figure 27b

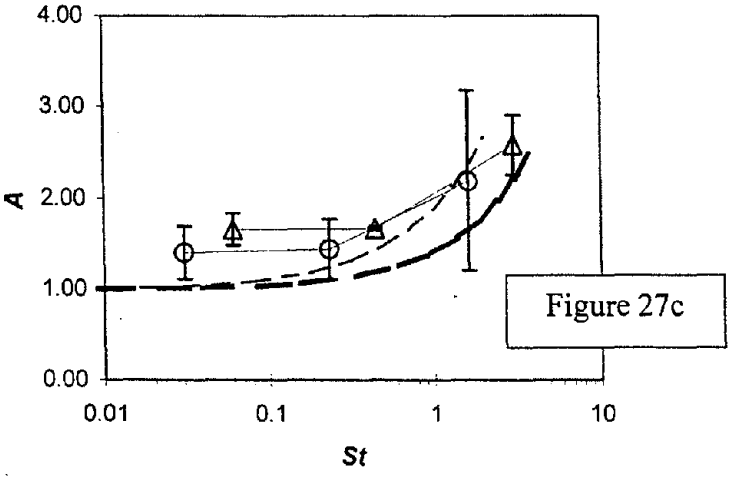

Figure 27c

The reproducibility of the data is seen to be generally good, though not as good as those obtained from the thin-walled sampler and disc-shaped sampler studies described earlier. This is to be expected since the conditions were more variable due to the rotation of the bluff body. Nevertheless, the relative standard deviation (RSD) values determined for most of the data (for the same set of conditions) are less than 10%, though they are generally higher for the larger particles. All sample masses exceeded the *LOQ* of 0.67 mg.

The general trends from the graphs show that orientation-averaged A decreases with increasing St for relatively low R-values ($R = 2$ and $R \approx 5.6$). For high R ($R = 15$), orientation-averaged A increases with increasing St. The graphs also show that A generally increases with increasing R. The magnitudes of these increases are highest for large St-values. As a side note, in Figure 27b, the R-values corresponding to the two samplers were slightly different[1], but they are deemed to

[1] Before the experiments were conducted, it was recognized that an IOM sampler with a smaller, modified orifice would be capable of operating at a lower flowrate than the original IOM sampler for equivalent values of R. Since part of the overall goal of the research was to develop a prototype low-flowrate personal inhalable aerosol sampler, there was interest in comparing the performance of this modified, low-flowrate IOM sampler with the original sampler. For the comparison, the flowrate of the modified IOM sampler was

be close enough to permit a graphical comparison of the performances of the two samplers under roughly equivalent conditions of R. Inspection of the data and confidence intervals indicates that there are no statistically significant differences in A (at the 95% confidence level) for the two r-values that are tested, for all conditions of R and St.

One of the goals of this study was to see how the performances of blunt aerosol samplers would change if they were placed at orientations with respect to the wind that were averaged over 360°, as opposed to when they were facing the wind (especially for large R-values). In order to make this comparison, the predicted values of A from the improved model in the disc-shaped sampler study (described in the previous section) were compared with the current experimental data, for equivalent values of St, R, and r. The comparison was made under the assumption that the different shapes of the samplers (where the bluff body was regarded as part of the sampler body in the case of the IOM sampler) would account for only small differences in A, compared to the more dominant effects of R, St, and possibly r. Earlier, Ogden and Birkett (1977) had concluded that detailed facial structure had little effect on the aerosol concentrations measured by model human heads.

Figure 27a clearly shows that, by rotating the bluff body and collecting orientation-averaged concentrations, A decreased with increasing St. At $R \approx 5$, (shown in Figure 27b), the orientation-averaged A-values initially decreased with increasing St (as they do in Figure 27a), but then increased at the highest St-value. Armbruster and Breuer (1982) had observed this exact same trend, at similar R-values when they examined the aspiration efficiency of human head models for windspeeds up to 8 m/s. In both Figures 27a and b, the comparison between the experimental data and model predictions is striking – the model prediction curves (from the disc-shaped sampler study) seem to very influential in pulling the orientation-averaged A-values upward at high St-values.

At $R = 15$, as shown in Figure 27c, R seems to play an even larger role in influencing orientation-averaged A. At this point, the orientation-averaged A measurements are almost indistinguishable (though slightly higher, overall) from those predicted by the facing-wind model. Here, R becomes the predominant factor in determining sampler performance, negating the seemingly secondary effects of sampler orientation and its associated effects on the influence of St. This trend had not been observed in the earlier studies because, prior to these experiments, such high values of R had never been tested. Such new knowledge opens up the new possibility of defining a threshold value of R above which the performances of samplers are not significantly affected by sampler orientation and can thus be predicted by models such as the one developed for disc-shaped samplers facing the wind. If this could be established, it would greatly enhance the ability to predict the performances of practical samplers under well-defined sampling conditions, since the aspiration efficiency models for samplers facing the wind are inherently much less complex than those for samplers at various wind orientations.

For the two values of r tested in these experiments, there were no significant differences in orientation-averaged A. This confirmed suspicions first raised in the earlier disc-shaped sampler study (see Section 6), which indicated that a two-fold difference in r does not have a large

---

somewhat arbitrarily set at 0.5 L/min. As a result, the R-value for the modified sampler was 5.88, compared to an R-value of 5.3 for the original IOM sampler operating at 2 L/min.

influence on A. In the current experiments, the effects of a similar two-fold difference in r on orientation-averaged A were even smaller. In fact, the two cases were statistically indistinguishable. The rotation of the bluff body seems to have reduced the effects of r on A. The question then remains: how far can the range of r can actually be stretched and still have a negligible influence on orientation-averaged A? Knowledge of this range would greatly aid in the development and testing of aerosol samplers, both personal and area, since it would provide information about the appropriate size of mannequins for testing personal samplers or the size of the instruments themselves, in developing area samplers. Such knowledge may also question the necessity of even using mannequins at all for testing personal samplers in the future. These issues will be explored in the next section.

Investigation of orientation-averaged aspiration efficiency A for a broad range of dimension ratio r

For the development and testing of personal inhalable aerosol samplers, the traditional protocols utilized so far by various researchers have had some common features. The samplers were usually mounted on life-size mannequins in large cross-section wind tunnels, and the mannequins were rotated continuously or stepwise, yielding orientation-averaged data for A. These protocols, however, were very expensive and time-consuming, due to the fact that the large wind tunnels themselves were quite expensive and they required large amounts of aerosol be generated inside them. There were also problems in maintaining uniform velocity and concentration profiles over the wind tunnel cross-sections, resulting in relatively poor reproducibility of experimental data. To combat these problems, alternative approaches have been sought for the development and testing of samplers. One such approach was recently proposed by Witschger *et al.* (1998) and Aizenberg *et al.* (2000). They described a simplified test protocol using an idealized, smaller-than-life-size torso, initially in a large wind tunnel but with the expectation that such a protocol may be used in smaller wind tunnels in the future. The simplified torso allowed the simultaneous measurement of aerosol concentrations at three or four different orientations with respect to the wind, thus reducing the number of experiments that needed to be conducted. Orientation-averaged A was determined as the average A of three or four wind orientations (0°, 90°, 180°, etc.). The later study (Aizenberg *et al.*) compared the performances of four commercial inhalable aerosol samplers used in conjunction with their simplified torso to those obtained from a life-size mannequin, and they found no statistically significant differences in sampler performance. Another approach, first proposed by Ramachandran *et al.* (1998), involved the use of scaling relationships between two physically equivalent sampling systems, where both the size of the mannequin and sampler would be scaled-down, to simulate aerosol performance in the full-scale using experiments conducted at a model-scale. This approach was investigated in the current research and it is one of the topics covered in the next section.

Regardless of which approach was used, there has been much speculation about the role of the bluff body in influencing sampler performance. Both the results from the earlier disc-shaped sampler study and those from Witschger and his colleagues' studies suggested that the size of the bluff body, as embodied in r, may not be significant over certain ranges of r. The purpose of this investigation, then, was to test the performance of the IOM sampler for a wide range of r in order

to potentially identify an r-value where it would in fact be significant in determining orientation-averaged A.

Two bluff bodies were employed for these next experiments, and both of them had a width-to-depth ratio of 2. However, these bluff bodies were modified from the previous ones in order to enable the samplers to be recessed into the body. This was done to better represent the way samplers would actually be mounted on workers in the real world, where the samplers would not project out significantly beyond the worker's torso, relative to the size of the torso. The modified bluff body is shown in Figure 28. The decision to modify the bluff body was also based on the slight positive bias in A that was found when IOM samplers were mounted on the original bluff body. Prior to this investigation, a small number of experiments were carried out with IOM samplers mounted on the original bluff body and the modified bluff body, respectively, to compare their performances. In order to magnify any differences in A, the samplers were tested directly facing into the wind, with R = 15, D = 120 mm, δ = 15 mm and d_{ae} = 13 μm. In the interest of time, only two repeats were done for each sampling configuration. The IOM sampler mounted on the original bluff body provided A-values of 1.55 and 1.47 and the IOM sampler mounted on the modified bluff body provided A-values of 1.16 and 1.22. These values were compared to those collected for a disc-shaped sampler (also tested in the wind tunnel) under the same exact conditions. It was found that the IOM sampler mounted on the modified bluff body provided very similar concentrations to those measured by the disc-shaped sampler (the disc-shaped sampler measured A-values of 1.21, 1.19 and 1.23), but significantly lower concentrations than those provided by the IOM sampler on the original bluff body. These results, in addition to the theoretical knowledge that A should be close to 1 for relatively small particles with low inertia, suggest that the modified bluff body would produce more accurate measurements of A in future experiments. The comparison between the performances of the IOM sampler on the modified bluff body and the disc-shaped sampler also suggests that their differences in shape did not significantly affect their measured A-values.

Figure 28

This provides some assurance that the correct assumptions were made in the previous study regarding the shapes of blunt samplers, that these shape effects were in fact secondary to the more dominant effects of St, R, and possibly r, in influencing orientation-averaged A.

For these experiments, IOM samplers were again chosen as representative blunt samplers, and they were tested in a variety of sampler configurations. Since the effects of R were investigated in the previous study and were well characterized, R was kept constant at 5.3 for these experiments. This R-value corresponded to an original IOM sampler operating at 2 L/min at a windspeed of 1 m/s, and it was partly chosen to see how the IOM sampler, operated at its prescribed flowrate, would perform against the inhalability curve when mounted on miniature bluff bodies or when used as a stand-alone sampler. As in the previous study, the IOM samplers were centrally mounted on the rotating bluff bodies and isokinetic samplers were used to measure the reference concentrations.

Now, two bluff bodies were used, with widths of 120 mm and 75 mm, respectively. In addition, the IOM sampler was mounted without any bluff body at all (i.e., it was suspended in the wind tunnel in isolation). Here, it is noted that the IOM sampler body itself had a width of 37 mm. Since the orifice diameters were 15 mm for all the sampling configurations, r-values of 0.125, 0.2 and 0.4 were achieved. Based on three particle sizes of fused alumina (d_{ae} = 6, 34, and 89.5 μm), St ranged from 0.003 to 1.62. Four repeats were done for each combination of r and St.

The experimental results are shown in Figure 29 (with open circles for r = 0.125, open triangles for r = 0.2 and crosses for r = 0.4). In general, it is seen that orientation-averaged A decreases with increasing St, as expected for inhalable aerosol samplers. In addition, there is a slight increase in A for the largest St-value, which probably reflects the influence of R (as concluded in the previous study for the disc-shaped blunt samplers). However, there are no statistically significant differences in performance[2] for the three sampling configurations. This is somewhat surprising in the view of the large range of r covered.

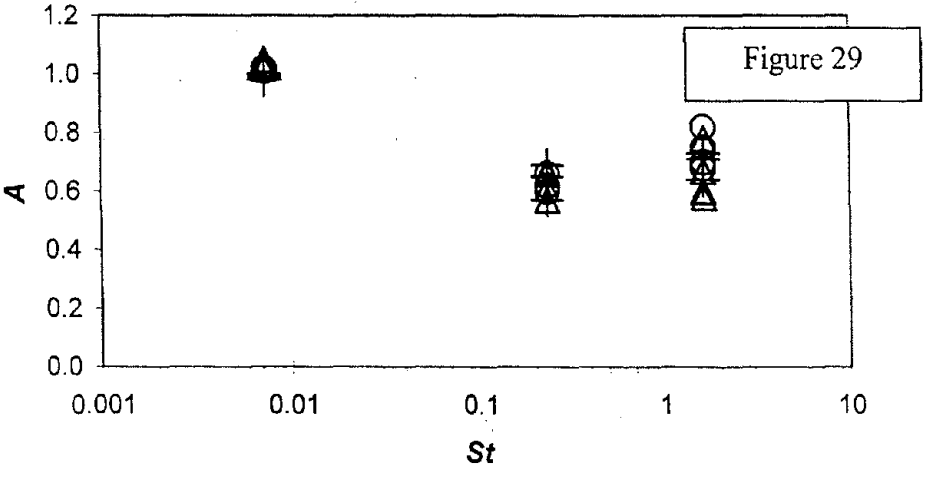

Figure 29

[2] One-way ANOVA was used to compare the A-values of the three samplers at each particle size at the 95% confidence level.

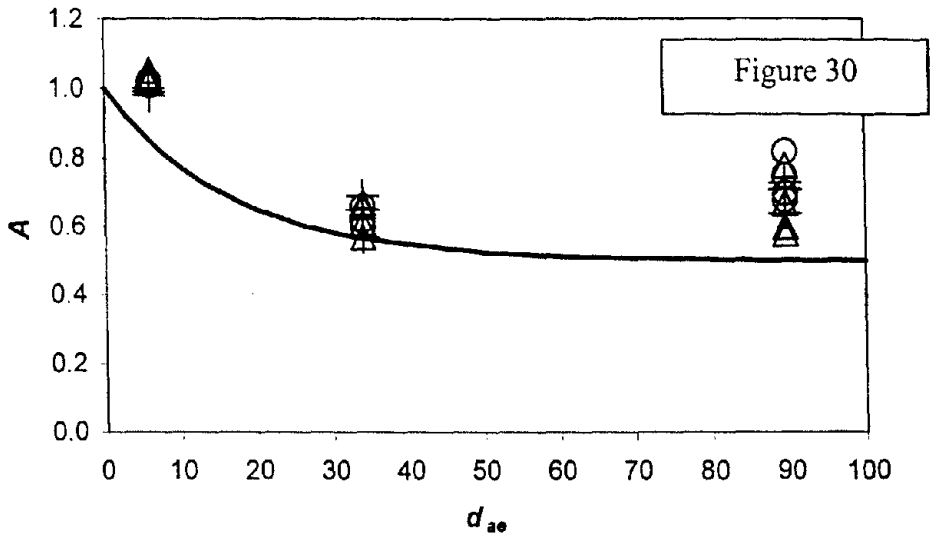

In order to compare how the IOM sampler performs against the inhalability curve in these experiments, Figure 30 presents the same results, this time expressing orientation-averaged A as a function of d_{ae} (since inhalability is defined in that way). Compared with the inhalability curve, the IOM sampler at its various configurations provides slightly higher A-values. But the fact that the data are reasonably close to the inhalability curve provides further evidence that the size of the bluff body plays only a minimal role in influencing the performance of the samplers (since the inhalability curve represents the performance of an IOM sampler when mounted on a life-size mannequin).

These experiments show no statistically significant differences in the performances of the three IOM samplers, for $r = 0.125$ to 0.4. Combined with knowledge gained from the previous study for the disc-shaped blunt sampler, orientation-averaged A was found to be independent of r over the full range from 0.066 to 0.4. Practically speaking, an r-value of 0.066 would correspond to an IOM sampler mounted on a 230 mm-width bluff body. This is about two-thirds the width of a typical life-size mannequin. An r-value of 0.4 would correspond to an IOM sampler by itself. By showing no differences in performance for these two vastly different sampling configurations, this investigation suggests that the IOM sampler would collect the inhalable aerosol fraction even when used as a stand-alone sampler.

It is important to note, however, that these observations were made for the specific sets of conditions investigated in the study. Only three particle sizes were examined and R was constant for all the experiments. While these observations may hold true for even a wide range of R, as minimal r effects were found for $R = 2$ to 15 in the previous study, more experiments would be needed to confirm such a surprising result. It would also be interesting to see if there is in fact a threshold r-value where r does significantly influence the orientation-averaged A. Or it may be the case that A is not significantly affected by r at all when it is orientation-averaged, in contrast to A for blunt samplers facing the wind, where r has been shown to play an obvious large role in determining A, especially in the comparison between thin-walled and disc-shaped samplers, as described earlier. In addition, while the IOM sampler performed reasonably well against the inhalability curve even though it was not used in the way it was designed to, all the sampling

configurations slightly overestimated orientation-averaged A compared to the curve. Since there was no obvious explanation for this bias, further discussion must be deferred to future investigations. Nevertheless, these observations provide evidence to suggest that the IOM sampler might not need to be mounted on life-size bluff bodies, or possibly even on bluff bodies at all, to accurately collect the inhalable aerosol fraction.

Conclusions from this part of the research

The first set of experiments described above are instrumental in establishing a hierarchy of effects on orientation-averaged A. It is clear that compared to r, St has a much larger influence on A. This is clear from the data where, for given R-value, A is seen to be primarily determined by St, and not by r. It is also clear, however, that the effects of St are overpowered by the effects of R in some cases. The pattern of behavior observed in Figures 27a and b, where the orientation-averaged A decreases as a function of St, no longer applies for $R = 15$. Here, the effects of sampler rotation appear to be greatly reduced, and the experimental measurements are very close to those for disc-shaped samplers facing directly into the wind. That notwithstanding, when considering the effects of R and St on orientation-averaged A, it would be difficult to say that one is more important than the other. The effects of R are greatest at high St-values, and the effects of St are greatest at high R-values. Both R and St, therefore, work synergistically in affecting orientation-averaged A. As seen in earlier sections, this had also been true for both thin-walled samplers and blunt samplers facing the wind, where the increase in A was greatest for high R and St-values. Thus, as concluded in those earlier studies, R and St are considered to be the most important factors in determining A, even when A is orientation-averaged with respect to the wind. As new knowledge had been obtained in the investigation of thin-walled and blunt samplers facing the wind at large velocity ratios, similar new knowledge has also been obtained for blunt samplers at averaged orientations with respect to the wind at large velocity ratios.

The effect of r discussed here presents a very intriguing question about the role of bluff bodies in testing personal samplers. While it is clear that, within the range of r tested in the first set of experiments, r has a negligible effect on orientation-averaged A, it is still not yet known how far the range of r might be stretched and yet still have a negligible effect. In addressing this question, the second set of experiments was conducted to investigate the orientation-averaged A of IOM samplers for a much wider range of r. Two important observations were made from the experimental results. One was that the orientation-averaged A for IOM samplers, plotted as a function of St, does not change for an r-range of 0.066 to 0.4. This is tantamount to saying that an IOM sampler mounted on a near life-size mannequin would provide the same aerosol concentration as one not mounted on anything. The second observation is that the aspiration efficiency curve of the IOM sampler is reasonably close to the inhalability curve. This provides further evidence that the bluff body itself does not play a major role in influencing orientation-averaged A.

Based on what has been learned from these two experiments, particularly regarding the effects of R and r on orientation-averaged A, a foundation has been established set for the development and testing of a new prototype inhalable aerosol sampler.

8. Development of a new low-flowrate prototype personal inhalable aerosol sampler

Introduction

We now describe the development of a low-flowrate prototype personal inhalable aerosol sampler. The development process took place in two main steps. The first step was the validation of the small-scale sampler testing system for testing personal inhalable aerosol samplers. Here, the results from the previous section suggest that the size of the bluff body on which samplers are mounted may not be an significant factor in determining their performances, at least over a broad range. Based on this observation, the performance of an IOM sampler mounted on a miniature, rotating bluff body in the small-scale system was determined for a large range of particle sizes, and these results were compared to those obtained from full-scale systems using large wind tunnels and life-size mannequins. The second step, addressed in this section, is the design and testing of the prototype sampler itself, using dimensional scaling principles. The prototype sampler is an exactly scaled-down version of the IOM sampler, where the orifice size and flowrate were reduced to achieve the same R and r as that of the IOM sampler mounted on a life-size mannequin. For the validation of the prototype sampler, its performance results were compared to both the inhalability curve and the performance of the IOM sampler in the small-scale system.

Background

Before moving on to the actual development of a new, prototype personal inhalable aerosol sampler, it was necessary to validate the performance of a reference inhalable aerosol sampler in the small-scale sampler testing system (i.e., the small wind tunnel and miniature bluff body), and thus validate the small-scale sampler testing system itself. As discussed earlier, two alternative approaches have recently been considered in the testing of such samplers in wind tunnels that are too small to accommodate life-size mannequins. The first approach was adopted by Witschger *et al.* and Aizenberg *et al.* when they proposed that samplers be tested on smaller-than-life-size, simplified bluff bodies, rather than on life-size mannequins, with the assumption that the performance of the samplers would not be significantly different in the two cases. They in fact found that the performances of four personal inhalable aerosol samplers obtained in their testing scheme were not significantly different than those obtained when they were mounted on life-size mannequins. The validity of this approach was also confirmed during the present research in the investigation of the effect of r on orientation-averaged A (described in the previous section), where it was found that over a large range of r, r did not have a significant effect on orientation-averaged A. The second approach was proposed by Ramachandran *et al.* (1998), and this involved the use of scaling relationships between two physically equivalent sampling systems, where both the size of the mannequin and sampler would be scaled down, to simulate aerosol sampler performance at full-scale using experiments conducted at small-scale. While this approach has been extensively theorized, it has not yet been tested experimentally. Since all the experiments in the current research were conducted in a small wind tunnel, one or both of these approaches needed to be taken in developing and testing inhalable aerosol samplers.

For the validation of the small-scale sampler testing system, the first approach was taken, and experiments similar to those described in the previous section were conducted. There the results

had suggested that the IOM sampler mounted on a small, rotating bluff body would still measure the inhalable aerosol fraction. However, only three particle sizes were tested. For a better comparison of the IOM sampler's performance against the inhalability curve and against those data obtained from large wind tunnels using life-size mannequins, orientation-averaged A-values were determined for six particle sizes.

For the dual purpose of developing a new, low-flowrate personal inhalable aerosol sampler and providing another validation of the small-scale sampler testing system, a dimensional scaling approach was adopted, where the new sampler was simply a scaled-down version of the original IOM sampler. This sampler was realized by incorporating an orifice adapter into the orifice of the original IOM sampler, effectively to reduce the size of the orifice to 6 mm. Both the orifice and sampling flowrate were scaled down so that the resulting r and R-values, respectively, were equivalent to those of the original IOM sampler mounted on a life-size mannequin in a large wind tunnel. To test the validity of the dimensional scaling approach in both the development of a new sampler and in the validation of the small-scale sampler testing system, the performance of the scaled-down IOM sampler was compared to the inhalability curve and the earlier large wind tunnel data, respectively. As a further, and perhaps more accurate, test of the prototype sampler's performance as an inhalable aerosol sampler, its performance was compared to that of the IOM sampler in the small-scale sampler testing system (as determined during the first validation of the small-scale sampler testing system). This comparison represented perhaps the most direct comparison against the inhalability criterion in the sense that, here, both samplers were subjected to the same conditions inside the small-scale sampler testing system. Therefore, any biases from using the small-scale sampler testing system, if present, would be reflected in both samplers, with the expectation that those biases would disappear if both samplers were operated at full-scale. As in the testing of the IOM sampler, orientation-averaged A-values were determined for six particle sizes.

Correction factors for appropriate calculations of aspiration efficiency

As shown earlier, the average particle concentrations changed as a function of their positions along the axis of the wind tunnel, due to particle settling and remixing, and the changes depended on the size of the particles and windspeeds. For a given experiment, in order to determine the true reference concentration for total aerosol at the location of the test sampler (which was located downstream from the isokinetic probe), a correction therefore needed to be applied to the isokinetic probe concentration. However, only three particle sizes were examined previously. In the new experiments described in this section, six particle sizes were tested. So a similar exercise needed to be done to determine the correction factors for these six particle sizes.

For the sake of improved accuracy, correction factors were now determined for eight particle sizes in the range of d_{ae} up to close to 100 μm range, including all six particle sizes that were examined in the study. Since the windspeed was kept constant at 1 m/s in these and all the subsequent experiments, corrections factors were determined only for this windspeed. Each correction factor (for each particle size) was determined as the average of three concentration ratios. The concentration ratios of isokinetic samplers placed 0.7 m and 1.2 m from the turbulence grid and along the center axis of the test section were determined. These locations

represented the positions of the isokinetic samplers and test samplers, respectively, for the main body of the research.

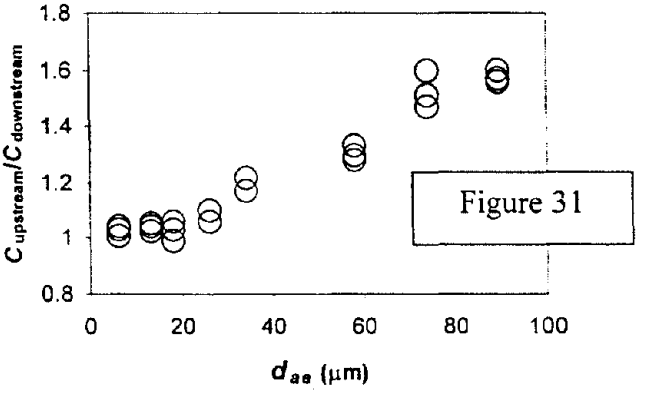

In determining A for the test samplers, correction factors equivalent to the ratio of concentrations measured at the upstream and downstream positions, respectively, were applied to the isokinetic sampler measurements (located upstream) to obtain true reference concentrations in the downstream positions. The ratios consistently increased as a function of d_{ae}. That is, the difference in total aerosol concentration from the upstream to downstream position was greater for larger particles. This trend is shown in Figure 31. The trend is not surprising since it is expected that gravity would play a larger role in reducing concentrations for larger particles due to particle settling. While it would be possible to obtain a smooth curve and regression equation based on these data, the actual average concentration ratios are used as correction factors for the current investigation since they are available for each particle size that was examined. The reproducibility of the concentration ratios is very good – the relative standard deviation (RSD) at each particle size was found to be less than 5%.

Validation of the small-scale sampler testing system

For these experiments, IOM samplers were centrally mounted on both sides of a 120 mm x 120 mm x 60 mm rotating bluff body (see earlier Figure 28). The flowrate was set at 2 L/min, which was prescribed for collecting the inhalable aerosol fraction in the original version of this instrument. As in the earlier experiments, U was kept constant at 1 m/s. Thus, R was constant at 5.3 for all the experiments. The r-value was also constant at 0.125. Fused-alumina powders of nominal grades F1200, F600, F400, F320, F280 and F240 were mechanically generated to produce aerosols of mass median d_{ae} 6, 18, 34, 58, 74 and 89.5 μm, respectively. Orientation-averaged A was determined as a function of d_{ae}, and four repeats were conducted for each particle size. For a direct comparison against the inhalability curve and large wind tunnel data, Figure 32 shows orientation-averaged A as a function of d_{ae}. Here the solid circles are our new data, while the closed circles are from Kenny *et al.* (1997) and the closed triangles from Mark and Vincent (1986).

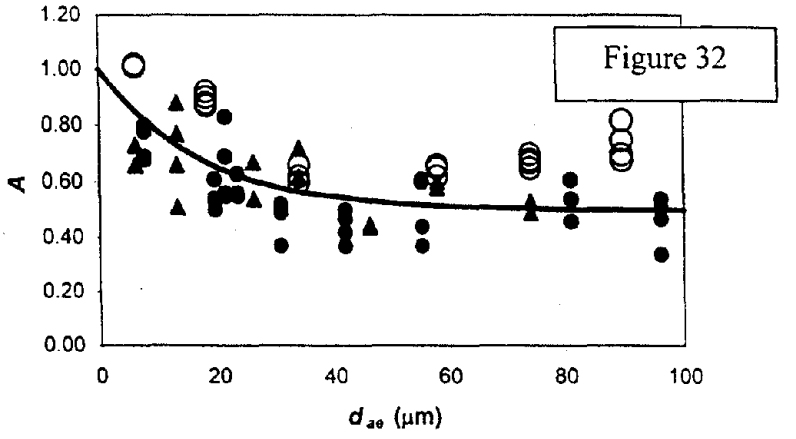

The reproducibility of the data is very good. The relative standard deviation (RSD) is seen to be less than 5 % for all particle sizes, except for the 89.5 μm particles, for which the RSD is 8 %. All sample masses exceeded the *LOQ* of 0.67 mg. By contrast, the RSDs of the earlier large wind tunnel data were as high as 22% for both Kenny *et al.* and Mark and Vincent for similar ranges of particle size.

The performance of the IOM sampler in the small wind tunnel is reasonably close to that of IOM samplers in large wind tunnels and to the inhalability curve. However, there does appear to be a small bias[3], with the IOM sampler in the small wind tunnel slightly over-sampling in relation to the IOM samplers in the large wind tunnels. The results, however, are consistent with those described in Section 7 for the same conditions, where orientation-averaged A began to increase for large particles after showing a plateau beginning at around 30 μm. One plausible reason for the bias between the small and large wind tunnel data is the fact that correction factors are applied to the isokinetic probe concentrations in the small-scale sampler testing system to account for particle losses due to gravity. Such corrections had not been considered in those earlier large wind tunnel experiments cited above. The corrections effectively reduce the reference total aerosol concentrations (c_0) used in the calculation of aspiration efficiency ($A = c/c_0$). If A-values determined in this way are compared to those where gravity corrections are not made, the former A-values would indicate an apparent over-sampling of aerosols compared to the latter A-values. Such effects would be greatest for large particles, due to the greater gravity corrections. In fact, Figure 32 shows that the bias is indeed greatest for the largest particles. Another possible reason for the bias is the fact that the Re_f (for the bluff body flow) in these studies (about 8,000) is significantly lower than that for the full-scale studies (about 20,000). Very recent emerging data have suggested that such Re_f-dependent effects may exist at these ranges of Re_f (Brixey *et al.*, as yet unpublished). Finally, other possible reasons are the differences in the shape and orifice location of IOM samplers mounted on small bluff bodies compared to those of IOM samplers mounted on life-size mannequins. The exact mechanisms for such biases are unknown. The biases, however, are probably not due to the difference in actual size of the bluff body and mannequin, since such biases were not observed for differences in r over a large range of r (see Section 7). In any case, these experiments confirm that while small

[3] The average difference in orientation-averaged A for the IOM sampler in the small wind tunnel versus the inhalability curve was 0.16, across all particle sizes.

positive biases are found, the small-scale sampler testing system overall is able to produce results for the IOM sampler that are similar to those obtained from large wind tunnels.

For the validation of the dimensional scaling approach first proposed by Ramachandran *et al.* (1998), a scaled-down version of the IOM sampler was developed. The sampler and bluff body were designed so that R and r would be equivalent to that of a full-size IOM sampler mounted on a life-size mannequin. According to Ramachandran *et al.* and Kenny *et al.* (2000), by keeping dimensionless variables such as R and r equivalent for the small-scale and large-scale sampler testing systems, and comparing the performances of the samplers across the same range of St, the measured orientation-averaged A-values would be equivalent for both systems. This is because orientation-averaged A is considered mainly as a function of R, r, and St. So, by keeping these dimensionless variables constant, the resulting A-values would also be constant.

Assuming that the original IOM sampler operates at a flowrate of 2 L/min and is mounted on the torso (say, 300 mm in width) of a life-size mannequin, the resulting R and r-values are 5.3 and 0.05, respectively. For a particle size range of 8 to 96 μm, which was the range of the large wind tunnel data, the corresponding St range is 0.007 to 1.87. To achieve the same r-value in the small-scale, the bluff body was scaled down from 300 mm to 120 mm in width and the orifice was scaled down from 15 mm to 6 mm in diameter. Likewise, in order to achieve the same R-value with the scaled-down orifice, the flowrate was reduced from 2 L/min to 0.32 L/min. For a particle size range of 6 to 89.5 μm, the corresponding St range in the small-scale system was 0.018 to 4.05. Table 15 shows a comparison of the specifications for both the original IOM sampler and the scaled down IOM sampler. To achieve the small geometry of the scaled-down sampler, the entry of the original IOM sampler was modified simply by adding a faceplate with the smaller orifice. The original and modified IOM samplers are shown in Figure 33 (see below).

	FULL-SCALE (Mark and Vincent, 1986; Kenny *et al.*, 1997)	**SMALL-SCALE** (present work)
d_{ae} (μm)	8 to 96	6 to 89.5
δ (mm)	15	6
D (mm)	300	120
U (m/s)	1	1
Flowrate, Q (L/min)	2	0.32
St	0.007 to 1.87	0.018 to 4.05
R	5.3	5.3
r	0.05	0.05

Table 15

For the experiments, scaled-down IOM samplers were centrally mounted on both sides of the rotating bluff body. Orientation-averaged A was determined for an St range from 0.018 to 4.05, using six particle sizes, and four repeats were obtained for each particle size.

The reproducibility of the data is very good – the RSD is less than 10 % for the full range of St that is being tested. Figure 34 shows that for the same conditions of R and r, and over the same range of St, the scaled-down IOM sampler has similar orientation-averaged A-values (triangles) as those obtained by the IOM sampler in large wind tunnels (solid circles and triangles for the

Kenny *et al.* and Mark and Vincent studies respectively). For *St*-values above about 2, direct comparison between the small and large wind tunnel data is not possible. As observed for the IOM sampler in the previous section, however, the scaled-down IOM samplers do seem to slightly over-sample compared to IOM samplers in the large wind tunnels, perhaps for the same reasons stated earlier. In any case, the general closeness of the data obtained in the small-scale and large-scale sampler testing systems indicates much promise for the dimensional scaling approach.

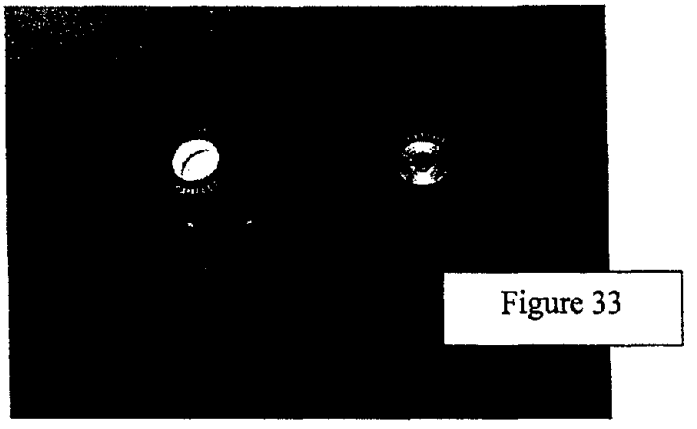

Figure 33

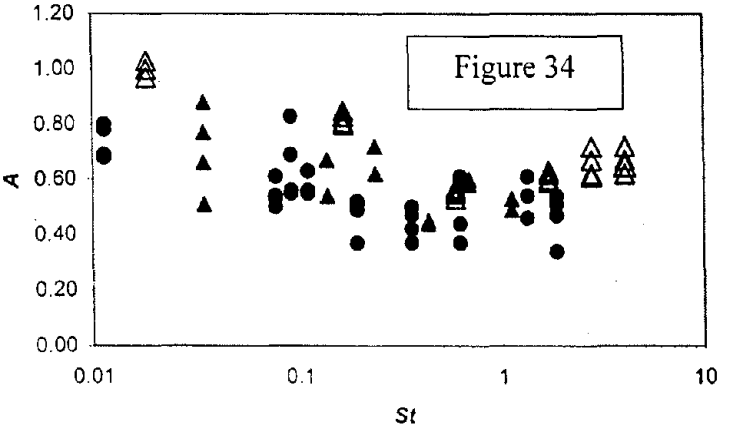

Figure 34

Development of a new, low-flowrate, personal inhalable aerosol sampler

The experiments on dimensional scaling approach had two main goals. The first was to test the validity of the dimensional scaling approach in designing small-scale sampler testing systems that could produce results comparable to those that would be obtained in full-scale sampler testing systems. This has been achieved. The second goal was to test the validity of the dimensional scaling approach in the development of new samplers by (a) comparing the performance of a scaled-down IOM sampler with the inhalability curve, and (b) comparing the performance of the scaled-down IOM sampler with that of a full-scale IOM sampler, when both were mounted on miniature bluff bodies in the small-scale sampler testing system.

As mentioned in the previous section, the reproducibility of the data is very good. Specifically, the RSD is less than 5 % for 6, 18, 34 and 58 μm particles, and the RSD is 8 and 6 % for 74 and 89.5 μm particles, respectively. All the samples, except for the ones corresponding to 89.5 μm particles, exceeded the *LOQ* of 0.67 mg. It was difficult to obtain large enough samples for the 89.5 μm particles because of the low sampling flowrate and tendency of the air compressor to overheat after running for extensive periods of time. The 89.5 μm samples did exceed the *LOD*, however, and their masses were approximately half that of the *LOQ*.

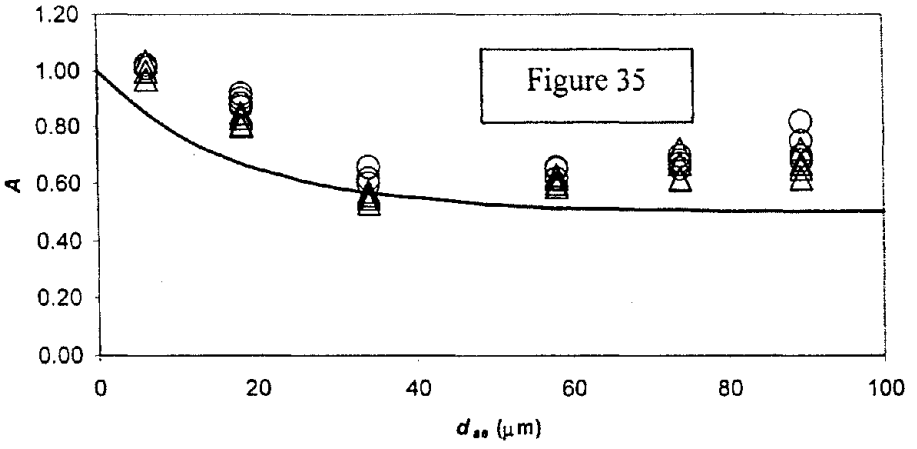

Figure 35 shows the performance the new sampler with respect to the inhalability curve (open triangles). This time, orientation-average A is expressed as a function of d_{ae} (since the inhalability curve is defined in this way). It is clear from this figure that the new sampler does indeed measure the inhalable aerosol fraction, evidenced by the close proximity of its performance with the inhalability curve. Figure 35 also shows that the performance of the scaled-down IOM sampler is nearly equivalent to that of the original IOM sampler (open circles) when both are tested on the same bluff body. There are no statistically significant differences (at the 95% confidence level) for any of the particle sizes that are examined. While it is clear that when compared against the inhalability curve, the scaled-down sampler does show a slight positive bias[4], when compared against the IOM sampler, these biases disappear. The small biases, therefore, may be attributed to the samplers being tested in the small-scale sampler testing system for the reasons suggested earlier. It is likely that the bias in the performance of the scaled-down IOM sampler would disappear, as it does for the full-size IOM sampler, if the former were mounted on a life-size mannequin in a large wind tunnel, or if it were mounted on actual workers in practical settings.

Conclusions from this part of the research

The experiments presented in this chapter marked a culmination of the laboratory phase of the research. The knowledge gained from the ideal sampling scenarios of thin-walled and disc-shaped samplers facing the wind was used to design increasingly complex experiments which

[4] This bias was slightly smaller than that obtained from the earlier comparison of the IOM sampler on the modified bluff body and the inhalability curve. The average difference in orientation-averaged A-values across all particle sizes, in this case, was 0.12.

ultimately led to the design and validation of a new, low-flowrate personal inhalable aerosol sampler.

Prior to testing the new sampler, the small-scale sampler testing system was validated by two different approaches. For the first validation, an IOM sampler was mounted on a miniature, simplified bluff body, and it was shown to closely provide the inhalable aerosol fraction for a wide range of particle sizes corresponding to the inhalability curve. For the second validation, a scaled-down version of the IOM sampler was designed and mounted, again, on the miniature bluff body. This, too, was found to closely provide inhalable aerosol fraction. In both cases, however, small positive biases were observed when comparing the experimental results to the inhalability curve and large wind tunnel data. These biases were attributed to the differences in how orientation-averaged A-values were obtained in the small-scale and full-scale sampler testing systems and perhaps other differences pertaining to the shapes of the bluff bodies and the sampler orifice locations. For the development of a low-flowrate, prototype personal inhalable aerosol sampler, the performance of a dimensionally scaled-down IOM sampler (also used to validate the small-scale sampler testing system) was compared to both the inhalability curve and that of the full-size IOM sampler, when both were tested in the small-scale sampler testing system. By scaling down the IOM sampler, the new sampler had a low flowrate of 0.32 L/min. When comparing its performance with the inhalability curve, small positive biases were observed. However, when its performance was compared to that of the IOM sampler, these biases disappeared. This gave further evidence that the small biases were attributed to the use of the small-scale system, and it was expected that those biases would not be present for both samplers in the full-scale. Thus, the new sampler was validated as a prototype, low-flowrate personal inhalable aerosol sampler.

While these experiments have provided considerable confidence in the performance of the new, low-flowrate sampler, it is recognized that such a characterization was obtained under relatively tightly controlled conditions in the laboratory. It is therefore considered important that the sampler should be tested under realistic field conditions as a further validation of its performance.

9. Field testing of the new, low-flowrate, prototype personal inhalable aerosol sampler

Introduction

Here we describe a field study that was conducted in three different lead industries in South Korea. The primary goal was to compare the performance of the new low-flowrate prototype personal inhalable aerosol sampler with that of the original IOM sampler when both samplers were mounted side-by-side on factory workers.

Background

When practical aerosol samplers are used to assess worker exposure to aerosols in typical work settings, it is inevitable that their relative performances will vary a great deal more than when they are tested in wind tunnels. This is because the conditions that determine the performance of such samplers are much more variable in work settings than they are in controlled laboratory

settings. With this in mind, the new prototype inhalable aerosol sampler was tested in the field against the original IOM aerosol sampler, with the latter as a reference for the inhalable fraction.

The study took place in South Korea through collaboration with Professor N.W. Paik at the Seoul National University (SNU) School of Public Health. Professor Paik provided contacts with inspectors from the Korean Occupational Safety and Health Agency (KOSHA, Inchon, Korea) who helped with the sampling trials. The samples were analyzed in the Industrial Hygiene Laboratory at SNU, which was equipped for metal analysis. External quality control was performed by the laboratory's participation in the inter-laboratory Proficiency Analytical Testing program organized by the U.S. National Institute of Occupational Safety and Health (NIOSH) and the American Industrial Hygiene Association (AIHA).

Lead was investigated for several reasons. First and foremost, it is a metal and therefore capable of being analyzed in very small quantities[5] using, for example, inductively coupled argon plasma atomic emission spectroscopy (ICP-AES). Since the sampling was conducted in actual field environments, it was expected that the concentration levels of aerosol would be very low compared to the very high concentrations that were generated in the wind tunnel. Secondly, lead represented a metal that was toxic to humans when deposited anywhere inside the respiratory tract, and so was an appropriate choice for inhalable aerosol sampling. The current TLV for elemental lead is 50 $\mu g/m^3$ (ACGIH, 2002), expressed as an 8-hour time-weighted average. Finally, the fact that the information obtained would provide useful information for KOSHA in their capacity to protect workers in the plants was a useful incentive for this collaboration.

Workplaces

The field study was conducted in three factories that utilized lead as a main source of their final products. All three were located in major industrial sectors near Seoul. They were a battery manufacturing plant, a paint production plant and a battery recycling plant. In each plant, the recruitment of subjects was carried out in full accordance with the University of Michigan guidelines for the use of human subjects.

The battery manufacturing plant produced lead-acid batteries for automobiles and industrial devices. There were a total of 80 workers on the factory floor and the work shifts were divided into daytime and nighttime shifts, with typically 8 to 12 hours per shift. Volunteers were identified from the casting and assembly operations. In the casting operation, molten lead was fed into a mold producing a thin, lattice-like cast. The casts were conveyed down a slide and joined with other casts molded in the same way. One of the workers inspected the casts and trimmed them or disposed them. The worker also applied cork spray between the casts to prevent them from sticking to one another. The worker then placed the accumulated casts on a cart and moved them to the lead oxide (PbO) coating operation. In the assembly operation, the grids were moved along a conveyer belt. A typical worker assembled outer casings around the grids and used a torch to seal the + and – knobs with the outer casing. The worker also placed various parts into the casing to form a complete battery. The factory was relatively modern, and many of the

[5] The estimated *LOD* of lead samples using ICP-AES is 1 μg, according the NIOSH Manuel of Analytical Methods (NIOSH, 1994)

processes were automated and ventilation hoods were installed above the furnaces. All the workers wore face-piece respirators (3M Company, St. Paul, MN) and gloves.

The paint production plant produced lead-based paint for ceramic painting and glass painting applications. It also produced lead-based raw materials for the manufacture of colored glass. There were 16 workers on the factory floor. None of them had specific job descriptions so it was difficult to associate particular tasks with specific individuals. The paint and colored-glass raw materials were produced in the following manner. Raw materials were fed into a mixer (the raw materials consisted of litharge (PbO) and silica, at approximately 3:1 by mass, and small amounts of other materials) and transported to a furnace by a pulley system. The material was melted in a furnace and cooled in a water tank. The resulting glass-like material was transported to a secondary mixer where the material was ground and blow-dried. This was then transported to a tertiary mixer and ground to a fine powder, after which color was added. The powder was either packaged into plastic containers and sold to glass manufacturers or was combined with pine oil and a solvent to produce lead-based paint. Compared to the battery plant, this facility was relatively old and generally unkempt. Ventilation hoods, however, were observed over the furnaces and hoppers and the workers wore face-piece respirators.

The battery recycling plant extracted the lead from lead-acid batteries and produced bars of lead. There were approximately 25 workers performing a variety of job tasks. Lead was extracted by first disassembling and segregating the battery into lead scrap and battery scrap and then feeding the lead scrap into a furnace. The molten lead was molded into ingots and transported to storage for exportation. As in the paint production plant, dust was observed along the floor and interior of the building. Ventilation hoods were installed above the furnace and the workers wore half-face respirators with replaceable cartridges.

Methods

Prototype low-flowrate sampler: The new sampler used in the field study was a slightly scaled-down version of the low-flowrate sampler described in the laboratory study (see previous section). Such scaling was permissible based on the excellent performance of the sampler scaling laws as outlined in the previous sections. The orifice was reduced to 5 mm, and correspondingly, the flowrate was reduced to 0.22 L/min. This enabled R to remain the same as for both the IOM sampler and the earlier scaled-down version (under the same windspeed conditions), with a slight decrease in r compared to the earlier version[6]. The new sampler is shown in Figure 38. The further reduced flowrate enabled the sampler to be used with the SKC Pocketpump (SKC Inc., Eighty-four, PA) which has a maximum flowrate of 0.225 L/min. High-flow and low-flow Gillian pumps (Sensidyne, Clearwater, FA) were also available through the industrial hygiene laboratory at SNU and these were used to operate the IOM and prototype samplers, respectively.

[6] Compared to an r-value of 0.05 for an IOM sampler mounted on a 300-mm torso (or for the 6-mm scaled-down IOM sampler on a 120mm bluff body), the r-value of the prototype sampler was 0.02. Since no differences in performance were found for an r-range of 0.05 to 0.4 (encompassing the range of r tested in chapters 6 and 7, it was assumed that a further reduction in r would not significantly influence the sampler's performance.

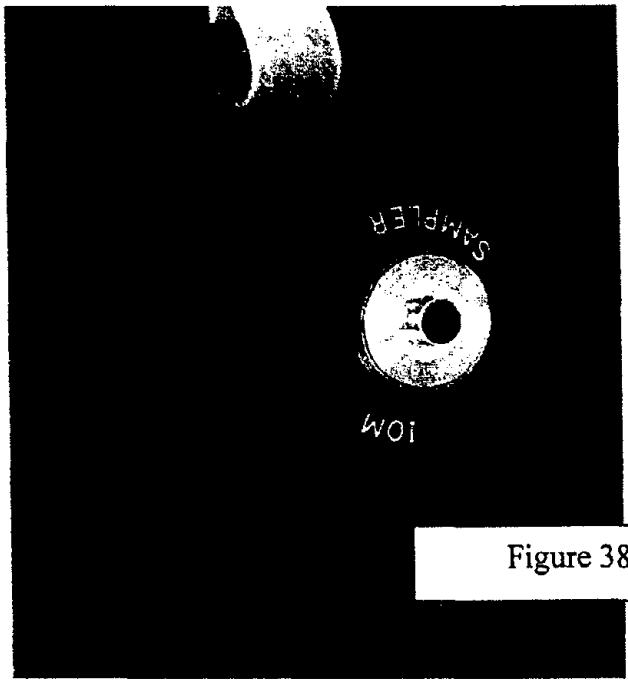

Figure 38

Sample collection: Thirty-nine sample pairs and 8 field blank pairs were collected from the three plants described above. Four of the sample pairs, however, were lost due to pump faults or torn filters. So a total of 35 sample pairs were available for lead analysis. Of these, 27 were personal sample pairs and 8 of them were area sample pairs. In any case, each sample pair consisted of a sample taken using the new prototype sampler and a sample taken using the original IOM sampler. For the personal samples, each volunteer subject wore one of each type of sampler during a work shift and both samplers were placed close together on the same side of the worker's torso in the lapel region. Each sampler was attached to its own sampling pump. The sampling tubes were taped together and the tubes and samplers were clipped or taped to the worker. For area samples, the samplers were taped to the walls at various locations throughout the plant. The prototype and IOM samplers were installed on the workers near the beginning of their shifts, taken off and paused during their lunch breaks, and then resumed until close to the end of their shifts. The resulting sampling durations were approximately 5 to 7 hours. Upon completion of sampling on a given day, the samplers were covered with laboratory sealing film (Whatman Inc., Clifton, NJ) and transported to the industrial hygiene laboratory at SNU. In addition to the 39 sample pairs, two sets of cascade impactor (Marple 290 Personal Cascade Impactor, Thermo Instrument Systems, Bedford, MA) samples were obtained from the paint production plant and battery recycling plant. These were installed as area samplers and used to estimate aerosol particle size distributions at the two locations. In the battery manufacturing plant, a total of 20 sample pairs and 4 field blank pairs were obtained in two days of sampling. Ten sample pairs and 2 field blank pairs were obtained from the casting and assembly operations, respectively. In the paint production plant, 8 sample pairs and 2 field blank pairs were obtained. Five of the sample pairs were personal samples and 3 were area samples. However, 2 sample pairs were lost due to pump failure or filter break-through. So a total of 6 sample pairs (4 personal and 2 area) were analyzed from this plant. Finally, in the battery recycling plant, 11 sample pairs and 2 blank pairs were collected, but due to a pump fault and torn filter, only 9

sample pairs were analyzed. Three of these pairs were personal sample pairs and 6 of them were area sample pairs.

Analytical methods: For the analysis of lead in the collected samples, the filters were removed from the sampling cassettes and put into 50-ml plastic centrifuge tubes (Corning Incorporated Life Sciences, Acton, MA). Any deposits on the inner walls of the cassettes were also put into the centrifuge tubes as part of the sample. The wall deposits were collected by wiping the insides of the cassettes with two or three mixed cellulose ester (MCE) filters (Millipore Corporation, Bedford, MA), depending on the size of the orifice. To facilitate the removal of wall deposits, the filters were dipped in Milli-Q water[7] prior to using them. MCE filters were used because they were readily dissolvable in nitric acid and therefore ideal for ICP-AES. Previously, Tsai *et al.* (1995a and 1996a) had similarly used alcohol-impregnated filters to collect the wall deposits from IOM samplers and 37-mm cassette samplers. Each sample was prepared according to an extensive, well-documented preparation procedure, based on the NIOSH Method 7300. Instead of the ashing technique described in the method, however, a microwave oven (CEM Model, MDS-2100, CEM Corporation, Matthews, NC) was used to quickly digest the samples and filters under high pressure prior to sample analysis. For the lead analysis, an ICP-AES instrument (Perkin-Elmer Model 3000DV, Perkin Elmer, Inc., Wellesley, MA) was used to quantify the sample masses. Appropriate reagent blanks and calibration standards were used to produce high quality results in conformance with NIOSH Method 7300.

Data analysis: The analysis of inter-sampler comparison data was based on the expression $E_{NEW} = S \cdot E_{IOM}$, where E_{NEW} is the measured aerosol concentration from the prototype new sampler, E_{IOM} is the measured concentration from the IOM sampler, and S is the regression coefficient. It was assumed that the relationship between E_{IOM} and E_{NEW} could be represented by a straight line passing through the origin[8]. This expression has been widely applied in observational studies such as this one (Tsai *et al.*, 1995a; Tsai *et al.*, 1996a; Spear *et al.*, 1997; Werner *et al.*, 1999; and others). Also similarly to these earlier studies, a weighted least squares (WLS) regression approach was adopted where all the results were weighted by the factor $1/(E_{IOM})^2$ in order to stabilize the residuals (Tsai, 1995). The WLS regression analyses were carried out using the statistical software package SPSS 10 (SPSS Science, Chicago, IL). Data records were excluded if either of the samples in a given sample pair were below the limit of detection (*LOD*). The *LOD*s were determined from the standard deviation of field blank lead masses using the equations described in an earlier section. Since the IOM sampler and prototype sampler field blanks were slightly different[9], two *LOD*s were determined – one for each sampler. The *LOD*s were determined to be 4.50 and 1.44 μg per sample for the IOM sampler samples and prototype sampler samples, respectively. Out of a total of 35 sample pairs, 2 samples were below the *LOD* and thus excluded from the data analysis. Although 9 of the sample masses were found to lie between the *LOD* and *LOQ*, they were not excluded in the analysis due to practical

[7] Milli-Q water (Millipore Corporation, Bedford, MA) is known to be completely free of lead and other metals (except for very trace amounts of boron, less than 13 parts per trillion).

[8] The zero intercept was based on the fact that both samplers should measure zero concentration simultaneously, if no aerosols were present.

[9] The field blanks for the IOM samplers contained one 25-mm MCE filter (for the cassette) and three 37-mm MCE filters (for wall deposits), and the field blanks for the prototype samplers contained three 25-mm MCE filters (one for the cassette and two for the walls).

considerations[10]. The removal of outliers was based on physical implausibility, following a similar approach used in the earlier field studies cited. Results from the previous section indicated that the IOM sampler and low-flowrate version had very similar performances in laboratory settings. Therefore, individual concentration ratios that fell outside the arbitrary but very broad range of $0.2 < E_{NEW}/E_{IOM} < 5.0$ were considered outliers. Three out of the remaining 33 sample pairs were removed in this way. Thus, out of a total of 35 sample pairs, 30 sample pairs were considered "good" sample pairs and included in the data analysis.

Results

The measured lead concentrations using the prototype and IOM sampler and the concentration ratios for each sample pair are shown in Table 17. Where possible, the exposure information is divided into four work areas based on either the work process or type of factory. But since the workers in the paint production plant and battery recycling plant did not have well-defined work areas, no divisions were made by work area in these plants. The results of the WLS regression analyses are summarized in Table 18. It is seen that the *S*-values range from 1.60 to 2.51 for the four work areas and the overall S-value for all the data is 1.89.

Plant/process description	E_{IOM} (µg/m^3)	E_{NEW} (µg/m^3)	E_{NEW}/E_{IOM}
Battery mfg/casting	44	177	4.06
Battery mfg/casting	49	47	0.96
Battery mfg/casting	29	27	0.91
Battery mfg/casting	47	42	0.89
Battery mfg/casting	38	34	0.89
Battery mfg/casting	68	62	0.91
Battery mfg/casting	45	90	1.99
Battery mfg/casting	65	173	2.68
Battery mfg/casting	49	74	1.51
Battery mfg/casting	59	821	13.87
Battery mfg/assembly	102	59	0.58
Battery mfg/assembly	33	4	0.12
Battery mfg/assembly	16	18	1.08
Battery mfg/assembly	70	126	1.81
Battery mfg/assembly	180	68	0.38
Battery mfg/assembly	120	123	1.02
Battery mfg/assembly	87	416	4.76
Battery mfg/assembly	103	1111	10.77
Battery mfg/assembly	56	72	1.29
Battery mfg/assembly	32	48	1.50
Paint production	267	218	0.82
Paint production	1775	9378	5.28
Paint production	4840	6462	1.34
Paint production	981	1166	1.19

[10] These samples were not removed for practical reasons. Their removal would reduce the number of "good" sample pairs from 30 to 21. Also, similar earlier studies (Tsai *et al.*, Werner *et al.*, and others) only removed samples with masses below the *LOD*.

Paint production	1122	4523	4.03
Paint production	2436	1575	0.65
Battery recycling	315	997	3.17
Battery recycling	131	594	4.53
Battery recycling	184	418	2.27
Battery recycling	372	1789	4.81
Battery recycling	351	396	1.13
Battery recycling	57	66	1.16
Battery recycling	111	396	3.57
Battery recycling	157	142	0.91
Battery recycling	330	348	1.06

Table 17

Work area	S	SE	N	R^2	LCL	UCL
Casting	1.64	0.37	9	0.72	0.92	2.36
Assembly	1.62	0.56	7	0.59	0.53	2.71
Paint production	1.60	0.62	5	0.63	0.39	2.82
Battery recycling	2.51	0.52	9	0.75	1.49	3.53
All work areas	1.89	0.25	30	0.66	1.40	2.38

Table 18

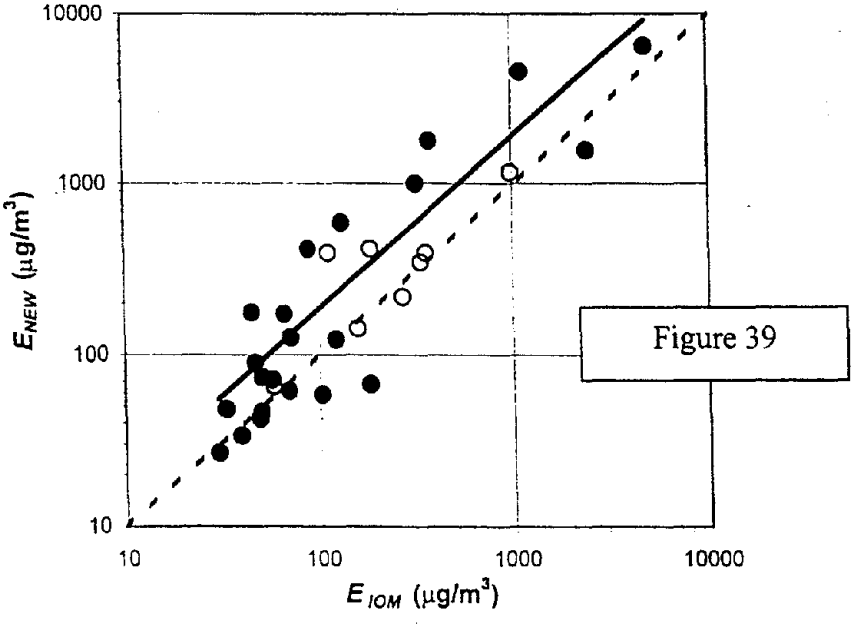

Figure 39

Figure 39 compares the concentrations as measured by the two samplers, where the solid circles relate to the pairs of personal samples and the open circles the pairs of area samples. The solid line is the one obtained from WLS regression while the dashed line represents the ideal 1:1. The graph indicates that, overall, the exposure ratios (E_{NEW}/E_{IOM}) are greater than unity, indicating that the prototype sampler measures higher exposures than the IOM sampler. It is seen that, in a few instances, the prototype sampler yields up to five times greater lead exposures than the IOM

sampler. For the area sample pairs, however, the prototype and IOM sampler exposures are very close to unity for six of the eight area sample pairs.

Particle size distributions for aerosols at the paint production plant and battery recycling plant, obtained using Marple-type personal cascade impactors, revealed mass median particle aerodynamic diameters of 9 and 20 μm respectively, with corresponding geometric standard deviations (GSD) are 5.04 and 3.93, respectively.

Discussion

The results of the inter-sampler comparisons indicated that the new, low-flowrate sampler generally measured higher lead exposures than the IOM sampler. The WLS regression showed that S was 1.89 for the 30 sample pairs that were analyzed. At first glance, these results were somewhat surprising, since the earlier wind tunnel experiments had shown no statistically significant differences in the performance of the two samplers (although, as already noted, a slightly scaled-up version of the prototype sampler was tested in those experiments). Upon closer inspection, however, it was clear that there was a large amount of variability in the measured lead concentrations. While 9 of the 30 sample pairs indicated that the new sampler measured more than twice the lead concentration obtained using the IOM sampler, 16 of the 30 sample pairs indicated that the exposure ratio E_{NEW}/E_{IOM} was less than 1.3. And for three of the four work areas, the 95% lower confidence limits (based on estimates of the standard error) of S were less than unity.

At this stage, based on this single short field study, we can only speculate about the factors that may have been responsible for the higher-than-expected S-values that were found. It is noted that 6 out of the 8 area sample pairs indicated that the two samplers measured very similar concentrations. These sample pairs were not susceptible to individual worker effects, and so there is the suggestion that sample losses may have occurred in some of the personal sample pairs, especially for the IOM sampler with its much larger inlet. In this regard, it was noted towards the end of the field study that some of the workers had been using compressed air to blow dust off of them prior to their lunch breaks, and this might well have resulted in the loss of some material from the IOM samplers.

Workplace comparisons

While there were obvious differences in the actual lead exposures measured in the three plants (see Table 17), the S-values for two of the plants (battery manufacturing and paint production) were very close to each other (see Table 18) and the S-value for the battery recycling plant was higher than those for the other plants. The variability of exposure, however, was such that there was insufficient statistical power to enable formal support of these conclusions. The higher S-value observed for the battery recycling plant may be related to the differences in particle size for this plant compared to that of the paint production plant (particle size distributions were only measured for these two plants, where the median particle aerodynamic diameters of the paint production plant and battery recycling plant were 9 and 20 μm, respectively). The previous similar field studies cited earlier had indicated that the differences in the performance of IOM samplers and 37-mm cassette samplers were more pronounced for work areas with coarser

aerosols. In the current investigation, the same observation was made and it was contrary to what was expected of the performances of the two samplers, where the wind tunnel experiments had shown similar performances for particles with d_{ae} up to 90 μm.

Conclusions from this part of the research

This field study was conducted to test the performance of a new, low-flowrate personal inhalable aerosol sampler in practical settings. Comparing its performance with that of a reference inhalable aerosol sampler when both were mounted on the same worker, it was found that the new instrument over-sampled the inhalable aerosol fraction, with a regression coefficient of 1.89 for 30 sample pairs. However, closer inspection of the exposure ratios (E_{NEW}/E_{IOM}) indicated that roughly half of them were within the range $0.80 \leq E_{NEW}/E_{IOM} \leq 1.30$. Sampling losses in the IOM sampler, both during sampling and sample analysis, may have resulted in the (perhaps) artificially high exposure ratios that were observed, especially since it was observed that most of the exposure ratios obtained from the area sample pairs were quite close to unity. The relatively small number of samples collected from three different plants also contributed to the increased variability of sampling data. Further studies would be necessary to produce more conclusive results. One such study is currently being carried out by Professor Pentti Kalliokoski and his colleagues in Finland. In this study, the performances of several samplers, including the new low-flowrate sampler and the original IOM sampler, are being determined in practical field settings. These results will provide a good complement to those obtained in this research.

10. Sampling for the thoracic fraction

Introduction

As described in Section 1, thoracic aerosol is defined as the fraction that may penetrate into the lung below the larynx. Criteria for the thoracic aerosol fraction were identified in the early 1980s. The one that has gained the most widespread acceptance is the PM_{10} definition that was proposed by the United States Environmental Protection Agency (EPA), intended to provide a metric for exposure that is relevant to a wide range of lung diseases. Standards based on this criterion have been in existence for many years, and have become the primary basis for controlling the exposures of human populations to aerosols in their living environments, not only in the USA for also in many other countries.

The definition for the thoracic fraction contained in Equation (2) (see Section 1) is the version adopted by the International Standards Organisation (ISO, 1983) and – later – ACGIH (see Vincent 1999). Although for practical purposes this is very close to the definition for PM_{10}, it is actually a more rigorous statement of the definition of what may enter the lung. This is because the thoracic fraction is expressed clearly as a sub-fraction of the fraction that is originally inhaled. This is the version that remains the basis of intended standards for workplace aerosol exposures, both as expressed by ACGIH and by many other bodies around the world. However, at the time of completing this research and writing this report, no such standards have yet actually been promulgated. Although several aerosol types have been suggested as candidates for occupational exposure limits (OELs) based on the thoracic fraction, none have yet been finalized. As a result, although there has been considerable discussion about samplers for the

thoracic fraction, motivation in the industrial hygiene community towards the development – and particularly the commercial availability – of such instrumentation has been weak.

In what follows, a description will be given of the design of a prototype personal low-flowrate thoracic aerosol sampler. It operates at the low flowrate of 0.32 L/min, the same as the low-flowrate personal inhalable aerosol sampler described above in Section 6. However, because no definitive reference sampler – operating at the more 'conventional' sampling flowrate (i.e., 2 L/min) – can yet be identified, comparative trials in the laboratory and in the field were not conducted. Nonetheless, important design work has been performed in order to realize the desired instrument, following closely what has been achieved for the inhalable fraction (see Section 8). This may be the subject of separate study at some point in the future.

Theoretical background

To design a sampler for the thoracic fraction first requires an entry that aspirates the inhalable fraction, followed by a pre-selector that has penetration characteristics matching the curve specified in Equation (2). Various physical options are available for the type of pre-selector that might be used. But in recent years, attention has been drawn to the use of porous plastic foam media. Gibson and Vincent (1981) were the first to propose such media as a pre-selector for the finer respirable fraction. Later, Vincent *et al.* (1993) proposed porous plastic foam as a pre-selector also for the thoracic fraction, specifically incorporated into a sampler whose entry matches that of the original IOM personal inhalable aerosol sampler. Other researchers have also explored the use of such media and, indeed, the same IOM/foam configuration. Through all this effort, one attraction of porous foam media for such applications has been the fact that the physical mechanisms governing aerosol penetration are essentially the same as those governing aerosol penetration through the airways of the human respiratory tract.

Porous plastic foam media are attractive options as aerosol sampler pre-selectors also because of their flexibility, versatility, availability and – importantly – low cost. Electron micrographs of the structure of such material reveal it as somewhat 'fibrous-like' and so having features that enable it, in the context of aerosol science, to be treated as filter media. Based on the available cumulative experimental data for the penetration of particles through such media, and the understanding that the physics of deposition inside such media is dominated by a combination of inertial and gravimetric forces, an empirical mathematical model embodying the penetration (P) of foam media was proposed (Vincent *et al.*, 1993), thus

$$-(d_f/t)\ \ln P = 54.86 St_f^{2.382} + 38.91 N_g^{0.880} \qquad (25)$$

in which

$$St_f = d_{ae}^2 \gamma^* U_F / 18 \eta d_f \qquad (26)$$

$$N_g = d_{ae}^2 \gamma^* g / 18 \eta U_F \qquad (27)$$

where, in addition to the variables already defined, U_F is the face velocity of the air approaching the foam media, and g is the acceleration due to gravity. Here, St_f is now the Stokes inertial parameter for describing the role of inertia in particle collection by the fibrous elements inside

the foam media, and N_g is the gravitational parameter describing the role of gravitational deposition. In the model described, inertial mechanisms dominate particle collection for fine particles or for high air velocities through the foam, and gravity dominates for large particles or low air velocities.

In addition, Vincent *et al.* studied the relationship between Po and d_f and showed the empirical relationship

$$d_f = \left(0.009633 Po^{-1.216}\right) \tag{28}$$

to be applicable and accurate over wide ranges of pore sizes.

Kenny *et al.* (2001) examined the robustness of the above model by reference to a comprehensive set of new experimental data, and found that it held up quite well. However, they stressed the importance of a reliable supply of foam media with consistent properties, specially closely-specified cell dimensions. Elsewhere, in studies of the filtration characteristics of foam media in relation to its potential practical applications in certain air cleaning situations, it was shown (Poon, 1997) that the internal physical characteristics of foam media obtained in the United States – in particular the microscopic physical dimensions and bulk porosity for a given nominal Po – are very close to those for foam media from a different manufacturer in Europe. This suggested good consistency in commercially-available media.

Design and construction of a low-flowrate personal thoracic personal aerosol sampler

Our design for a personal thoracic aerosol sampler was based on an extension of the new low-flowrate personal inhalable aerosol sampler described in the previous section. Briefly, the prototype sampler used in the field study described there operated at a flowrate of 0.22 Lpm, lower than the one emerging from the laboratory study (see Section 8) in order that it could be used with the low-flowrate personal sampling pumps that are commercial available. The sampler dimensions were adjusted according in order to be consistent with the scaling laws for aspiration efficiency that have been shown throughout this research to be applicable to such sampling systems. That prototype inhalable aerosol sampler now provides the basis for the corresponding prototype thoracic aerosol sampler. The important new ingredient is the insertion of a pre-selector with particle penetration characteristics (at the chosen flowrate) that are close to the thoracic aerosol conventional curve defined in the ACGIH set of criteria (Vincent, 1999) and elsewhere (see also Figure 1).

Here, as in the case of the corresponding higher-flowrate thoracic aerosol sampler described by Vincent *et al.* in 1993, an appropriate foam plug was inserted into the inlet nozzle, carefully chosen with respect to pore dimensions and external dimensions to provide a penetration curve closest to that of the ideal thoracic aerosol curve. These choices were made by a trial-and-error application of the model embodied above in Equations (25) to (28). Table 16 summarizes the technical specifications of the new instrument. The predicted performance of the chosen foam (based on the mathematical model described above) plug is shown in Figure 36.

Table 16	
Sampling flowrate	0.22 Lpm
Inlet diameter	5 mm
Plastic foam pore size	45 pores per inch (ppi)
Foam plug diameter	5 mm
Plug length	3.5 mm

To realize the desired thoracic sampler, the foam plug described in Table 16 is simply inserted into the entry of the inhalable version of the sampler first shown in Figure 38, and pushed in far enough that its end is flush with the lip of the entry. The complete assembly is shown below in Figure 39.

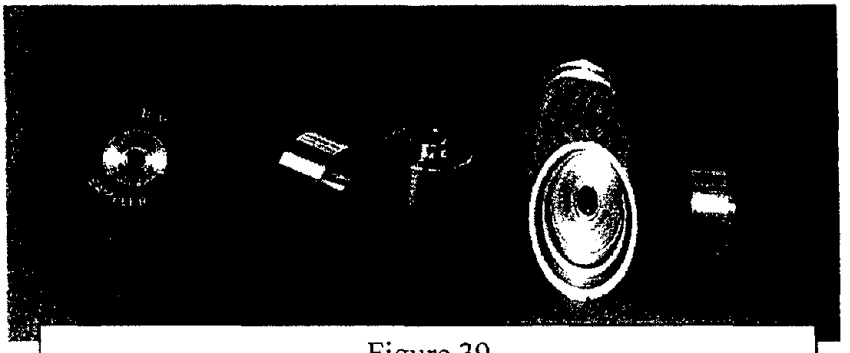

Figure 39

Left: 0.22 Lpm inhalable aerosol sampler
Center: a pair of inlet nozzles with foam inserts
Right: Cassette (disassembled) and a pair of foam plugs

The foam plug described in Table 26 (and shown above) is very small. Because the foam media itself is very pliable, it is very difficult to cut the plug to the required dimension. Therefore we developed special procedures by which to prepare the plugs of the desired external dimensions. In this procedure, small sheets of the 45 ppi foam of thickness 5 mm were cut (approximately 120 mm x 150 mm in size) and placed into the base of a small baking tray into which molten paraffin wax (melting point, 50°C) was carefully poured until the foam was sufficiently immersed. The baking tray, complete with foam and wax, was placed into a pre-warmed oven at 60°C and allowed to sit for up to one hour, with periodic squeezing of the foam with tweezers, to ensure that air bubbles were removed from within the body of foam sheet. The baking tray was removed from the oven and allowed to cool to room temperature, enabling the wax to solidify. The solid wax/foam substrate was removed from the tray and wax/foam plugs were cut with the aid of a specially fabricated sharp stainless steel cutter on a suitable cutting surface. The wax plugs were trimmed to their correct length (3.5 mm) by the use of a safety razor blade. The advantage of using this particular wax technique was that it afforded little deformation during cutting, allowing for production of truly cylindrical foam plugs. After trimming, the wax was simply removed by first heating the plugs on a raised mesh above the baking tray, allowing the majority of the wax to simply melt out of the foam into the tray below, with the residues being

removed by washing the plugs in a kerosene based de-waxing solvent (Wax-Out, Fisher Scientific). The use of such temperature and solvent were found not to adversely affect the foam substrates. Foams plugs were then 'greased' by washing in a 10% (by weight) solution of petroleum jelly dissolved in xylene and the solvent allowed to evaporate, leaving a petroleum jelly residue on the foams. 'Greasing' ensured that particle bounce and blow-off from the foam substrates was minimized when in use. The foam plugs were inserted into the ends of the sampler inlets, with the face of the foam plug flush with the sampler inlet. The sampler was then used in the usual manner, with particles collected onto the filter cassette (and collected on the internal walls below the foam) being measured with an appropriate gravimetric or chemical technique.

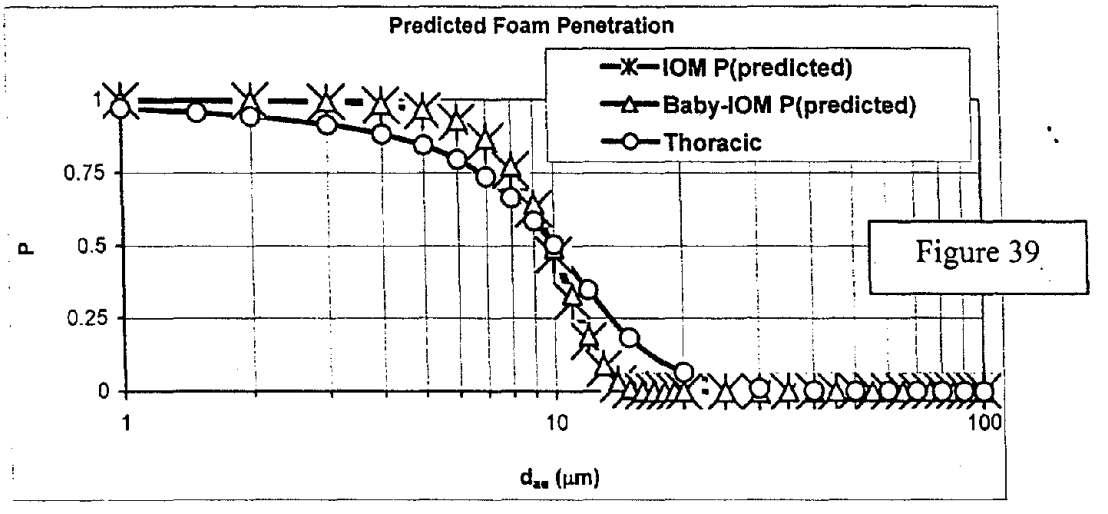

Figure 39

Conclusions from this part of the research

This short exercise has showed that it is possible to extend what was learned during the development of the low flowrate inhalable aerosol sampler (see Sections 8 and 9) to a corresponding low flowrate thoracic aerosol sampler. Although a prototype instrument was built, to demonstrate the technical feasibility of constructing such an instrument, it was decided once the project got under way not to perform extensive testing with this instrument. As mentioned near the beginning of this report, the desire in the industrial hygiene community to have available a range of personal sampling instruments has receded in recent years as new standards (e.g., from ACGIH) have not yet embraced the thoracic aerosol criterion. With this in mind, it was decided not to undertake a full laboratory study to characterize the new instrument. Nor were any field studies carried out.

11. **Final summary and conclusions from the research**

This research proved the hypothesis that it is indeed possible to develop sampling instruments with desired performance characteristics based on an improved knowledge of the physics of

aerosol sampling. The primary part of the research was a set of laboratory investigations leading to the development of a prototype low-flowrate sampler for the inhalable aerosol fraction. The path to this goal stimulated a number of important new advances in aerosol sampling science, resulting in a number of publications for major aerosol science and industrial hygiene journals, some of which have already appeared and others which will be published in due course. The desired endpoint of a new low-flowrate sampler for the inhalable fraction was achieved successfully.

The research revealed both the benefits and limitations of previous aerosol sampling models in their ability to predict sampler performance. Numerous wind tunnel experiments characterized the performance of samplers with simple and complex shapes, over wide ranges of conditions never investigated before, and improved semi-empirical models were developed for predicting sampler performance. This greatly narrowed the gap between current knowledge of aerosol sampling under ideal conditions and that pertaining to sampling under more realistic conditions. Finally, the research demonstrated that it is possible to accurately characterize the performances of personal aerosol samplers using a small-scale sampler testing system. The sampler testing system and methods developed for this research enabled the testing and validation of the performances of aerosol samplers with a high degree of reproducibility, at relatively low cost, and in short periods of time. It is expected that the future development of aerosol samplers will increasingly utilize such simplified testing systems, including the use of direct-reading instrumentation that would significantly reduce the costs, labor, and time requirements even further. This indeed is the subject of other NIOSH-funded research being carried out in our laboratory and which will be completed and reported later in 2003.

In conclusion, it is believed that the progress that has been achieved in this project will greatly facilitate the future development of new sampling devices. This in turn will aid industrial hygienists in their ability to characterize workers' aerosol exposures and ultimately preserve the health of people in aerosol-laden workplace environments.

The following publications derived directly from this research have already appeared:-

Paik, S.Y. and Vincent, J.H. (2002), Filter and cassette mass instability in ascertaining the limit of detection of nhalable airborne particulate, *American Industrial Hygiene Association Journal*, 63, 698-702.

Paik, S.Y. and Vincent, J.H. (2002), Aspiration efficiency for thin-walled nozzles facing the wind and for very high velocity ratios, *Journal of Aerosol Science*, 33, 705-720.

Paik, S.Y. and Vincent, J.H. (2002), Aspiration efficiencies of disc-shaped blunt nozzles facing the wind, for coarse particles and high velocity ratios, *Journal of Aerosol Science*, 33, 1509-1523.

Brixey, L.A., Paik, S.Y., Evans, D.E. and Vincent, J.H. (2002), Experimental studies to develop new aerosol samplers and methods for their evaluation, *Journal of Environmental Monitoring*, 4, 633-641.

Several more are in preparation.

ACKNOWLEDGEMENTS

The PI and his Co-Investigators are grateful for the financial support that was received in the form of the NIOSH-CDC Grant No. RO1-OH-03687-03. In addition we are grateful for support provided by the School of Public Health at the University of Michigan that enabled acquisition of the wind tunnel that was used throughout this work. Finally we wish to acknowledge the help of the skilled technicians in the Workshop in the Department of Chemistry at the University of Michigan who built most of the units and systems tested during the research.

REFERENCES

Aizenberg, V., Grinshpun, S.A., Willeke, K., Smith, J., and Baron, P.A. (2000), Measurement of the sampling efficiency of personal inhalable aerosol samplers using a simplified protocol, *Journal of Aerosol Science*, 31, 169-179.

American Conference of Governmental Industrial Hygienists (ACGIH) (2002), *Threshold limit values for chemical substances and physical agents, and biological exposure indices*, ACGIH, Cincinnati, OH.

American Society of Testing and Materials (ASTM) (2000), ASTM Standard practice for controlling and characterizing errors in weighing collected aerosols (ASTM D 6552), ASTM.

Armbruster, L. and Breuer, H. (1982), Investigations into defining inhalable dust, *Annals of Occupational Hygiene*, 26, 21-32.

Badzioch, S. (1959), Collection of gas-borne dust particles by means of an aspirated sampling nozzle, *British Journal of Applied Physics*, 10, 26-32.

Baines, W.D. and Peterson, E.G. (1951) , An investigation of flow through screens, *Transactions of the ASME* , 467-480.

Bartley, D.L. (1998), Inhalable aerosol samplers, *Applied Occupational and Environmental Hygiene*, 13, 274-278.

Belyaev, S.P. and Levin, L.M. (1974), Techniques for collection of representative aerosol samples, *Journal of Aerosol Science*, 5, 325-338.

British Medical Research Council (BMRC) (1952), Recommendations of the BMRC panels relating to selective sampling, From the Minutes of a joint meeting of Panels 1, 2 and 3.

Buckingham, E. (1914), On physically similar systems: illustrations of the use of dimensional equations, *Physics Review*, 4, 345-376.

Chung, K.Y.K. and Ogden, T.L. (1986), Some entry efficiencies of disklike samplers facing the wind, *Aerosol Science and Technology*, 5, 81-91.

Davies, C.N. (1968), The entry of aerosols into sampling tubes and heads, *British Journal of Applied Physics*, Ser 2, 921-932.

Davies, C.N. and Subari, M. (1982), Aspiration above wind velocity of aerosols with thin-walled nozzles facing and at right angles to the wind direction, *Journal of Aerosol Science*, 13, 59-71.

DiNardi, S.R. (1995). *Calculation Methods for Industrial Hygiene*, Van Nostrand Reinhold, New York, NY.

Durham, M.D. and Lundgren, D.A. (1980), Evaluation of aerosol aspiration efficiency as a function of stokes' number, velocity ratio and nozzle angle, *Journal of Aerosol Science*, 11, 179-188.

Federation of the European Producers of Abrasives (FEPA) (1993), FEPA standard for bonded

abrasive grains of fused aluminium oxide and silicon carbide, FEPA 42-GB-1984 R1993.

Gibson, H. and Ogden, T.L. (1977), Some entry efficiencies for sharp-edged samplers in calm air, *Journal of Aerosol Science*, 8, 361-365.

Hangal, S. and Willeke, K. (1990), Overall efficiency of tubular inlets sampling at 0-90 degrees from horizontal aerosol flows, *Atmospheric Environment*, 24A, 2379-2386.

Hinds, W.C. and Kuo, T.-L. (1995), A low velocity wind tunnel to evaluate inhalability and sampler performance for large dust particles, *Applied Occupational and Environmental Hygiene*, 10, 549-556.

Jayasekera, P.N. and Davies, C.N. (1980), Aspiration below wind velocity of aerosols with sharp-edged nozzles facing the wind, *Journal of Aerosol Science*, 11, 535-547.

Kenny, L.C., Aitken, R.J., Chalmers, C., Fabries, J.F., Gonzales-Fernandez, E., Kromhout, H., Lidén, G., Mark, D., Riediger, G., and Prodi, V. (1997), A collaborative European study of personal inhalable aerosol sampler performance, *Annals of Occupational Hygiene*, 41, 135-153.

Kenny, L.C., Aitken, R.J., Beaumont, G. and Görner, P. (2001), Investigation and application of a model for porous foam aerosol penetration, *Journal of Aerosol Science*, 32, 271-285.

Kerr, S.M., Muranko, H. and Vincent, J.H. (2002), Personal sampling for inhalable aerosol exposures of carbon black manufacturing industry workers, *Applied Occupational and Environmental Hygiene*, 17, 681-692.

Li, S.N. and Lundgren, D.A. (1999), Weighing accuracy of samples collected by IOM and CIS inhalable samplers, *American Industrial Hygiene Association Journal*, 60, 235-236.

Lidén, G. (1994), Performance parameters for assessing the acceptability of aerosol sampling equipment, *Analyst*, 119, 27-33.

Lidén, G. and Bergman, G. (2001), Weighing imprecision and handleability of the sampling cassettes of the IOM sampler for inhalable dust, *Annals of Occupational Hygiene*, 45, 241-252.

Lipatov, G.N., Grinspun, S.A., Shingaryov, G.L., and Sutigin, A.G. (1986), Aspiration of coarse aerosol by a thin-walled sampler, *Journal of Aerosol Science*, 17, 763-769.

Mark, D., Vincent, J.H., Gibson, H., and Witherspoon, W.A. (1985), Applications of closely graded powders of fused alumina as test dusts for aerosol studies, *Journal of Aerosol Science*, 16, 125-131.

Mark, D. and Vincent, J.H. (1986), A new personal sampler for airborne total dust in workplaces, *Annals of Occupational Hygiene*, 30, 89-102.

Mark, D. (1990), The use of dust-collecting cassettes in dust samplers, *Annals of Occupational Hygiene*, 34, 281-291.

McCrae. J. (1913), The ash of silicotic lungs, Publication of the South African Institute of Medical Research, Johannesburg, South Africa.

Mendenhall W. and Beaver, R (1994), *Introduction to Probability and Statistics*, Duxbury Press, Belmont, CA.

National Institute of Occupational Safety and Health (NIOSH) (1994), NIOSH Manual of Analytical Methods (NMAM®), 4th ed., DHHS (NIOSH) Publication 94-113.

Ogden, T.L. and Birkett, J.L. (1977), The human head as a dust sampler, In: *Inhaled Particles IV* (W.H. Walton, Ed.) Pergamon Press, Oxford, U.K., 93-105.

Pankhurst, R.C. (1964), *Dimensional Analysis and Scale Factors*, Butler and Tanner Ltd., U.K.

Parratt, L.G. (1961), *Probability and Experimental Errors in Science*, John Wiley and Sons, Inc., New York, NY.

Poon, W.S. (1997), Dust filtration and loading by fibrous and foam media, Ph.D. Thesis, University of Minnesota, Minneapolis, MN.

Ramachandran, G., Sreenath, A., and Vincent, J.H. (1998), Towards a new method for experimental determination of aerosol sampler aspiration efficiency in small wind tunnels, *Journal of Aerosol Science*, 29, 875-891.

Rüping, G. (1968), The importance of isokinetic suction in dust flow measurement by means of sampling probes, *Staub-Reinhalt. Luft* (English translation), 28 (4), 1-11.

Smith, J.P., Bartley, D.L., and Kennedy, E.R. (1998), Laboratory investigation of the mass stability of sampling cassettes from inhalable aerosol samplers, *American Industrial Hygiene Association Journal*, 59, 582-585.

Spear, T.M., Werner, M.A., Bootland, J., Harbour, A., Murray, E.P., Rossi, R., and Vincent, J.H. (1997), Comparison of methods for personal sampling of inhalable and total lead and cadmium-containing aerosols in a primary lead smelter, *American Industrial Hygiene Association Journal*, 58, 893-899.

Sreenath, A., Vincent, J.H., and Ramachandran, G. (1999), New experimental studies of basic performance characteristics of aerosol samplers, *Applied Occupational and Environmental Hygiene*, 14, 624-631.

Sreenath, A., Ramachandran, G., and Vincent, J.H. (2002), Aspiration characteristics of idealized blunt aerosol samplers at large angles to the wind, *Journal of Aerosol Science*, 33, 871-881.

Stairmand, C.J. (1941), Sampling gas-borne particles, *Engineering*, 152, 141-143, 181-183.

Tsai, P.J. (1995) *Health-related aerosol exposures of the nickel industry workers*. Ph.D. thesis, University of Minnesota, Minneapolis, MN.

Tsai, P.J. and Vincent, J.H. (1993), Impaction model for the aspiration efficiencies of aerosol samplers at large angles with respect to the wind, *Journal of Aerosol Science*, 24, 919-928.

Tsai, P.J., Vincent, J.H., Wahl, G., and Maldonado, G. (1995a), Occupational exposure to inhalable aerosol in the primary nickel production industry, *Occupational and Environmental Medicine*, 52, 793-799.

Tsai, P.J., Vincent, J.H., Mark, D., and Maldonado, G. (1995b), Impaction model for the aspiration efficiencies of aerosol samplers in moving air under orientation-averaged conditions, *Aerosol Science and Technology*, 22, 271-286.

Tsai, P.J., Vincent, J.H., Wahl, G.A., and Maldonado, G. (1996a), Worker exposure to inhalable and 'total' aerosol during nickel alloy production, *Annals of Occupational Hygiene*, 40, 651-669.

Tsai, P.J., Vincent, J.H., and Mark, D. (1996b), Semi-empirical model for the aspiration efficiencies of personal aerosol samplers of the type widely used in occupational hygiene, *Annals of Occupational Hygiene*, 40, 93-113.

Tufto, P.A. and Willeke, K. (1982), Dependence of particulate sampling efficiency on inlet orientation and flow velocities, *American Industrial Hygiene Association Journal*, 43, 436-443.

Vaughan, N.P., B. D. Milligan, and Ogden, T.L. (1989), Filter weighing reproducibility and the gravimetric detection limit, *Annals of Occupational Hygiene*, 33, 331-337.

Vincent, J.H. (1987), Recent advances in aspiration theory for thin-walled and blunt aerosol sampling probes, *Journal of Aerosol Science*, 18, 487-498.

Vincent J.H. (1989), *Aerosol Sampling: Science and Practice*, John Wiley and Sons Ltd, Chichester, U.K.

Vincent J.H. (Ed.) (1999), *Particle Size-Selective Sampling of Particulate Air Contaminants*,

ACGIH, Cincinnati, OH.

Gibson, H. and Vincent, J.H. (1981), The penetration of dust through porous foam filter media, *Annals of Occupational Hygiene*, 24, 205-215.

Vincent, J.H. and Mark, D. (1982), Applications of blunt sampler theory to the definition and measurement of inhalable dust, *Annals of Occupational Hygiene*, 26, 3-19.

Vincent, J.H., Emmett, P.C., and Mark, D. (1985), The effects of turbulence on the entry of airborne particles into a blunt dust sampler, *Aerosol Science and Technology*, 4, 17-29.

Vincent, J.H., Stevens, D.C., Mark, D., Marshall, M. and Smith, T.A. (1986), On the aspiration characteristics of large-diameter, thin-walled aerosol sampling probes at yaw orientations with respect to the wind, *Journal of Aerosol Science*, 17, 211-224.

Vincent, J.H. and Mark, D. (1990), Entry characteristics of practical workplace aerosol samplers in relation to ISO recommendations, *Annals of Occupational Hygiene*, 34, 249-262.

Vincent, J.H., Mark, D. and Aitken, R.J. (1993), Porous plastic foam filtration media: their penetration characteristics and applications in particle size-selective sampling, *Journal of Aerosol Science*, 24, 929-944.

Vincent, J.H., Ramachandran, G., Thomassen, Y., and Keeler, G.J. (1999), Application of recent advances in aerosol sampling science towards the development of improved sampling devices: the way ahead, *Journal of Environmental Monitoring*, 1, 285-292.

Vitols, V. (1966), Theoretical limits of errors due to anisokinetic sampling of particulate matter, *Journal of the APCA*, 16, 79-84.

Voloshchuck, V.M. and Levin, L.M. (1968), Some theoretical aspects of aerosol aspiration (large Stokes' numbers), *Izv. Akad. Nauk. ser. Fizika Atm. Okeana* (English translation), No. 4.

Werner, M., Vincent, J.H., Thomassen, Y., Hetland, S., and Berge, S. (1999), Inhalable and "total" metal and metal compound aerosol exposures for nickel refinery workers, *Occupational Hygiene*, 5, 93-109.

Wilsey, P.W., Vincent, J.H., Bishop, M.J., Brosseau, L.M. and Greaves, I.A. (1996), Workers' exposures to inhalable and 'total' oil mist aerosol in a metal machining shop, *American Industrial Hygiene Association Journal*, 57, 1149-1153.

Witschger, O., Willeke, K., Grinshpun, S.A., Aizenberg, V., Smith, J., and Baron, P.A. (1998), Simplified method for testing personal inhalable aerosol samplers, *Journal of Aerosol Science*, 29, 855-874.

Zenker, P. (1971), Investigations into the problem of sampling from a partial flow with different flow velocities for the determination of the dust content in flowing gases, *Staub-Reinhalt. Luft* (English translation), 31, 30-36.

INVENTION

One invention arose out of this project, the new low flowrate (0.22 L/min) personal inhalable aerosol sampler. This instrument is based on the original IOM (2 L/min) personal inhalable aerosol sampler, developed at the Institute of Occupational Medicine, Edinburgh, U.K. during the 1980s. This instrument is described in the following patents:-

> Lynch, G., McLuckie, P., Mark, D. and Vincent, J.H. (1985), Improvements in dust collection (A personal dust sampler. . .), UK Patent Application No. 2,158,234 (published November 6th 1985); U.S. Patent No. 4,675,034

The new invention is described in the disclosure submitted to the University of Michigan's Director of Licensing in March 2002. No commercial development has yet taken place, but interest has been expressed by a leading manufacturer of industrial hygiene sampling apparatus.

Disclosure

A. Description of invention

Abstract of invention

This invention was developed as part of an effort to sample the inhalable aerosol fraction from the ambient atmosphere at very low air flowrates, and thus enable the existing IOM personal inhalable aerosol sampler (SKC Ltd., Blanford Forum, Hants, U.K.) to be used with lightweight sampling pumps for personal aerosol exposure monitoring. The low-flowrate IOM sampler adapter is composed of stainless steel, and it fits inside the orifice of the IOM sampler.

Detailed description

The low-flowrate IOM sampler adapter is a short stainless steel tube with thick walls. On one end of the tube, there is a thin protruding lip. The diameter of the tube orifice is 5 mm, which provides a sampling velocity of 0.187 m/s when the sampling flowrate is 0.22 L/min. This sampling velocity plays a critical role in enabling the sampler to collect the inhalable aerosol fraction under many practical sampling situations.

The adapter enables the IOM sampler, which requires a sampling flowrate of 2 L/min, to function as a low-flowrate sampler, sampling at 0.22 L/min. The IOM sampler, then, can be used in combination with very light sampling pumps (with maximum flowrates much lower than 2 L/min) and still collect the inhalable aerosol fraction. Currently, there is no sampler that can accurately collect the inhalable aerosol fraction at a flowrate less than approximately 2 L/min.

Below is a picture of the IOM sampler and IOM sampler with low-flowrate adapter (left) and the low-flowrate adapter by itself (right).

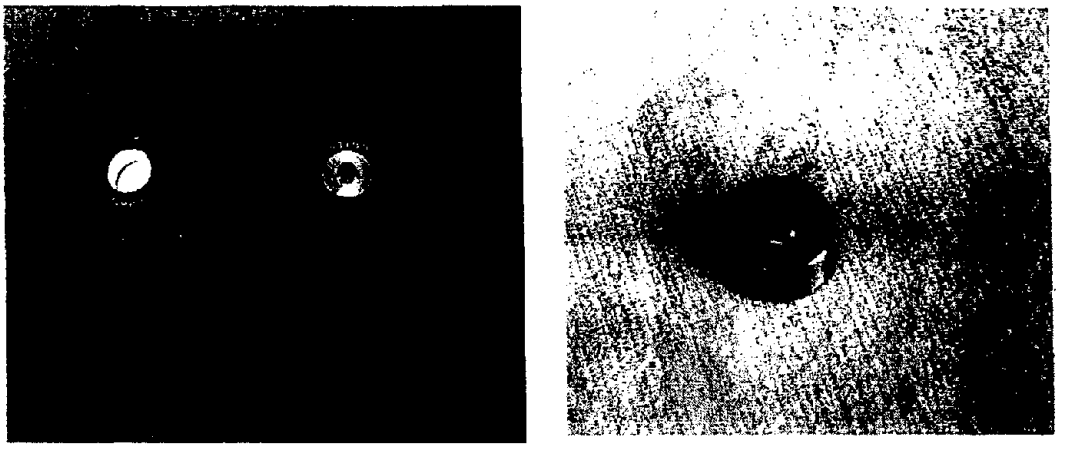

The outer diameter of the low-flowrate IOM sampler adapter is 15 mm, the internal diameter is 5 mm, and the length is 8 mm. The length of the protruding lip is 2 mm, with a thickness of 0.25 mm. The adapter fits snugly inside the orifice of the IOM sampler.

Simulations and working models

In order to investigate sampler aspiration efficiencies, A, for very low flowrates, experiments were conducted in our laboratory using a wide range of flowrates, as low as 0.082 L/min, for simplified disc-shaped samplers facing the wind. An existing model for blunt samplers facing the wind was modified, using our experimental data, to include this wide range of flowrates[11]. Results indicated that the diameter of the disc had a small effect on aspiration efficiency, at least when r (the ratio of the diameter of the sampling orifice and disc, respectively) was in the approximate range 0.05 to 0.10 (see below - predictions based on the modified model are for the IOM sampler and our low-flowrate prototype). Since it is expected from blunt sampling theory that bluff body effects are more pronounced when samplers are facing the wind, we thought that the difference we saw due to r would be even smaller for orientation-averaged aspiration efficiency[12]. Thus, we wanted to test our prototype (the IOM sampler with low-flowrate adapter in place), which differs from the IOM sampler only in r ($r = 0.041$ for our prototype; $r = 0.125$ for the IOM sampler), and see how its orientation-averaged aspiration efficiency would compare to that of the IOM sampler.

[11] Paik, S. and Vincent, J.H. (2002) Aspiration efficiency for blunt samplers facing the wind and for high velocity ratios, J. Aerosol Sci., submitted.

[12] Orientation-averaged aspiration efficiency is the index for sampler performance according to the inhalability convention.

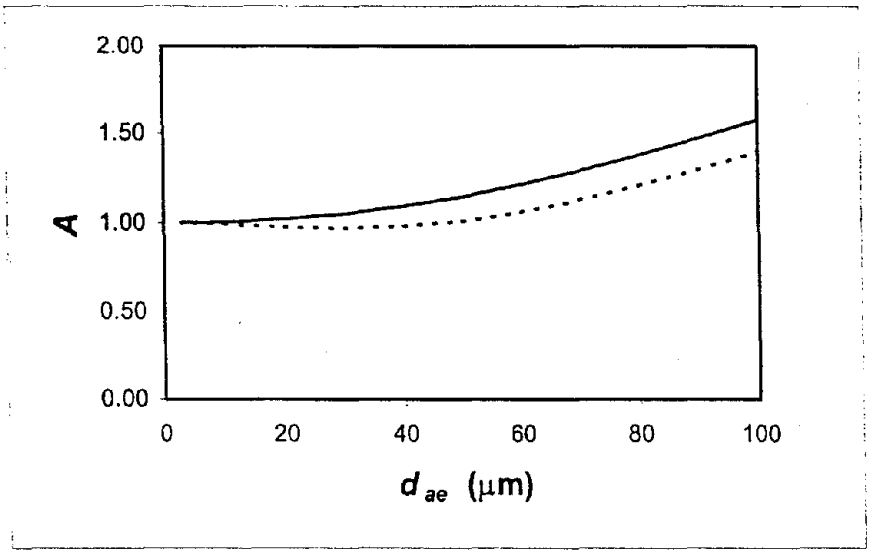

(These experiments were done in Summer 2001. Predictions are based on the modified blunt sampling model for $r = 0.041$ and $r = 0.125$. Dotted line represents A for $r = 0.041$ and solid line represents A for $r = 0.125$)

Experimental data

Based on the insights mentioned above, we decided to compare the performance of a low-flowrate prototype (slightly larger than our current proposed prototype) with an IOM sampler, both mounted on a 120 mm-wide rotating bluff body, and thus corresponding to r-values of 0.05 and 0.125, respectively. This sampling scenario is representative of practical sampling situations in ambient aerosol monitoring, and similar such studies have been done elsewhere. Results from these experiments indicated that the performances of the prototype and the IOM sampler were very close indeed. The slight positive bias in our data compared to the inhalability criterion was likely due to our experimental set-up, which utilized a small wind tunnel. Nevertheless, we concluded that our proposed low-flowrate prototype, which is a slightly smaller version of the prototype we tested, would be sufficient as an alternative to the IOM sampler when measuring the inhalable aerosol fraction.

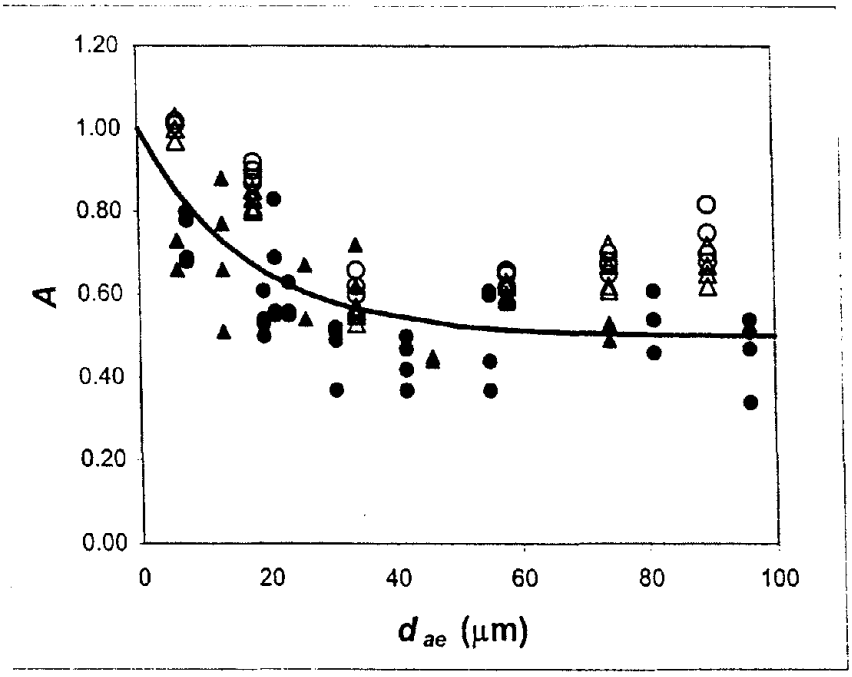

(These experiments were done in Fall 2001. Open circles represent IOM sampler data, open triangles represent prototype sampler data, solid triangles and circles represent data from earlier large wind tunnel studies, and solid line represents the inhalability curve)

c. As an alternative to the low-flowrate adapter, which is used in combination with the existing IOM sampler, a completely new sampler can be developed, consisting of a sampling cassette similar to the IOM cassette, except with a smaller orifice. In addition, our results show that the sampling velocity is of primary importance in determining aspiration efficiency, more so than bluff body effects. Therefore, adapters or cassettes with varying orifice diameters can be constructed and used with sampling pumps of varying flow capacities, as long as the sampling velocity remains constant. The low-flowrate adapter can also be constructed of various materials, including plastic and Teflon, in order to facilitate the analysis of samples collected. Due to the lower flowrate, it may be necessary to analyze the samples with methods more sensitive than gravimetry, such as ICP-MS (Inductively-coupled plasma mass spectrometry) or AAS (Atomic Absorption Spectrometry), in which case a sampling cassette and adapter made of plastic or Teflon would be more favorable than stainless steel to the acid digestion required by these methods.

B. **Similar technologies**

The IOM personal inhalable aerosol sampler (SKC Ltd., Blanford Forum, Hants, U.K.) is very similar to this invention. The invention, in fact, is used in conjunction with the IOM sampler, since it fits inside the orifice of the sampler. The invention represents a new use of the IOM sampler, enabling it to sample the inhalable aerosol fraction at a very low flowrate. However, as mentioned in A3c, it is not limited to being used with the IOM sampler and the new knowledge gained can be applied to the development of new generations of aerosol samplers.

Alternatives: The flowrate and orifice diameter can be manipulated, as long as the sampling velocity is close to 0.187 m/s. For applications that require large amounts of sample, for example, the flowrate can be very high so long as the orifice diameter is increased accordingly. Likewise, if an even lower flowrate is desired, the orifice can be made smaller, so long as the mass sampled can be detected and quantified by whatever analytical method is used. Inductively-coupled plasma mass spectrometry (ICP-MS), for example, can analyze masses on the order of nanograms.

C. **Market potential for the invention**

This invention, used with the IOM sampler, allows the user to collect the inhalable aerosol fraction when mounted on the body of the wearer. It is unique in that it can be used with a lightweight, low-flowrate sampling pump. Currently, there is a commercial sampling pump called the "Pocket Pump", available by SKC, which only weighs 5 ounces and provides flowrates up to 0.225 L/min. The invention would be used for industrial hygiene and environmental sampling applications. It would find special wide use among young children, women, and the elderly, to whom it may be too inconvenient to wear heavier sampling pumps for extended periods of time.